Composite Framed Buildings under Fire-Induced Progressive Collapse: Computational Analysis and Design Recommendations

by

Thi Thu Ha Nguyen

A dissertation submitted in partial fulfillment
of the requirement for the degree of
Doctor of Philosophy
(Civil Engineering)
in the University of Michigan
2017

Doctoral Committee:

Associate Professor Ann E. Jeffers, Chair
Professor Sherif El-Tawil
Associate Professor Jason Paul McCormick
Professor Peter David von Buelow

Thi Thu Ha Nguyen

hanguyen@umich.edu

ORCID iD: 0000-0002-6648-4103

ACKNOWLEDGEMENTS

I would like to express a special thanks to my Ph.D. advisor and mentor, Prof. Ann Jeffers. This dissertation research would not be possible without her great guidance. Her humility, her compassion with students, and her generosity towards other people has been an example for me to become a better person and contribute more to the society. It is a great pleasure to work with Prof. Jeffers as a student.

I also want to thank my Ph.D. committee, Prof. El-Tawil, Prof. McCormick, and Prof. Buelow, for spending their precious time providing me helpful feedback and helping me complete the dissertation. I also really appreciate the support from my colleagues in the research group, including Jason Martinez, Paul Beata, Ning Liu, and Alyssa Desimone.

I am very grateful for the love from my family and friends, and the support of the department of Civil and Environmental Engineering, and the University of Michigan - Ann Arbor.

TABLE OF CONTENTS

LIST OF TABLES

LIST OF FIGURES

ABSTRACT

Empirical and scientific evidence suggests that buildings may be susceptible to fire-induced progressive collapse if they are not specifically designed to resist the effects of fire. Although prior studies have shed some light on the problem, there is still a lack of quantitative research on structural robustness in fire, leading to a gap in building codes related to fire-induced progressive collapse. This dissertation aims to address these issues by proposing a comprehensive method for quantifying structural robustness in fire, which integrates the existing standards on structural performance at room temperature and fire protection requirements. Additionally, a macro-element model for beam-to-column connections was developed to offer an accurate analysis at a reasonable computational cost. Test data from experimental studies on moment-resisting structures at room temperature and elevated temperatures were used to validate the appropriateness of the connection model. 2D and 3D macro-element models were developed to explore the robustness of composite steel structures against fire-induced progressive collapse. Sequentially coupled thermal-structural analysis using an explicit dynamic approach in ABAQUS was adopted for the analysis. The elements used in the 3D model include beam-column elements for the steel beams and columns, shell elements for the reinforced concrete slabs, and kinematic coupling constraints for the connections. The 3D model was validated against the experimental data of the Cardington Fire Test 3 and was employed to investigate 10-story composite buildings exposed to various fire scenarios. It was found that failure of the insulation materials determined the time limit of the structure in most cases. Although the buildings were sufficiently designed for progressive collapse at room temperature and one-hour rated fire protection was applied for all steel members, the buildings could only withstand less than an hour of fire. In other words, prescriptive design is insufficient to ensure the robustness in fire. Additionally, several design improvements were explored to study the effectiveness of different structural enhancement strategies. It was found that increasing fire protection applied to the columns or increasing the capacity of the columns was the most effective approach for the moment-resisting framed building considered in this study.

CHAPTER 1. INTRODUCTION

Chapter 1 provides the background and motivation for the research. It describes the research objectives within the context of the current literature, that is, investigating the structural performance of buildings in resistance to progressive collapse in fire. It also summarizes the structure of this dissertation.

1.1. Motivation

The dissertation aims to investigate the performance of building structures in fire events, especially the structural resistance to progressive collapse in fire. It is motivated by statistical and scientific evidence of considerable risk and catastrophic consequence of structural fire in buildings.

Structural fires have attracted very low interest among structural engineers and are rarely considered in building design aside from prescriptive measures given in building codes. This is partly due to their low probabilities of occurrence (i.e., the fire probability in buildings is 0.3-0.5% per year in the U.S. [1]) and small region of impact (i.e., a structural fire typically only affects an individual building). Meanwhile earthquakes, which affect large areas encompassing several buildings and infrastructure, have been intensely studied and widely accepted as a requirement in structural design. However, while earthquakes are restricted to earthquake-susceptible areas, structural fires may occur anywhere and at any time. In fact, despite their low probabilities of occurrence, structure fires have a high total number of incidents and tremendous associated costs. According to National Fire Protection Association (NFPA) [2], there were roughly 490,000 structure fire incidents, which caused 2,700 deaths, 14,000 injuries, and $10 billion property damage on average each year from 2009 to 2015 in the U.S. Approximately, one of every four households will have a reported home fire in an average lifetime [3]. In contrast, each year in the U.S., earthquakes cause $4.4 billion loss, the majority of which are located on the West Coast (i.e., California, Washington, and Oregon). [3]

Another reason for the low interest in structural fires is the public trust in the active fire protection systems, which include smoke detection systems and fire suppression systems. In reality, approximately 40-50% of high-rise buildings in the U.S. are not equipped with sprinklers; even where sprinklers were present, 13% of them failed to function effectively when fires occurred, according to NFPA's 2007-2011 survey [4]. The major reasons for sprinkler failures were system shut-offs before fire, water inability to reach fire, and insufficient released water [4]. The height of the building also poses additional challenges for evacuating occupants and suppressing fires (e.g., high pressure required to pump water to high floors). This, in turn, may enable fire to spread vertically and horizontally within the building. This is evidenced in the study done by Cowlard et al. [5], in which a third of structural fire incidents in high-rise buildings surveyed had fire on multiple floors.

Moreover, sustainability, particularly green building design, has been a major trend in civil engineering. High-rise buildings with LEED certified designs have been in high demand in urban areas. However, the environmentally-friendly and energy-efficient features in green buildings have posed significant risks of structural fire [6]-[8]. For example, roof gardens and photovoltaic solar panels hinder fire fighters from entering buildings and suppressing fires [6]. Additionally, solar panels have caused many fire incidents [7]. The open space concept with vertical openings (e.g., atriums) [8] and the removal of partition walls conflicts with the compartmentation approach, that is commonly used in fire protection engineering. Passive energy buildings also use flammable materials in wall linings and external cladding [6]. The recent fire at Grenfell Tower (London, UK) in June 2017, which started on the fourth floor, spread to the top of the 24-story building due to the exterior aluminum claddings, and killed at least 12 people [9] shows the potential dangers of using flammable materials in claddings.

In addition to the probability of fire occurrence and the issues modern buildings face with regards to fire safety, the risk of structural fire is substantiated by many real-life fire incidents in buildings. One of the most severe fires in history is the Great Chicago Fire in 1871, which burned for around three days, killed 300 people, destroyed roughly 3.3 square miles of Chicago, and left around 100,000 residents homeless [10]. The reason for this great conflagration was the lack of adequate fire detection and suppression systems, the use of flammable building materials, and the weather conditions at the time [10]. While the Great Chicago Fire led to substantial advancements in fire

safety engineering, fires continue to pose a significant problem in structures. As this dissertation focuses on collapse resistance, Table 1.1 summarizes several notable incidents of structural fires that led to the partial or entire collapse of mid- and high-rise buildings.

Table 1.1. *Notable structural fire incidents*

Event	Causes of collapse	Structure & Fire proofing
First Interstate Bank Building (1988) [11] Partial collapse	- Fire started in an open-plan office area of the 12th floor and spread to four floors above - Results: fire lasted for 3 hr 40 min; nearly 5 floors are burned out; external claddings of the 12th-16th floors were destroyed and fell to the ground; structural damage in a secondary beam and several floor decks; 40 deaths and 40 injuries	- 62-story framed structure - Steel columns and beams; composite floor with concrete slab on profile steel deck - Steel columns and beams are fire protected; no fire stopping, no fire compartmentation - No automatic sprinklers
World Trade Center Building 1 & 2 (2001) [12,13] Entire collapse	- The impact of the aircraft crash led to severe damage and localized loss of the 93rd-99th floor (i.e., 35 exterior columns and 6 core columns were cut off, insulation of 43 core columns and truss was stripped), followed by vigorous fires on multiple floors - The loss of water for firefighting and sprinkler system caused the fire to spread uncontrollably	- 1362-foot-high “framed-tube” structure - Steel columns, beams, and trusses; concrete-steel composite floor system - All beams, trusses, and columns were fire protected; no fire protection was applied on the underside of the metal deck of the composite slab - Automatic sprinklers

	- Result: WTC 1 collapsed after 102 min; WTC 2 collapsed after 56 min; around 2,600 deaths	
World Trade Center Building 7 (2001) [12,13] Entire collapse	- Due to the debris from the collapse of WTC 1, fire was ignited in more than 10 floors near the southwest corner of WTC 7, and several exterior walls were damaged - The interruption of public water supply (due to the collapses of WTC 1 and 2) made the sprinkler system unable to suppress the fire, leading to wide spread of fire; columns and beams were heated beyond the critical temperatures and failed. - Results: WTC 7 entirely collapsed after seven hours in fire; no casualties	- 610-foot-high frame structure - Steel columns and beams; concrete-steel composite floor system - All beams, trusses, and columns were fire protected; no fire protection was applied on the underside of the metal deck of the composite slab - Automatic sprinklers
Windsor Tower, Spain (2005) [14] Partial collapse	- Fire started on the 21st floor during the building renovation process, fire spread rapidly to all floors above the second floor due to incompletion of fire protection and fire stopping - Results: After 20 hours in fire, Windsor Tower was severely	- 32-story "core" structure with 2 rigid floors, “open plan” concept - Reinforced concrete core, interior columns, beams, and slab; steel exterior columns - Fire protection for steel exterior columns was not complete (under construction); compartmentation and

	damaged (progressive collapse of floors and columns above the 17th floor); no casualties	fire stopping for vertical openings was not complete - Sprinklers were not completely furnished
Faculty of Architecture Building, Delft Univ., Netherlands (2009) [15] Partial collapse	- Fire started on the sixth floor of the North section (from a coffee vending machine) and spread to all the floors above the sixth floor despite manual fire suppression efforts - Results: After seven hours in fire, the loss of slab (due to excessive deflection) initiated the progressive collapse of the North section of the building; no casualties	- 13-story reinforced concrete framed structure, sitting on top of a series of 6 semi-independent 3-story structures - Part of the building had "open plan" concept (double height floors with large windows) - No sprinklers
Plasco Shopping Center, Teheran, Iran (2017) [16] Entire collapse	- Fire started on the 10th floor (from a leak in a small gas cylinder) and spread to the upper floors - Results: After more than three hours in fire, entire building collapsed due to the failure of the steel structure at high temperatures; at least 30 deaths including 20 firefighters	- 17-story residential and commercial building with many garment stores - Steel columns and beams, concrete-steel floor system - No sprinklers, empty fire extinguishers; fire safety standards were ignored

Some important lessons can be learned from these fire events, as follows:

- Active fire protection (e.g., fire sprinkler systems and firefighting) and compartmentation help to prevent fire from spreading throughout buildings and reduces damage. However, in many cases active systems may not function due to the loss of water supply or difficulties for firefighters to access the fire.

- Vertical openings and large glass windows, which are common in high-rise buildings, pose risks of spreading fire throughout the building. Adequate fire stopping and compartmentation should be applied in these situations to avoid uncontrollable fires.

- Applying insulation on steel members helps reduce the impacts of fire on load-bearing capacity, thereby mitigating the risk for collapse of the building (e.g., fire protection on steel members of First Interstate Bank prevented the progressive collapse of the building even after nearly 4 hours of fire).

- Spray-applied fire resistive material (SFRM) which is often used for insulation can be damaged under impact, significantly lowering the structural fire resistance and resulting in the collapse of the building in fire (e.g., SFRM was stripped in the airplane crash into WTC 1 and 2). This situation should be addressed in the structural analysis of buildings subjected to multi-hazard threats.

- Reinforced concrete structures may perform better in fire than steel structures without fire insulation (e.g., in the Windsor Tower fire, unprotected concrete core and concrete columns remained robust while unprotected steel columns buckled and collapsed).

- Structural redundancy can mitigate progressive collapse in fire (e.g., in the Windsor Tower fire, the rigid floors transferred the loads from buckled steel columns to the remaining concrete core and concrete columns, and helped resist the further collapse of the building).

In addition to the statistics and the real-life events where buildings collapsed partially or entirely due to structural fires, multiple theoretical studies have proved that long fire exposure may lead to progressive collapse of buildings. More specifically, during a long fire, significant thermal expansion followed by catenary action of the heated floor system during fire can produce significant lateral deflections in columns, which can then lead to global collapse of the building. A study done by Lange et al. [24] used 2D finite element models to analyze a 12-story composite

steel frame with an interior core and perimeter moment frame subjected to a three-floor exponential fire curve. It was concluded that during fire, the perimeter columns were initially pushed outward due to the thermal expansion of the heated floors, then pulled inward due to the significant deflection and catenary action of the floors [24]. Eventually the perimeter heated columns buckled, initiating the progressive collapse of the building.

Research by Garlock and Quiel [25] investigated a 38-story steel moment frame in realistic fire scenarios that included a temperature-time curve involving three phases - heating, stabilizing, and cooling - using 2D finite element analyses. Only one exterior bay of the frame was subjected to fire and the fire spread vertically from the 22nd floor to the 30th floor. It was found that during the heating phase, the heated beams expanded and caused the perimeter columns to deform laterally. When the beams and columns reached the limit state under the combined effect of axial forces and bending moments, plastic hinges would form, increasing the potential for structural collapse [25]. The study also showed that the beams bracing the perimeter columns were crucial to maintaining stability of the perimeter columns, and thus they were suggested to have a higher fire protection level than other beams in the building [25].

Another study done by Agarwal and Varma [26] showed conclusions of column failures in corner compartment fire scenarios. The research used 3D finite element models to analyze two 10-story composite buildings of identical plan layout, i.e., one with a rigid core in the center and the other with a perimeter moment resisting frame. Parametric design fire curves were used for the corner fire on the fifth floor. The analysis predicted that both structures experienced column failures during fire: the building with the rigid core experienced buckling of the perimeter columns, and the building with perimeter moment frame experienced buckling of the interior column [26].

Moreover, it is widely understood in structural engineering that the loss of column(s) can lead to the partial or entire collapse of a building. Examples are the entire collapse of the World Trade Center Building 7 (2001) [12,13], which was initiated by the fire-induced failure of interior columns, and the partial collapse of the Alfred P. Murrah Federal Building during the Oklahoma City bombing attack (1995) [27], which caused the column failure. The loss of column(s) is also considered in building codes (e.g., ASCE 7 [28]) as a significant initiator of building collapse.

In brief, there is theoretical and empirical evidence that mid-rise and high-rise buildings are in a considerable risk of structural fires, which may lead to column failures and progressive collapse (if there is insufficient redundancy). Therefore, to improve life safety and structural resilience in buildings, it is necessary to understand structural behavior in resistance to fire-induced progressive collapse.

1.2. Research background

To investigate structural performance against progressive collapse in fire, it is vital to understand structural performance against progressive collapse at room temperature, which has been long been studied in research and considered in building codes. The American Society of Civil Engineering (ASCE) Standard ASCE 7 defines "progressive collapse" as "the spread of an initial local failure from element to element that eventually results in the collapse of an entire structure or a disproportionately large part of it" [28]. The loss of a column is a widely-used scenario of a local failure initiating progressive collapse [29-31].

Research has investigated progressive collapse at room temperature at various scales and levels, ranging from sub-assemblies (e.g., Sadek et al. [29] with both experimental and computational analyses), 2D multi-story frames (e.g., Khandelwal et al. [30] with computational analyses), to 3D full-scale buildings (e.g., Alashker et al. [3] with computational analyses). Sadek et al. [29] investigated the failure mechanisms of a steel sub-assembly consisting of three columns connecting with two beams via moment connections, in which the middle column was removed. Khandelwal et al. [30] studied 2D ten-story steel frames (i.e., an intermediate moment frame and a special moment frame) subjected to the sudden loss of an interior column on the first floor, and found that catenary action developed in the gravity bay at large deformation and provided additional resistance against progressive collapse. Investigating a ten-story composite building with the loss of a perimeter column, Alashker et al. [31] concluded that the slab could reduce the deformations and redistribute loads from the removed column to the adjacent columns.

Progressive collapse at room temperature has also been considered in building codes [28,32-33]. In the U.S., guidelines for progressive collapse resistant design at room temperature are provided by the General Service Administration (GSA) [32] and the Unified Facility Criteria (UFC) [33]. There are two major approaches to progressive collapse, namely Direct Design and Indirect Design.

- *Direct Design Approaches* explicitly consider the resistance against progressive collapse during the design process [32]. These include: (1) the Alternate Path method (i.e., requiring the structure to be capable of bridging over a missing structural element and localizing the extent of damage), and (2) the Specific Local Resistance method (i.e., requiring the structure or parts of it to provide sufficient strength to resist a specific load or threat) [33].

- *Indirect Design Approaches* implicitly consider the resistance against progressive collapse by providing minimum strength, continuity, and ductility [33]. ASCE 7 [28] provides suggestions for improving structural integrity, including: (1) suitable plan layout, (2) integrated system of ties, (3) returns on walls, (4) changing span directions of floor slabs, (5) load-bearing interior partitions, (6) catenary action of the floor slab, (7) beam action of the walls, (8) redundant structural systems, (9) ductile detailing, (10) additional reinforcement for blast and load reversal (if considering in design), and (11) compartmentalized construction.

Progressive collapse threat at elevated temperature (e.g., in fire) has been recently investigated in research but is non-existent in design guidelines. Porcari et al. [34] summarized recent findings on the mechanisms related to fire-induced progressive collapse, including the effect of restraint, stiffness, and bracing. When analyzing a ten-story building subjected to corner fire, Agarwal and Varma [26] found that reinforcement in the floor system could contribute to better load redistribution and resistance against fire-induced progressive collapse. Using OpenSees software, Jiang et al. [35] investigated the fire-induced collapse mechanisms of 2D frames. Quiel and Marjanishvili [36] studied fire following an extreme event (i.e., blast or impact) that causes failure of a column in a steel frame. Using SAFIR software with 2D fiber-beam elements and ASTM E119 standard fire curve, the authors estimated the time to initiate collapse as well as the impact of fire insulation [36]. Also using SAFIR and 2D analyses of a 38-story frame, Neal et al. [37] showed that meeting the progressive collapse design requirements was insufficient to prevent buildings from collapse in fire. The authors further discussed the effect of different parameters including fire protection, fire type, and location of the fire-blast event.

Additionally, to effectively mitigate progressive collapse in fire, it is crucial that structural robustness in fire be quantified. U.S. building codes (i.e., UFC [33] and ASCE/SEI 41-06 [38]) offer guidelines for performance levels and acceptance criteria to evaluate structures at room temperature. There are three different performance levels (i.e., Immediate Occupancy, Life Safety,

and Collapse Prevention) and two categories of the Acceptance Criteria (i.e., deformation-controlled actions and force-controlled actions); each performance level requires different limit values and coefficients in the Acceptance Criteria. However, the Acceptance Criteria do not consider elevated temperature, leaving uncertainty for design against progressive collapse in fire. Meanwhile, there are building codes for structural fire protection but only for laboratory tests on single structural components or assemblies, such as ASTM E119 Standard Test Methods for Fire Tests of Building Construction and Materials [39]. ASTM E119 identifies three performance criteria for fire protection, i.e., insulation, integrity, and stability, but there are no specific guidelines on how to assess these criteria for the entire structural system.

There are very few quantitative studies on structural performance in fire. Most research on structural fire engineering focuses on qualitative understandings such as failure mechanisms [24-26,35] and factors influencing structural failure in fire [24-26,34,37]. Among those few quantitative studies, Garlock and Quiel [25] proposed formulae for calculating capacity of non-uniformly heated components, which is useful for structures in fire, but it does not provide a method to evaluate the entire structural system. Meanwhile, Quiel and Marjanishvili [36] investigated structural robustness at the system-wide level by estimating the collapse time of a steel frame in fire, but they presented no details on how to quantitatively determine if a building was approaching imminent collapse. Moreover, although the significance of fire protection on structural robustness in fire is evidenced in multiple studies [25,36-37], the performance of fire protection materials has not been considered in any research on structural robustness evaluation. Insights into failure of fire insulation at large deformation are presented in studies on spray-applied fire resistive materials (e.g., Braxtan and Pessiki [40] and Arablouei and Kodur [41]) but they have not been integrated into research and guidelines for structural robustness.

1.3. Knowledge gaps and research objectives

Along with building codes for structural performance at room temperature, prior studies have shed some light on the structural resistance against progressive collapse at room temperature and elevated temperatures (i.e., in fire). However, there are some major limitations which may cause inconsistency in research and design for the fire-induced progressive collapse condition, as summarized below:

- There is a lack of guidelines for structural design in fire, concerning both progressive collapse and structural robustness evaluation.

- Prior research has provided qualitative understandings of structural performance in fire, but no quantitative method of evaluating the global structural robustness in fire has been presented. This poses a challenge for the performance-based design of buildings for fire conditions.

- There is a disconnect between research on structural performance in fire and research on fire protection materials. This can pose a risk of inadequate evaluation of building robustness in fire if ignoring the failure of insulation materials under combined fire and extreme loads.

- Beam-to-column connections play an important role in the global structural robustness but have been improperly considered in structural fire analyses (i.e., connections are primarily modeled as simple joints). This can lead to inaccuracy, even overestimation of structural capacity, in analyses of fire-induced progressive collapse. Several studies proposed simplified models for beam-to-column (BC) connections but very few have been validated against test data at elevated temperature. Prior to this thesis, there was no fire-validated model for welded flange-bolted web connections, which are commonly used in the U.S.

This dissertation addresses these knowledge gaps through full-scale analyses of building structures subjected to fire-induced progressive collapse. The focus is composite steel framed structures (i.e., steel columns and beams, and reinforced concrete slabs that act compositely with the beams), a widely-used structural type for mid- and high-rise buildings. The finite element method (e.g., ABAQUS software) was adopted thanks to its ability to accurately predict structural performance in complex loading conditions (i.e., fire and progressive collapse) at a reasonable computational cost. A comprehensive method for quantifying structural robustness in fire is presented (in Chapter 2) to provide a practical guideline for design and future research on fire-induced progressive collapse. For better accuracy and computational efficiency of large-scale structural analyses, this dissertation proposes a simplified model (i.e., macro-element model) for welded unreinforced flange-bolted web (WUF-B) connection, which was validated against experimental data at room temperature and elevated temperatures (as described in Chapter 3). The methodology is applied to 2D (Chapter 4) and 3D (Chapter 5) structural models to assess the performance of moderate-rise structures.

1.4. Structure of dissertation

Chapter 1 presents an introduction to the research presented herein regarding structural robustness of buildings against fire-induced progressive collapse, focusing specially on computational analyses and performance evaluation. It includes motivation, review of previous research, and research objectives.

Chapter 2 presents a comprehensive method of quantifying structural robustness in fire, which takes into account current guidelines (i.e., ASCE, UFC, and ASTM E119) and scientific insights related to this matter. It includes three criteria (i.e., insulation, integrity, and stability) and proposes the term "time limit" to measure the maximum time the structure can remain robust in fire. If adopted in building codes, this method can provide transparency for design practice and consistency among research studies on fire-induced progressive collapse.

Chapter 3 presents a simplified (or macro-element) model for beam-to-column connection, which was validated against experimental data at room temperature and elevated temperatures. The focus is on the welded unreinforced flange-bolted web (WUF-B) connection, which is commonly used in seismic building design in the U.S. The proposed model can easily be adapted for the shear tab connection as well as provide adequate accuracy for structural analysis in fire at a reasonable computational cost.

Chapter 4 presents 2D analyses of moment resisting frames in resistance to fire-induced progressive collapse. It provides insights into the failure mechanisms, the critical fire case for progressive collapse design, and estimates the time limit of structure in various fire scenarios. The analyses also adopted the macro-element connection model to ensure accuracy at a reasonable computational cost.

Chapter 5 presents the complete methodology of using 3D macro-element model to analyze composite buildings under fire-induced progressive collapse threats. It describes major components of the analysis, including thermal analysis, structural analysis, and method of quantifying structural robustness in fire. The Cardington corner compartment test was used to validate the appropriateness of the 3D model.

Chapter 6 presents examples of applying the 3D analysis to evaluate the structural robustness of composite buildings in resistance to fire-induced progressive collapse. Two types of structure are studied and compared against each other, one consisting of perimeter moment frames and interior gravity frames (called as Structure A), and the other consisting of a central core and gravity frames (called as Structure B). The results of the 3D analysis of Structure A was also compared with results in Chapter 4 to explore the differences between the 2D and 3D analyses. Additionally, a parametric study was conducted to analyze the effectiveness of different strategies for design improvement.

Chapter 7 summarizes the research conclusions on structural robustness against fire-induced progressive collapse. It also describes the limitations of this dissertation and discusses possible areas for future research.

Reference

[1] Code Consultants, Inc. (2012). "Fire Probability and Frequency. In: Fire Flow Water Consumption in Sprinklered and Unsprinklered Buildings." *SpringerBriefs in Fire*. Springer, New York, NY. <http://link.springer.com/chapter/10.1007%2F978-1-4614-8109-6_7> (Mar. 1, 2017)

[2] National Fire Protection Association. (2016). "Fire Statistics and Reports - Structure Fires." <http://www.nfpa.org/news-and-research/fire-statistics-and-reports/fire-statistics/fires-in-the-us/overall-fire-problem/structure-fires> (Mar. 1, 2017).

[3] Federal Emergency Management Agency (FEMA) (2000). "HAZUS®99 Estimated Annualized Earthquake Losses for the United States." Washington, DC <http://www.disastersrus.org/emtools/earthquakes/FEMA366.pdf> (May 1, 2017)

[4] Hall, J. (2013). "U.S. Experience with Sprinklers." *National Fire Protection Association*, Quincy, MA.

[5] Cowlard, A., Bittern, A., Abecassis-Empis, C., Torero, J. (2013). "Some Considerations for the Fire Safe Design of Tall Buildings." *International Journal of High-Rise Buildings*, Vol 2, No 1, 63-77

[6] Krause, U., Grosshandler, W., Gritzo, L. (2012). "The International FORUM of Fire Research Directors: A Position Paper on Sustainability and Fire Safety." *Fire Safety Journal*, Vol 49, 79-81

[7] Meacham, B. (2012). "Fire Safety Challenges of Green Buildings." *FPRF Fire Safety and Sustainable Building Symposium*. Chicago, IL, Nov 7 - 8 2012.

[8] Spadafora, R. (2012). "Atrium Features and Firefighting Tactics." *Fire Engineering*, Vol. 165, Iss. 3 <http://www.fireengineering.com/articles/print/volume-165/issue-3/features/atrium-features-and-firefighting-tactics.html> (May 1, 2017)

[9] Bilefsky, D., Hakim, D., Walsh, M. (2017) "The London Fire: What We Know". *New York Times*. <http://www.nytimes.com/2017/06/14/world/europe/uk-london-fire-grenfell-tower.html?mcubz=0> (July 1, 2017)

[10] Wikipedia. "Great Chicago Fire." < https://en.wikipedia.org/wiki/Great_Chicago_Fire> (May 1, 2017)

[11] One Stop Shop in Structural Fire Engineering. "Building Fires - First Interstate Bank Fire, Los Angeles." *University of Manchester*, UK. <http://www.mace.manchester.ac.uk/project/research/structures/strucfire/CaseStudy/HistoricFires/BuildingFires/interstateBank.htm> (May 1, 2017)

[12] Lew, H.S., Bukowski, R.W., Carino, N.J. (2005). "NIST NCSTAR 1-1. Federal Building and Fire Safety Investigation of the World Trade Center Disaster: Design, Construction, and Maintenance of Structural and Life Safety Systems." *National Institute of Standards and Technology*.

[13] One Stop Shop in Structural Fire Engineering. "Building Fires - World Trade Center Towers Collapse, New York." *University of Manchester*, UK. <http://www.mace.manchester.ac.uk/project/research/structures/strucfire/CaseStudy/HistoricFires/BuildingFires/worldTradeCenter.htm> (May 1, 2017)

[14] One Stop Shop in Structural Fire Engineering. "Building Fires - The Windsor Tower Fire, Madrid." *University of Manchester*, UK. <http://www.mace.manchester.ac.uk/project/research/structures/strucfire/CaseStudy/HistoricFires/BuildingFires/default.htm> (May 1, 2017)

[15] Engelhardt, M., Meacham, B., Kodur, V., Kirk, A., Park, H., Straalen, I., Maljaar, J., Weeren, K., Feijter, R., Both, K. (2013). "Observations from the Fire and Collapse of the Faculty of Architecture Building, Delft University of Technology." *Proc., 2013 Structures Congress*, ASCE, Pittsburgh, PA, 1138-1149.

[16] Hafezi, P. (2017). "Tehran Building Collapse Kills at Least 20 Firefighters: Mayor." *Reuters*. < http://www.reuters.com/article/us-iran-building-idUSKBN1530YP> (July 1, 2017)

[17] Scawthorn C., Eidinger J.M., and Schiff A.J., 2005. "Fire following earthquake. Technical Council on Lifeline Earthquake Engineering, Monograph No. 26." *American Society of Civil Engineers (ASCE)*, Reston, VA.

[18] Keller, W., Pessiki, S. (2012) "Effect of Earthquake-induced damage to spray-applied fire-resistive insulation on the response of steel moment-frame beam-column connections during fire exposure." *J. Fire Protection Engineering*, 22(4), 271-299.

[19] Sekizawa, A., Ebihara, M., Notake, H. (2003) "Development of Seismic-induced Fire Risk Assessment Method for a Building." *Proc., International Association of Fire Safety Science 7th International Symposium*, 309-320.

[20] Wilkinson, S., Grant, D., Williams, E., Paganoni, S., Fraser, S., Boon, D., Mason, A. and Free, M. (2013). "Observations and Implications of Damage from the Magnitude 6.3 Christchurch, New Zealand Earthquake of 22 February 2011," *Bull Earthquake Eng.*, v 11, 107-140. DOI 10.1007/s10518-012-9384-5.

[21] Braxtan, N., Pessiki, S. (2011). "Post-Earthquake Fire Performance of Sprayed Fire-Resistive Material on Steel Moment Frames." *J. Structural Engineering*, 137(9), 946-953.

[22] Baird, A., Palmero, A., Pampanin, S. (2011). "Facade Damage Assessment of Multi-Story Buildings in the 2011 Christchurch Earthquake." *Bulletin of the New Zealand Society for earthquake engineering*, special issue 44, number 4. <http://www.nzsee.org.nz/db/SpecialIssue/44(4)0368.pdf> (July 1, 2017)

[23] Meacham B. (2016). "Post-Earthquake Fire Performance of Buildings: Summary of a Large-Scale Experiment and Conceptual Framework for Integrated Performance-Based Seismic and Fire Design." *Fire Technology*, 52, 1133–1157.

[24] Lange, D., Roben, C., Usmani, A. (2012). "Tall Building Collapse Mechanisms initiated by Fire: Mechanisms and Design Methodology." *Engineering Structures*, 36, 90-103.

[25] Garlock, M., Quiel, S. (2007). "The Behavior of Steel Perimeter Columns in a High-Rise Building under Fire." *Engineering Journal*, 44(4), 359-372.

[26] Agarwal, A., Varma, A. (2014). "Fire Induced Progressive Collapse of Steel Building Structures: The Role of Interior Gravity Columns." *Engineering Structures*, 58, 129-140.

[27] Wikipedia. "Oklahoma City Bombing." <http://en.wikipedia.org/wiki/Oklahoma_City_bombing> (July 1, 2017)

[28] Standards ASCE 7. (2013). "Minimum Design Loads for Buildings and Other Structures." *American Society of Civil Engineers (ASCE).*

[29] Sadek F., Main J., Lew H., Robert S., Chiarito V., El-Tawil S. (2010). "An Experimental and Computational Study of Steel Moment Connections under a Column Removal Scenario." NIST Technical Note 1669, *National Institute of Standards and Technology*, Gaithersburg, MD.

[30] Khandelwal K., El-Tawil S., Kunnath S., Lew H. (2008). "Macromodel-Based Simulation of Progressive Collapse: Steel Frame Structures." *ASCE J. Structural Engineering*, v 134 (7), 1070-1078.

[31] Alashker, Y., Li H., El-Tawil S. (2011). "Approximations in Progressive Collapse Modelling." *Structural Engineering*, v 137 (9), 914-924.

[32] U.S. General Service Administration. (2003). "Progressive Collapse Analysis and Design Guidelines for New Federal Office Buildings and Major Modernization Projects." Washington, D.C.

[33] Unified Facilities Criteria. (2009). "Design of Buildings to Resist Progressive Collapse. Department of Defense." Washington, D.C.

[34] Porcari G., Zalok E., Mekky W. (2015). "Fire Induced Progressive Collapse of Steel Building Structures: A Review of the Mechanisms." *Engineering Structures*, v 82, 261-267.

[35] Jiang J., Li G-Q., Usmani A. (2014). "Progressive Collapse Mechanisms of Steel Frames Exposed to Fire." *Advances in Structural Engineering,* v 17 (3), 381-398.

[36] Quiel S., Marjanishvili S. (2012) "Fire Resistance of a Damaged Steel Building Frame Designed to Resist Progressive Collapse." *J. Performance of Constructed Facilities*, v 26 (4), 402-409.

[37] Neal M., Garlock M., Quiel S., Marjanishvili S. (2012). “Effects of Fire on a Tall Steel Building Designed to Resist Progressive Collapse.” *ASCE Proc. 2012 Structures Congress,* Chicago, IL, 246-256.

[38] ASCE/SEI 41-06. (2007). “Seismic Rehabilitation of Existing Buildings.” *American Society of Civil Engineers (ASCE)*, Reston, VA.

[39] ASTM. (2000). “Standard Test Methods for Fire Tests of Building Construction and Materials.” ASTM E119, American Society for Testing and Materials, West Conshohocken, PA.

[40] Braxtan, N., Pessiki, S. (2011)."Bond Performance of SFRM on Steel Plates Subjected to Tensile Yielding." *J. Fire Protection Engineering,* v 21 (1), 37-55.

[41] Arablouei, A., Kodur, V. (2015). "Critical Factors Governing Crack Propagation at the Interface of Fire Insulation and Slender Steel Trusses." *ASCE J. Structural Engineering,* v 141 (12).

CHAPTER 2. STRUCTURAL ROBUSTNESS IN FIRE

Chapter 2 presents a comprehensive method to quantify structural robustness in fire. It extends current methods for quantifying structural robustness to include hazards related to fire-induced collapse. The method includes three criteria (i.e., insulation, integrity, and stability) and proposes the term "time limit" to measure the maximum time the structure can remain robust in fire. If adopted in building codes, it can provide clarity for design practice and consistency among research studies on fire-induced progressive collapse.

2.1. Introduction

The methodology of determining structural robustness at room temperature is provided in the U.S. design guidelines and standards. Both UFC [1] and ASCE/SEI 41-06 [2] provide quantitative guidance to determine structural robustness at room temperature. However, there is no similar guideline for quantifying structural robustness in fire. At room temperature, structural robustness can be determined based on two criteria, namely force-controlled actions and deformation-controlled actions. The limits and coefficients for each criterion are different depending on the desired performance level (i.e., immediate occupancy, life safety, or collapse prevention). Because structural response in fire is far more complicated than that at room temperature (i.e., due to strength degradation and thermal expansion of materials at elevated temperature), the current guidelines cannot be directly applied to evaluate structural performance in fire.

Structural robustness in fire has been studied in recent research but no known research has provided a way to quantify the robustness of the structural system. This can leave discrepancy among research on structural evaluation as well as uncertainty in structural design for fire hazards. The majority of current research on structural fire engineering evaluates structural performance qualitatively, as summarized in the following categories:

(1) *Failure mechanisms of building structures in fire*: Lange et al. [3] found that buckling in perimeter columns leads to building failure. Garlock and Quiel [4] concluded that plastic hinges in beams and columns lead to building failure. Agarwal and Varma [5] found that buckling in perimeter columns or interior columns leads to building failure. Jiang et al. [6] reported that the dominant failure mode is downward collapse of the heated floor and lateral drift of the frames above the heated floor.

(2) *Effects of different components on the global structural performance in fire*: Agarwal and Varma [5] investigated the role of interior gravity columns and the effect of slab reinforcement in steel composite buildings subjected to fire. Lange et al. [3] described the effect of strong floor and weak floor on the failure of building. Bailey [7] explored the effect of composite floor on structural response in fire. Sun et al. [8] identified the effect of lateral bracing to the structural robustness in fire.

(3) *Effects of different factors on structural performance in fire*: Neal et al. [9] evaluated the effect of fire protection, fire type, and fire location. Porcari et al. [10] described the effect of restraint, stiffness, and bracing. Garlock and Quiel [4] reported on the effect of fire protection applied on columns and beams.

Very few studies have provided a quantitative assessment of structures in fire, and even when a quantitative assessment is conducted, it is done only at the component level (e.g., columns, beams, slabs, or connections). For example, Garlock and Quiel [4] evaluated the performance of beams and columns in fire by using two ratios: the axial load ratio P/P_y and the moment ratio M/M_P. Garlock and Quiel [4] also proposed a method to calculate load-bearing capacity of non-uniform heated beams and columns. To address the combined effect of axial force and moment, Garlock and Quiel [4] plotted the combined P and M plastic capacity envelope; once the analysis hit this envelop, the structure failed. Sarraj [11] proposed a method to calculate the capacity and stiffness of a fin plate connection, which was verified against experimental tests at ambient and elevated temperature. The load-bearing capacity of composite floor in fire has also been investigated by Bailey et al. [7,11]. A study done by Quiel and Marjanishvili [9] estimated the collapse time of a steel framed building in fire as well as the correlation between fire protection and the time to collapse. Although the time to collapse is a viable metric for evaluating structural robustness in fire, no details on

failure criteria (or how to quantitatively determine if a building collapses) was mentioned by Quiel and Marjanishvili [9].

On the other hand, research in building materials has provided significant understandings on the performance of fire protection materials. These findings unfortunately have not been integrated into evaluating structural robustness in fire. More specifically, the failure of sprayed fire resistive material (SFRM) at large strain has been observed in lab tests by Braxtan and Pessiki [12], and Arablouei and Kodur [13]. An important thing to note is that high deformation (i.e., high strain) is very common in fire events, and when fire protection loses its effectiveness (due to cracking, delamination, or fall-off), the temperature in steel members will quickly reach the critical limit (i.e., 500-600°C), leading to structural collapse. An example is the collapse of World Trade Center towers, which were initiated by the delamination of fire insulation under the action of impact/explosion following the aircraft crash [14]. Therefore, it is necessary to consider limiting strains in heated structures in order to prevent the failure of the fire protection, which can result in structural collapse in fire. While this dissertation focuses on preventing insulation damage, there may be other insulation or integrity criteria for the holistic design of structural fire protection such as partition walls.

For the reasons above, a comprehensive method to quantify structural robustness in fire was proposed. This method incorporates principles of evaluating structural robustness at room temperature (provided in the U.S. design guidelines), and up-to-date scientific findings on structural behavior in fire and the performance of fire protection materials.

2.2. Method background

The proposed method is based on two sets of design criteria (i.e., acceptance criteria [1,2] and fire protection criteria [15]) and two sets of research findings (i.e., capacity of non-uniformly heated members [4], and failure of fire insulation materials [12-13]), as described in the Section 2.2.1 to Section 2.2.4. Section 2.2.5 identifies the correlation between these literature materials and provides a solid foundation for the methodology of quantifying structural robustness, which is presented in Section 2.3.

2.2.1. Acceptance criteria

Both UFC (for progressive collapse design) [1] and ASCE/SEI 41-06 (for seismic design) [2] offer guidance for performance levels and acceptance criteria. There are three different levels of performance, namely:

(1) Immediate Occupancy (IO): after hazards, the building sustains minimal damage to its structural elements and only minor damage to its nonstructural components

(2) Life Safety (LS): after hazards, the building may experience extensive damage to its structural and nonstructural components but the risk of casualties is low

(3) Collapse Prevention (CP): after hazards, the building may pose a significant risk to life safety due to failure of nonstructural components, but the collapse of entire building is prevented

Acceptance criteria are classified into two categories, deformation-controlled actions and force-controlled actions. The deformation-controlled limit state is mostly determined by rotation at the connections (or beam ends). The force-controlled limit state is mostly determined by the Demand over Capacity Ratio (DCR), which combines the effect of axial forces and bending moments [2], as described below:

$$\text{For } \frac{N}{N_{CL}} < 0.2,\ DCR = \frac{N}{2N_{CL}} + \frac{M_x}{m_x M_{CEx}} + \frac{M_y}{m_y M_{CEy}} \le 1.0 \tag{2-1}$$

$$\text{For } 0.2 \le \frac{N}{N_{CL}} \le 0.5,\ DCR = \frac{N}{N_{CL}} + \frac{8}{9}\left(\frac{M_x}{m_x M_{CEx}} + \frac{M_y}{m_y M_{CEy}}\right) \le 1.0 \tag{2-2}$$

$$\text{For } \frac{N}{N_{CL}} > 0.5,\ DCR = \frac{N}{N_{CL}} + \frac{M_x}{M_{CEx}} + \frac{M_y}{M_{CEy}} \le 1.0 \tag{2-3}$$

where N, M_x, M_y = axial force and bending moment in the member due to applied loads; N_{CL} = lower bound compression strength of the member; M_{CEx}, M_{CEy} = expected bending strength of the member; and m_x, m_y = factor for member bending, defined based on the performance level and the ratio N/N_{CL}.

The limits differ depending on the performance level (i.e., IO, LS, or CP), the beam type (i.e., primary or secondary), and the beam's slenderness. For example, for LS level and non-slender beams, the rotational limit is $6\theta_y$ (for primary beams) and $9\theta_y$ (for secondary beams), where θ_y is the yield rotation) [2].

ASCE/SEI 41-06 [2] provides further details on calculating DCR and the rotation limits for different analysis procedures including linear static, linear dynamic, nonlinear static, and nonlinear dynamic. However, it does not consider fire (or elevated temperature) in the analysis.

2.2.2. Fire protection criteria

Building code requirements for structural fire protection are based on laboratory tests on single structural components or assemblies, in accordance with ASTM E119 (Standard Test Methods for fire tests of building construction and materials) [15]. In these tests, individual structural components or assemblies (e.g., floor-ceilings, columns, beams, and walls) are exposed to heating conditions in a furnace, following a specified fire curve (e.g., ASTM E119 standard fire curve, ASTM E1529 standard hydrocarbon fire) [15].

There are three performance criteria in the ASTM E119 standard tests, i.e., insulation, integrity, and stability (or load-bearing capacity):

(1) Insulation: for assemblies functioning as separator for two parts of a building (e.g., floor-ceilings and walls), the temperature rise at the unexposed surface of the specimen shall not exceed 139°C (282°F) for average temperature rise and 181°C (358°F) for maximum temperature rise.

(2) Integrity: for assemblies like floors, roofs, and walls, the formation of openings through which flames and hot gases can pass shall not occur.

(3) Stability (or load-bearing capacity): for load-bearing assemblies, the test specimen shall not collapse in such the way that it no longer performs the load-bearing function.

This set of three fire protection criteria is the principle of the proposed methodology of quantifying structural robustness in fire. The other performance criteria and research knowledge can

complement the general requirements defined in the fire protection criteria, as detailed in Section 2.2.5.

2.2.3. Capacity of heated members

To evaluate the fire behavior of beams and columns, Garlock and Quiel [4] presented two ratios: (1) the axial force ratio defined as the ratio of the analysis axial load to axial yield strength, P/P_y; and (2) the moment ratio defined as the ratio of the analysis moment to the plastic moment capacity, M/M_P.

For non-uniform heating, Garlock and Quiel [4] proposed to discretize a member's cross-section into heated fibers, each of which has uniform temperature and stress. The yield strength, P_y, and plastic moment, M_P, of the unevenly heated members are obtained by summing up the yield strength and plastic moment of each heated fiber, as follows [4]:

$$N_{CL} = \sum_{i=1}^{n} A_i k_{y,\theta i} \sigma_y \tag{2-4}$$

$$M_{CE} = \sum_{i=1}^{n} A_i z_i k_{y,\theta i} \sigma_y \tag{2-5}$$

where N_{CL} and M_{CE} = compression strength and bending strength of the member; A_i = area of each discretized fiber; z_i = distance from plastic neutral axis to the centroid of each fiber; $k_{y,\theta i}$ = yield stress reduction factor computed from the temperature of each fiber; σ_y = yield stress of the steel.

2.2.4. Failure of fire protection

To limit the temperature rise in steel members, fire protection is adhered to the exterior surface of the steel. Many studies [12,13] have shown that extreme loads can cause damage to insulations (e.g., SFRM) via the effect of large strains. It is important because large strains are expected in events related to structural fire and progressive collapse. Once the insulation loses its effectiveness, the temperature in steel members can quickly reach the critical limit (i.e., 500-600°C), resulting in structural collapse.

A study done by Braxtan and Pessiki [12] showed that at large deformation, SFRM could crack or detach from the steel members to accommodate the large strain. Detachment is more prevalent with the dry-mix SFRM while cracking is more prevalent with the wet-mix SFRM. In their experimental tests, wet-mixed SFRM cracked as early as $\varepsilon = 2.4\varepsilon_y$; dry-mixed SFRM detached at $\varepsilon = 3.6\varepsilon_y$ (yielding strain of SFRM $\varepsilon_y = 0.0016$). In another study on crack propagation of fire insulation, done by Arablouei and Kodur [13], the progression of delamination was very rapid, such that for medium density gypsum-based SFRM, delamination was completed within a range as low as steel yield strain ($\varepsilon_y = 0.002$). BS 5950 Handbook [16] shows that there is possibility of cracks and detachment of fire protection in beams at the deflection between span/40 and span/30 or strain exceeding 1.5%.

Additionally, research has shown that extreme events like earthquakes can damage the fire protection system and increase the risk of uncontrollable fire in buildings. The findings can be categorized into damage in active fire protection and damage in passive fire protection, as summarized below:

(1) Active fire protection may be ineffective after earthquake: Discovering fire may be difficult due to panic after an earthquake [17]; structural/non-structural damage can hinder sprinkler systems and firefighting efforts (e.g., damage in fire sprinkler system and fire doors was reported to be over 40% in 1994 Northridge earthquake and 30% in 1995 Kobe earthquake [18]); egress systems may be destroyed (e.g., interior stairs collapsed and impeded safe evacuation in 2010 and 2011 Christchurch earthquakes [19]); the response of fire department may be delayed due to the damage to the station itself or the transportation and communication networks [19].

(2) Passive fire protection is prone to losing its function during earthquake: SFRM is susceptible to cracking, debonding, and spalling under the earthquake loads [20,21]; compartmentation is highly prone to be damaged during earthquakes (e.g., breakage of windows and glass façades was observed in Christchurch earthquake [22], cracking in the concrete slabs, the exterior façade, and the interior partition systems was experienced in the University of California - San Diego shake table experiments [23] of a five-story building). This is important for buildings post-earthquake because the damage in

compartmentation can lead to significant fire spread through compartments and floors, as well as the loss of structural capacity due to ineffective fire insulation can lead to progressive collapse.

2.2.5. Correlation between references

Comparing the acceptance criteria (provided by UFC [1] and ASCE/SEI 41-06 [2]) and fire protection criteria (provided by ASTM E119 [15]), it can be seen that force-controlled actions align well with the stability (or load-bearing capacity) criterion, and deformation-controlled actions align well with the integrity criterion.

The two ratios proposed by Garlock and Quiel [4] (i.e., P/P_y and M/M_P) are similar to the force-controlled actions (i.e., demand over capacity ratio or DCR) of the acceptance criteria. However, DCR of the acceptance criteria is more adequate because it accounts for the combined effect of axial force and moment. The Garlock and Quiel's method of calculating capacity P_y and M_P for non-uniformly heated elements can be integrated into the DCR formula for structures in fire.

Findings on failure of SFRM at high deformation (i.e., strains and deflections) complements the insulation criterion (i.e., to prevent unacceptable rise in temperature at the unexposed surface of structures) of the fire protection criteria. They indicate that the strains developing in structural elements should be limited to avoid damage/failure of fire insulations.

2.3. Method of quantifying structural robustness in fire

The proposed method takes the principles of Fire Protection Criteria and improves it by adding other guideline and research findings accordingly. More specifically, it entails evaluating structures according to three limit states, namely insulation, integrity, and stability, as summarized in Table 2.1 and detailed below.

This method also follows three levels of performance as defined in the Acceptance Criteria. Different performance level (i.e., IO, LS, CP) requires different values for allowable limits (e.g., strain limit, deflection limit). The structure is defined to fail when a large part of the structure reaches the limit state (i.e., insulation, integrity, or stability).

The term “time limit” (or “collapse time”) is used to quantify the structural robustness in fire. Time limit is defined as the maximum duration of ISO 834 standard fire exposure that the structure can withstand before failure. Time limit can be very useful when comparing the robustness of different structures in resistance to fire and progressive collapse. More specifically, the one having longer time limit (i.e., can withstand fire for a longer period of time) is the more robust one (assuming that they are exposed to the same fire scenario).

Table 2.1. *Three criteria for quantifying structural robustness in fire*

Criterion	Purpose	Requirements	Measurements
Insulation	To prevent the failure of fire protection materials	Limit displacements in heated columns and beams: $\Delta \le \Delta_{\lim it}$ ($\Delta_{\lim it}$ depends on types of insulation materials)	- Deflections in beams - Lateral displacements in columns
Integrity	To prevent fire spread from the room of origin => Prevent formation of openings which allow flames and hot gases to pass through	- Limit vertical deflections of slabs: $\Delta \le \Delta_{\lim it}$ ($\Delta_{\lim it}$ depends on performance level; $\Delta_{\lim it} = L_{span}/20$ for LS) - Limit rotations at beam ends $\theta \le \theta_{\lim it}$ ($\theta_{\lim it}$ depends on performance level and beam’s slenderness)	- Deflection of slabs - Rotation at beam ends
Stability	To prevent the loss of load-bearing capacity of structures	Limit Demand over Capacity Ratio: $DCR \le 1$ - Columns: *DCR* combines the effects of axial forces and moments - Beams and connections: DCR takes effect of internal forces separately	- Axial forces and moments in columns - Axial forces, shears, and moments at beam ends (or connections)

There is a different value of time limit associated with each criterion, assuming the two remaining criteria are not violated (i.e., the structural failure associated with other criteria is ignored) at that time. In this dissertation, the denotation is following:

$T_{stability}$ = time limit associated with the stability criterion

$T_{integrity}$ = time limit associated with the integrity criterion

$T_{insulation}$ = time limit associated with the insulation criterion

Then the time limit T of the structure is the minimum of all three values of time limit above, i.e.,

$$T = min\ (T_{stability},\ T_{integrity},\ T_{insulation}) \tag{2-6}$$

2.3.1. Stability criterion

The stability criterion aims to prevent the loss of load-bearing capacity of structure. In other words, the internal force (caused by applied loads and fire) must not exceed the capacity, i.e., Demand over Capacity Ratio (DCR) must not exceed 1. The DCR follow the Acceptance Criteria [2] and Garlock and Quiel's formulae [4] for non-uniformly heated elements, as described below:

For columns, DCR follows the Eqs. (2-1) - (2-3).

For beams and connections,

$$DCR = \frac{P}{P_{CL}} \leq 1.0 \tag{2-7}$$

where P = internal force (i.e., axial force, shear, or moment) in the member due to applied load; P_{CL} = expected capacity (i.e., axial force, shear, or moment) of the member.

In case of non-uniform heating, the cross-section of each member can be discretized into several fibers. The axial force capacity P_{CL} and moment capacity M_{CE} are calculated as the sum of axial force and moment (respectively) of heated fibers [4], as shown in Eqs. (2-4) and (2-5).

The measurement needed for structural assessment includes the internal forces (axial forces and moments) in columns, and internal forces at beam ends (axial forces, shears, and moments). In the structural analysis, a good way to determine the time limit associated with the stability criterion

$T_{stability}$ is to plot the time history of the axial forces and lateral displacements in columns. Column buckling can be noticed by the sudden changes in the axial forces (i.e., a significant decrease up to zero in the axial force of buckled column along with significant increases in the axial forces of the adjacent columns) and the lateral displacements (i.e., a significant increase in the absolute value of displacements in buckled column). Practically, $T_{stability}$ is usually the time when axial forces in columns go to zero. For adequate accuracy, it is recommended to check the DCRs in every minute (of fire exposure) around the time of sudden changes in the axial forces and up to the time that the computational analysis terminates. It is noted that because the capacities of members are dependent on temperature, the capacities of members are different every minute in fire. Generally, $T_{stability}$ determined based on the time history plot of the axial forces in columns is smaller than the time when the DCR exceeds 1. To be conservative, the smaller value is chosen as the time limit associated with the stability criterion.

2.3.2. Integrity criterion

The integrity criterion aims to prevent fire spread from the room of origin by prohibiting the formation of openings that allow hot gases and flames to pass through.

The integrity criterion requires the limiting of the vertical deflections of composite slabs and the rotations at the beam ends (or the rotation at connections). The slab deflection limit aims to prevent fire from traveling vertically from floor to floor. The rotation limit at the beam ends (or connections) aims to prevent fire from traveling laterally from room to room and to avoid connection failure due to large deformation.

Currently, there is no guideline for slab deflection limit in fire condition and further research may be needed to determine the accurate slab deflection limit for preventing vertical fire traveling. In this dissertation context, *L/20* is proposed as the slab deflection limit (where *L* is the span of slab) for Life Safety performance level in fire, based on the deflection limit state of steel beams for fire resistance in BS 5950 [16]. It can be seen that *L/20* is far higher than *L/250* as the slab deflection limit at room temperature for serviceability. The rotation limit at beam ends (or connections) follows the Acceptance Criteria [2], and varies depending on the performance level (i.e., IO, LS, or CP), the beam type (i.e., primary or secondary), and the beam's slenderness. For example, for LS

level and non-slender beams, the rotational limit is $6\theta_y$ (for primary beams) and $9\theta_y$ (for secondary beams), where θ_y is the yield rotation [2].

The measurement needed for structural assessment includes the deflections of slabs, and the rotations at beam ends (or connections). In the structural analysis, a good way to determine the time limit associated with the integrity criterion $T_{integrity}$ is to plot the time history of the maximum deflections of all heated beams and heated slabs. $T_{integrity}$ is the earliest time when a connection's rotation or slab's deflection reaches its corresponding limit.

2.3.3. Insulation criterion

The insulation criterion aims to prevent the failure of fire insulation material, prohibiting the temperatures in heated steel members from exceeding the critical temperatures.

The insulation criterion requires the limiting of strains in heated columns and beams, $\varepsilon \le \varepsilon_{\lim it}$ where $\varepsilon_{\lim it}$ depends on the types of insulation materials in use. It is based on the studies by Braxtan and Pessiki [12] and Arablouei and Kodur [13], as well as BS 5950 Handbook [16]. In computational analysis, the values of strains are significantly dependent on the mesh size and thus they are less reliable than the values of displacements. Therefore, limiting displacements (i.e., deflections in beams and lateral displacements in columns) are used for defining the insulation criterion. According to BS 5950 Handbook [16], the limiting deflection in beams is taken as $L_{span}/40$ (i.e., equivalent to 1.5% strain limit) and the limiting lateral displacement in columns is taken as 120 mm.

The measurement needed for structural assessment includes the deflections of beams and lateral displacements of columns. To determine the time limit associated with the insulation criterion $T_{insulation}$, the first step is to identify the time T_1 when insulation material starts to fail (i.e., deflection of a beam exceeds $L_{span}/40$ or lateral displacements of a column exceeds 120 mm) in the structural analysis. Once the insulation in a steel member fails, the temperature in that member is assumed to be uniform along the length and recalculated by the thermal analysis, where the fire protection is removed at time T_1. Fig. 2.1 illustrates the temperature growth in a steel beam when the insulation fails. Subsequently, the structural analysis is reconducted with the new temperature for

that member. The time when the structural system starts to fail (according to stability and integrity criteria) in the updated structural analysis is the time limit associated with insulation criterion.

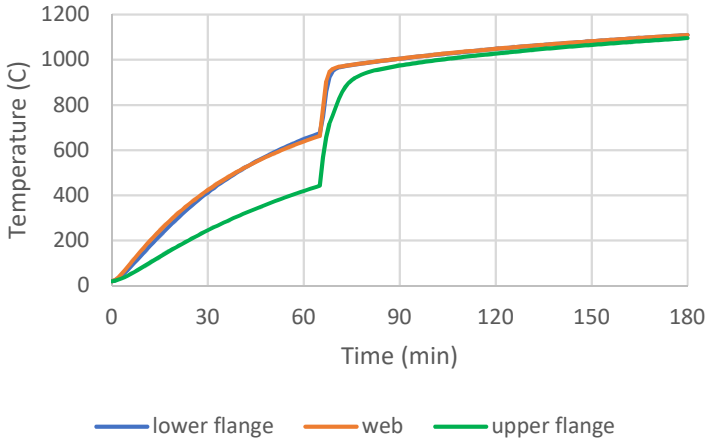

Fig. 2.1. *Temperature in a beam with insulation material failure at 65 min*

2.4. Conclusion and limitations

2.4.1. Conclusions

The proposed method of quantifying the structural robustness in fire of an entire building structure is to check three criteria, i.e, insulation, integrity, and stability. This method complements the existing building codes on structural performance at room temperature including the acceptance criteria [1,2] and the fire protection criteria [15]. The insulation criterion aims to prevent the failure of fire insulation materials and requires the limiting of deflections in beams and lateral displacement in columns. The integrity criterion aims to prevent the spread of fire from the room of origin and requires the limiting of deflections of the slabs and rotations at the connections. The stability criterion aims to prevent the loss of load-bearing capacity of the structure and requires the limiting of internal forces (i.e., $DCR \leq 1$). The limiting values and coefficients associated with these criteria can vary depending on different desired performance level, i.e., immediate occupancy, life safety, or collapse prevention.

The structure is defined to fail when a large part of its reaches the limit state (i.e., insulation, integrity, or stability). To quantify the structural robustness, the term “time limit” is used and defined as the maximum duration of ISO 834 standard fire exposure that the structure can

withstand before failure. Each performance criterion associates with a different time limit (e.g., the time limit associated with stability $T_{stability}$ is determined based on stability criterion only, regardless the insulation and integrity criteria) and the time limit of the structure is the minimum of three values of time limit, i.e., $T = min\ (T_{insulation}, T_{integrity}, T_{stability})$.

2.4.2. Limitations

For the insulation criterion, this study proposed the deflection limit of $L_{span}/40$ for heated beams and lateral displacement limit of 120 mm for heated columns. These values are based on BS 5950 Handbook [16] for steel structures in fire. For better accuracy, it is recommended to conduct experimental tests on the failures of the fire insulation material used in the building or to obtain the information from the manufacturer (if existing). Moreover, this study did not consider other limits which may belong to the insulation criterion such as the story drift (i.e., research on post-earthquake buildings reported the damage of fire protection materials under the extreme lateral loads).

The integrity criterion was proposed to include the limiting of slabs' deflections and connections' rotations. Other factors which can affect the integrity performance such as partition walls and claddings were not considered in this study.

Reference

[1] Unified Facilities Criteria. (2009). “Design of Buildings to Resist Progressive Collapse. Department of Defense.” Washington, D.C.

[2] Standards ASCE/SEI 7. (2013). “Minimum Design Loads for Buildings and Other Structures.” *American Society of Civil Engineers (ASCE).*

[3] Lange, D., Roben, C., Usmani, A. (2012). “Tall Building Collapse Mechanisms initiated by Fire: Mechanisms and Design Methodology.” *Engineering Structures*, 36, 90-103.

[4] Garlock, M., Quiel, S. (2007). “The Behavior of Steel Perimeter Columns in a High-Rise Building under Fire.” Engineering Journal*,* 44(4), 359-372.

[5] Agarwal, A., Varma, A. (2014). “Fire Induced Progressive Collapse of Steel Building Structures: The Role of Interior Gravity Columns.” *Engineering Structures*, *58,* 129-140.

[6] Jiang J., Li G-Q., Usmani A. (2014). “Progressive Collapse Mechanisms of Steel Frames Exposed to Fire.” *Advances in Structural Engineering,* v 17 (3), 381-398.

[7] Bailey, C.G. (2004). “Membrane Action of Slab/Beam Composite Floor Systems in Fire.” *Engineering Structures*, v 26 (12), 1691–1703.

[8] Sun, R., Huang, Z., Burgess, I. W. (2012). “The Collapse Behaviour of Braced Steel Frames Exposed to Fire.” J. Construction Steel Research, v 72, 130-42.

[9] Neal M., Garlock M., Quiel S., Marjanishvili S. (2012). “Effects of Fire on a Tall Steel Building Designed to Resist Progressive Collapse.” *Proc., 2012* Structures Congress*, ASCE, Chicago, IL,* 246-256*.*

[10] Porcari, G. F., Zalok, E., Mekky, W. (2015). Fire Induced Progressive Collapse of Steel Building Structures: A Review of the Mechanisms, *Eng. Struct.*, 261-267.

[11] Bailey, C. G. (2001). “Membrane Action of Unrestrained Lightly Reinforced Concrete Slabs at Large Displacements.” *Engineering Structures*, v 23 (5), 470-483.

[12] Braxtan, N., Pessiki, S. (2011)."Bond Performance of SFRM on Steel Plates Subjected to Tensile Yielding." *J. Fire Protection Engineering,* v 21 (1), 37-55.

[13] Arablouei, A., Kodur, V. (2015). "Critical Factors Governing Crack Propagation at the Interface of Fire Insulation and Slender Steel Trusses." *ASCE J. Structural Engineering,* v 141 (12).

[14] NIST (National Institute of Standards and Technology). (2008). “Final Report on the Collapse of World Trade Center Building 7, NIST NCSTAR 1A.” NIST, Gaithersburg, MD.

[15] ASTM. (2000). “Standard Test Methods for Fire Tests of Building Construction and Materials.” ASTM E119, American Society for Testing and Materials, West Conshohocken, PA.

[16] Lawson, R., Newman, G. (1990). “Fire Resistant Design of Steel Structures - A Handbook to BS 5950: Part 8”. *The Steel Construction Institute*, SCI publication 080.

[17] Scawthorn C., Eidinger J.M., and Schiff A.J., 2005. “Fire following earthquake. Technical Council on Lifeline Earthquake Engineering, Monograph No. 26.” *American Society of Civil Engineers (ASCE)*, Reston, VA.

[18] Sekizawa, A., Ebihara, M., Notake, H. (2003) “Development of Seismic-induced Fire Risk Assessment Method for a Building.” *Proc., International Association of Fire Safety Science 7th International Symposium*, 309-320.

[19] Wilkinson, S., Grant, D., Williams, E., Paganoni, S., Fraser, S., Boon, D., Mason, A. and Free, M. (2013). “Observations and Implications of Damage from the Magnitude 6.3 Christchurch, New Zealand Earthquake of 22 February 2011,” *Bull Earthquake Eng.*, v 11, 107-140. DOI 10.1007/s10518-012-9384-5.

[20] Keller, W., Pessiki, S. (2012) “Effect of Earthquake-induced damage to spray-applied fire-resistive insulation on the response of steel moment-frame beam-column connections during fire exposure.” *J. Fire Protection Engineering*, 22(4), 271-299.

[21] Braxtan, N., Pessiki, S. (2011). “Post-Earthquake Fire Performance of Sprayed Fire-Resistive Material on Steel Moment Frames.” *J. Structural Engineering*, 137(9), 946-953.

[22] Baird, A., Palmero, A., Pampanin, S. (2011). “Facade Damage Assessment of Multi-Story Buildings in the 2011 Christchurch Earthquake.” *Bulletin of the New Zealand Society for earthquake engineering*, special issue 44, number 4. <http://www.nzsee.org.nz/db/SpecialIssue/44(4)0368.pdf> (July 1, 2017)

[23] Meacham B. (2016). “Post-Earthquake Fire Performance of Buildings: Summary of a Large-Scale Experiment and Conceptual Framework for Integrated Performance-Based Seismic and Fire Design.” *Fire Technology*, 52, 1133–1157.

CHAPTER 3. MACRO-ELEMENT MODEL FOR BEAM-TO-COLUMN CONNECTION

Chapter 3 presents a simplified (or macro-element) model for beam-to-column (BC) connection, along with validation against experimental data at room temperature and elevated temperatures. The focus is welded unreinforced flange-bolted web (WUF-B) connections, which is commonly used in seismic building design in the U.S. It addresses the need of developing an accurate model for beam-to-column connections in fire at a reasonable computational cost. The study also seeks to determine whether WUF-B connections can provide adequate strength and ductility to resist progressive collapse in fire. The majority of this chapter was presented in Nguyen et al. [1].

3.1. Introduction

As mentioned in Section 1.1, there is a considerable risk of structural fires and fire-induced progressive collapse in mid- and high-rise buildings, and hence it is necessary to understand structural performance in resistance to fire-induced progressive collapse. Research and experimental tests have suggested the significant contribution of beam-to-column connections to the overall structural robustness, especially in preventing collapse in fire [2-5]. However, BC connections are often ignored in computational analyses, most of which treat them as simple joints (either fully fixed or pinned joints). Several other studies have paid attention to BC connections and use more accurate simulation models including brick-element model and macro-element model. Table 3.1 summarizes these three approaches in terms of the brief description of methodology, advantages and disadvantages (in terms of accuracy, ease of use, and computational cost), and examples of studies that use these approaches.

Table 3.1. *Different approaches of modeling beam-to-column connections*

Approach	Methodology	Advantages	Disadvantages	Study examples
Simple joint model	BC connections are modeled as a fully fixed or pinned joint (i.e., stiffness is either rigid or zero, depending on the direction of restrained disp.)	- Easy and quick to model - Computationally cheap - Reasonably accurate for structural analysis at room temperature	May be inaccurate for structural analysis in fire or complicated loading condition	- Elgazhouli and Izzuddin (2004) [6] - Foster et al. (2007) [7] - Garlock and Quiel (2007) [8] - Quiel and Marjanishvili (2009) [9] - Neal et al. (2012) [10]
3D brick element model	BC connections are modeled exactly as they are in reality; 3D high-resolution finite elements (i.e., brick element) are used to construct the BC connection	- Accurate for structural analysis even in complicated loading conditions - Capable to capture deformations in reality	- Slow and complicated to model - Causing numerical challenges due to contact issues - Computationally expensive	- Sarraj et al. (2007) [11] shear tab connection - Khandelwal and El-Tawil (2007) [12] WUF-B connection - Dai et al. (2010) [13] different connection types - Sadek et al. (2010) [5] WUF-B connection
Macro-element model	BC connections are modeled as a non-linear spring or a system of those; each spring represents a component of the	- Reasonably efficient in modeling - Computationally cost-effective - Reasonably accurate for	- Still complicated to model in 3D large-scale building analysis - Computationally expensive for 3D	- Sarraj's thesis (2007) [14] shear tab connection - Khandelwal et al. (2008) [15] WUF-B connection

	connection with different failure mechanism	structural analysis at room temperature and in fire	large-scale building analysis	- Yu et al. (2009) [16] web cleat connection - Alashker et al. (2011) [17] WUF-B connection - Agarwal and Varma (2014) [18] shear tab connection

Simple joint model is the most common approach thanks to the ease of modeling and computational efficiency. It is reasonably accurate when analyzing building structures at room temperature but not so in fire condition. It is because of the thermal expansion along with material strength degradation of steel elements at elevated temperatures, which result in significant deformations and reduction in capacity and stiffness of BC connections. The assumption to consider BC connections as fully rigid or pinned therefore may be invalid in fire condition. However, in large-scale models especially a 3D analysis of an entire building, simple joint model is still adopted for computational cost reason. Some examples are studies done by Elgazhouli and Izzuddin [6] and Foster et al. [7] simulating a composite floor system subjected to fire.

3D brick element model provides high accuracy at high computational cost. It is usually utilized in research which focuses only on BC connections at a structural component or sub-assembly level; the high computational cost is acceptable given the small scale of structures under study. Some examples are Sarraj et al. [11] on performance of shear tab connection, Khandelwal and El-Tawil [17] on performance of WUF-B connection, Dai et al. (2010) [13] on structural performance of different connection types, and Sadek et al. [5] on a steel sub-assembly using WUF-B connections.

Macro-element model balances out the pros and cons of the other approaches - reasonable accuracy at reasonable computational cost. Sarraj [14] presented a macro-element model for a shear tab (or fin plate) BC connection, based on the failure mechanisms and components of the connection that were observed in experiments and high-resolution FE analyses. The BC connection is in fact a system of non-linear springs, whose stiffness describes the force-deformation behavior of a component of the connection. As described in Fig. 3.1, the connection was represented by a system

of springs: shear tab in bearing, bolt in shear, beam web in bearing, and fin plate - beam web friction. The force-deformation relationship of each spring was determined by form-fitting to the results of experimental tests [14]. The connection model proposed by Sarraj [14] was verified at room temperature and elevated temperatures. This model was also adopted in full-scale 3D analyses done by Agarwal and Varma [18], which simulated a 10-story building against fire-induced progressive collapse. Agarwal and Varma [18] is among very few studies adopting BC connection model in entire building analyses at the full-scale 3D level. The computational cost and numerical challenges when considering BC connections in 3D component-element models were not mentioned in Agarwal and Varma [18].

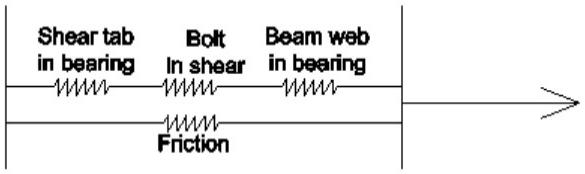

Fig. 3.1. *Sarraj [14] - macro-element model for the fin plate BC connection*

Khandelwal et al. [15] proposed macro-element models for shear and moment BC connections which used bolted fin plates. The majority of this model is similar to that of Sarraj [14] (i.e., a system of springs representing interaction between fin plate - bolt - beam web) but adding a panel zone spring, as shown in Fig. 3.2. Using FE software LS-DYNA with explicit dynamic analyses, Khandelwal et al. [15] also integrated their proposed connection model into 2D frames investigating progressive collapse at room temperature. However, the Khandelwal et al.'s model did not consider the behavior change of BC connection at elevated temperature.

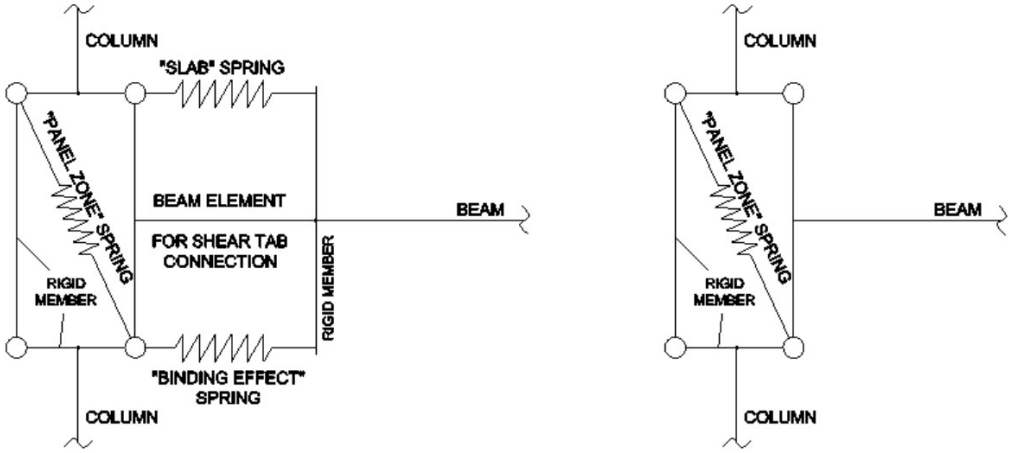

Fig. 3.2. *Khandelwal et al. [14] - macro-element model for shear and moment BC connection*

Yu et al. [16] developed macro-element model for another type of BC connection, the web cleat connection, as shown in Fig. 3.3. Similar to Sarraj [14] and Khandelwal et al. [15], Yu et al. [16] used a system of springs which includes bolt in tension, web cleat, bolt in shear, beam web in bearing, and beam lower flange in contact with column. The most noticeable difference is the introduction of web cleat spring, which is modeled as a system of two cantilever beams; each beam has concentrated forces and forms plastic hinges at both ends [16]. The model proposed by Yu et al. [16] was also verified at room temperature and elevated temperatures.

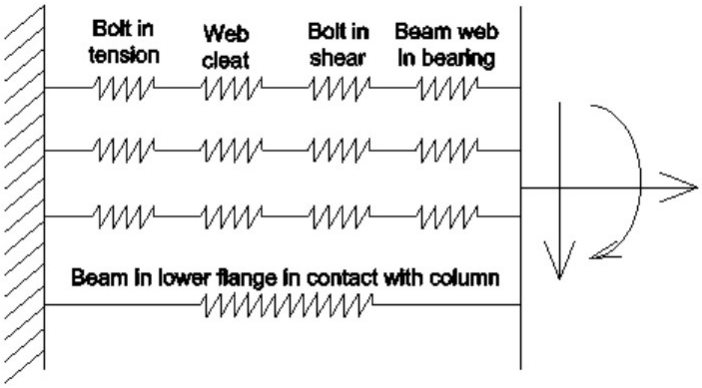

Fig. 3.3. *Yu et al. [16] - macro-element model for web cleat BC connection*

Alashker et al. [17] is another study analyzing an entire building in 3D models with the consideration of BC connections. Alashker et al. [17] developed two types of 3D models: (1) M1 using shell elements for structural components and shear tab BC connections (the shear tab is modeled as a single row of shell elements whose thickness and stress-strain characteristics are derived from the

strength and deformation of the connection), and (2) M2 using beam-column elements (the shear tab is modeled using a single beam element and a binding spring which represents the contact between the beam flange and column flange) [17]. Compared to shell element model, beam-column element model had higher computational efficiency (i.e., M2 ran 230 times faster than M1) [17]. Alashker et al. [17] also argued that the panel zones presented in Khandelwal et al. [15] provided insignificant contribution to the collapse response of the prototype building, and thus panel zone springs were omitted in the Alashker et al.'s model.

In brief, macro-element model is the most appropriate approach of modeling beam-to-column connections at elevated temperature because of its ability to provide accurate prediction at a reasonable computational cost. Several studies have proposed macro-element models for various types of beam-to-column connections, the majority of which have been validated against test data at room temperature. There are very few connection models with validation at elevated temperatures, including Sarraj [14] for shear tab connections, Yu et al. [15] for web cleat connections, and Wang et al. [18] for extended end plate connections.

WUF-B is a common type of BC connections in moderately seismic design and progressive collapse resistant design in the U.S. [5]. Khandelwal et al. [15] and Alashker et al. [17] proposed macro-element models for WUF-B connections at room temperature but there is no model for them at elevated temperatures (or in fire). Furthermore, no studies have assessed its capabilities to redistribute loads in a structure that experiences column loss in fire. To address this issue, this chapter presents a macro-element model for WUF-B connections with validation against test data at room temperature and elevated temperatures. It also investigates the performance of WUF-B connections within a frame subassembly subjected to multi-hazard threats (i.e., column loss and fire). Two scenarios are considered: column loss (e.g., due to blast or impact) followed by fire, and column loss that occurs during fire.

3.2. Model for WUF-B connections

Two types of models are proposed for WUF-B connections, i.e., high-resolution model (i.e., using 3D brick elements) and macro-element model (i.e., using beam-column elements and spring elements). They both use finite element method (i.e., ABAQUS) for analysis. Although the high-resolution model for WUF-B connection is not new in research, its main purpose here is to verify

the accuracy of using ABAQUS for analyzing the connection's performance in extreme loading conditions, and to validate the macro-element model.

3.2.1. High-resolution model

As shown in Fig. 3.4, the WUF-B connection is composed of a shear tab that is welded to the flange of the column and bolted to the web of the beam. To achieve moment resistance, the top and bottom flanges of the beam are welded to the face of the column. Stiffeners are added to the column to prevent distortion at the joint.

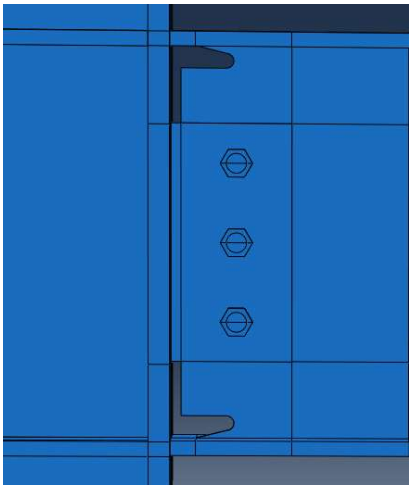

Fig. 3.4. *WUF-B connection*

To model the subassemblies (i.e., beams connecting to columns by WUF-B connections), a high-resolution finite element model was produced in ABAQUS [20] using 3D brick elements with material and geometric nonlinearities. The material properties at elevated temperature were taken from Eurocode 3 [21] with 0.5% strain hardening. The models used true stress and strain defined in the following formulae:

$$\varepsilon_{\text{true}} = \ln\left(1 + \varepsilon_{\text{nominal}}\right) \tag{3-1}$$

$$\sigma_{\text{true}} = \sigma_{\text{nominal}}\left(1 + \varepsilon_{\text{nominal}}\right) \tag{3-2}$$

where σ_{true} and $\varepsilon_{\text{true}}$ are the true stress and strain, and σ_{nominal} and $\varepsilon_{\text{nominal}}$ are the nominal stress and strain.

The WUF-B connection is composed of bolted and welded components. The welds were modeled using tie constraints between the connected components. The interactions between bolted components (i.e., between the bolt and beam web, between the bolt and shear tab, and between the beam web and shear tab) were modeled using interaction elements, which were defined as having "hard" contact in the normal direction and penalty friction with a friction coefficient of 0.3 in the tangential direction.

The multiple contact surfaces posed significant challenges in obtaining a stable solution. Therefore, implicit and explicit models were compared in the validation study. The implicit model required less computational time but artificial damping was needed in order to achieve numerical convergence. The magnitude of artificial damping depends on the structure, the applied load, and the temperature and is determined based on experience and trial-and-error. For preventing spurious structural behaviors due to excessive damping, the artificial damping energy must be checked and ensured that it is less than 10% of the internal energy, according to the suggestion in Dai et al. [13]. On the other hand, the explicit model can simulate the response beyond structural instability. However, explicit models often require significant computational time, depending on the mesh size, the number of elements, and the loading duration. In the explicit model, kinetic energy should not exceed 10% of internal energy for quasi-static procedures [22]. The total duration in the explicit model needed to be long enough to reduce dynamic effects. Here, a duration between 1.0 - 1.1 s was found to be sufficient.

3.2.2. Macro-element model

The macro-element, or component-based, model aims to provide high accuracy and computational efficiency for structural analysis of BC connections. It was introduced and calibrated to the high-resolution model, and then validated against the experimental data at room temperature (i.e., in Sadek et al. [5]) and elevated temperatures (i.e., in Mao et al. [23]). The concept of the macro-element model is to use beam-column elements to model the beams and columns, and a system of springs and rigid links to model the connection between the beam and column, as shown in Fig. 3.5. The spring system accounts for all possible failure mechanisms occurring at the connection, depending on the type of connection. In the WUF-B moment connection, the failure mechanisms consist of plate bearing (shear tab and beam web), bolt shear, friction between shear tab and beam web, and

compressive or tensile failure in the beam flange due to yielding or local buckling. The component model was developed based on the failure mechanisms observed in experimental tests and simulations [5,16,23-24] as well as component-based models for shear connections, as introduced by Sarraj [14] and panel zone spring proposed in Khandelwal et al. [15]. Each spring was modeled as a connector element in ABAQUS with non-linear relationship between force and displacement.

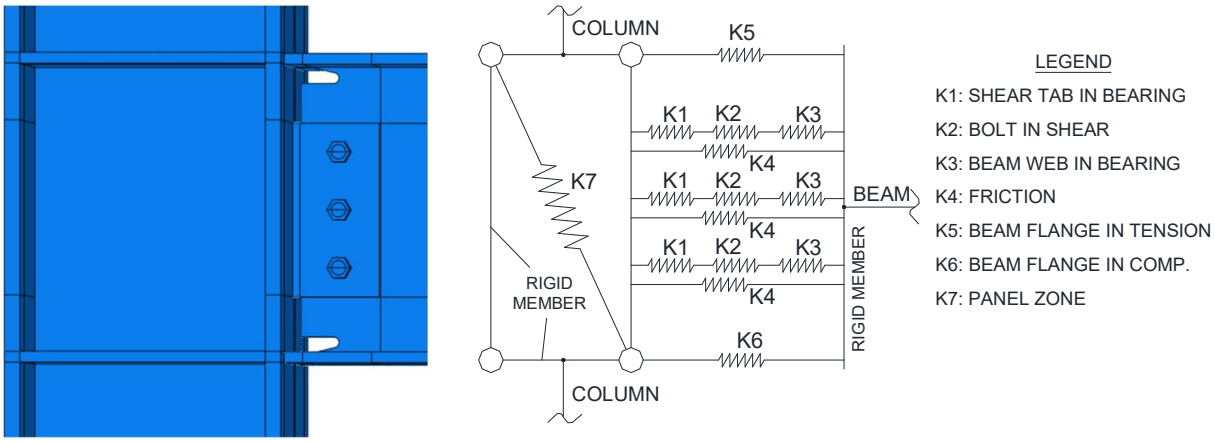

Fig. 3.5. *Macro-element model for the WUF-B connection*

Each bolted component is characterized by a system of series springs (representing the shear tab in bearing, the bolt in shear, and the beam web in bearing) in parallel with a friction spring (representing the contact between the beam web and the shear tab). The equivalent horizontal stiffness of this spring system follows the formulae for springs in parallel and in series:

$$K_e = K_s + K_4 \tag{3-3}$$

where

$$\frac{1}{K_s} = \frac{1}{K_1} + \frac{1}{K_2} + \frac{1}{K_3} \tag{3-4}$$

Here, K_e is the equivalent stiffness of the spring system at one bolt, K_4 is the frictional stiffness, K_1 is the stiffness associated with the shear tab in bearing, K_2 is the stiffness associated with the bolt in shear, K_3 is the stiffness associated with the beam web in bearing.

The equivalent stiffness K_e can also be represented by the relationship in load, F, and displacement, Δ, between the springs, i.e.,

$$F_e = F_s + F_4 \tag{3-5}$$

$$\Delta_e = \Delta_s = \Delta_4 \tag{3-6}$$

where

$$F_s = F_1 = F_2 = F_3 \tag{3-7}$$

$$\Delta_s = \Delta_1 + \Delta_2 + \Delta_3 \tag{3-8}$$

The magnitudes of stiffness K_1, K_2, and K_3 were determined based on the finite element analysis of the lap joint test, as shown in Fig. 3.6. In the lap joint test, one end of the shear tab is fixed and an axial load is applied evenly at the other end of the beam web. The strength of this joint depends on the bearing capacity of shear tab, the shear capacity of bolt, and the bearing capacity of the beam web.

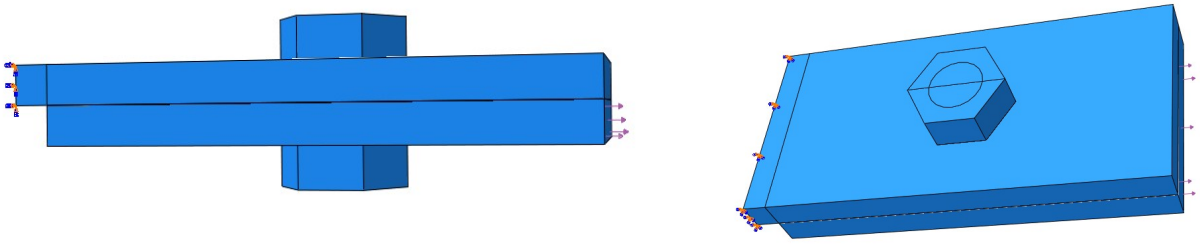

Fig. 3.6. *Lap joint*

The macro-element model adopted the formulas proposed by Sarraj [14] for the axial force-displacement relationships in plate bearing and bolt shear. The formulae were modified here based on calibration to the connections tested by Mao et al. [23]. For a plate in bearing (i.e., K_1 for shear tab in bearing and K_3 for beam web in bearing), the relationship between the bearing displacement, Δ_b (mm), and the bearing force, F_b (N), is as following:

$$\frac{F_b}{F_{b,Rd}} = \frac{\psi \bar{\Delta}}{\left(1 + \bar{\Delta}^{0.5}\right)^{\alpha}} \tag{3-8}$$

where

$$\bar{\Delta} = \frac{\Delta_b K_i}{F_{b,Rd}} = \frac{\Delta_b K_i}{\min\left(e_2, 2.76 d_b\right) f_u t} \tag{3-9}$$

K_i is the initial stiffness (N/mm) which is composed of three parts, i.e.,

$$\frac{1}{K_i} = \frac{1}{K_{br}} + \frac{1}{K_b} + \frac{1}{K_v} \tag{3-10}$$

where

$$K_{br} = \Omega t f_y \left(d_b / 25.4\right)^{0.8} \tag{3-11}$$

$$K_b = 32 E t \left(e_2 / d_b - 0.5\right)^3 \tag{3-12}$$

$$K_v = 6.64 G t \left(e_2 / d_b - 0.5\right) \tag{3-13}$$

Here, $F_{b,Rd}$ is the nominal plate strength; K_{br}, K_b, K_v is the bearing, bending, and shear stiffness; t is the thickness of the plate (mm); E, G, f_y are the Young's modulus, shear modulus, and yield strength of the plate material (N/mm^2); d_b is the diameter of the bolt (mm); e_2 is the distance from the bolt to the end of plate; ψ, α, Ω are temperature-dependent parameters that are determined by calibration to the finite element model of the lap joint test. For the connection studied here, the parameters ψ, α, Ω are shown in Table 3.2.

Table 3.2. *Temperature-dependent parameters for plate in bearing*

Temperature (°C)	ψ	α	Ω
20	1.05	3.00	1000
100	1.05	3.00	1000
200	1.15	3.10	600
300	1.20	3.10	500
400	1.30	3.15	450

500	1.30	3.20	450
550	1.30	3.15	450
600	1.40	3.30	400
650	1.40	3.20	400
700	1.40	3.40	350
800	1.50	3.30	350
900	1.70	3.30	350

For the bolt in shear (i.e., K_2), the relationship between the bolt shear deformation Δ_v (mm) and the shear force F_v (N) is as follows:

$$\Delta_v = \xi \frac{F_v}{K_{v,b}} + \phi \left(\frac{F_v}{F_{v,Rd}} \right)^{\beta} \tag{3-14}$$

$$F_{v,Rd} = 0.6 f_{ub} A_s \tag{3-15}$$

where

$$K_v = 0.15 G A_s / d_b \tag{3-16}$$

Here, f_{ub} is the tensile strength of the material for bolt (N/mm^2); A_s is the nominal unthreaded area of the bolt (mm^2); ξ, ϕ, β are temperature-dependent parameters that are determined by calibration to the finite element model of the lap joint test. For the connection studied here, the parameters ξ, ϕ, β are shown in Table 3.3.

Table 3.3. *Temperature dependent parameters for bolt in shear*

Temperature (°C)	ξ	ϕ	β
20	0.40	0.53	6
100	0.40	0.53	6
200	0.40	0.50	5.5
300	0.40	0.50	5
400	0.40	0.50	4
500	0.40	0.40	4

550	0.40	0.30	4
600	0.35	0.17	4
650	0.35	0.14	4
700	0.35	0.14	4
800	0.35	0.15	4
900	0.35	0.10	4

The nonlinear relationships between force and deformation of the bolted components are shown in Fig. 3.7 for temperatures of 550°C and 650°C.

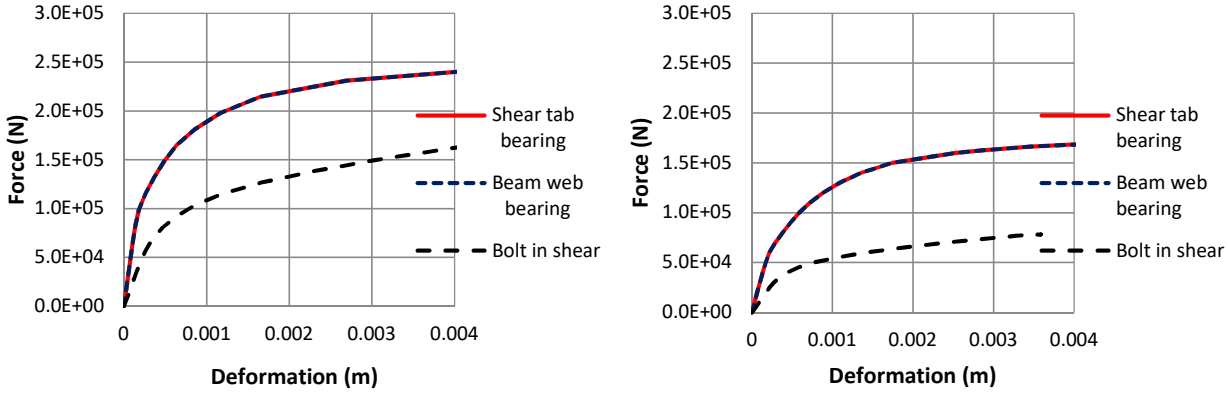

(a) 550℃ *(b) 650°C*

Fig. 3.7. *Force-deformation relationship of the bolt component at 550°C and 650°C*

The force and deformation for beam flange in tension or compression (i.e., K_5 and K_6) is calculated as a plate under axial load, i.e.,

$$F_{bf} = \sigma A_f \tag{3-17}$$

$$\Delta_{bf} = \varepsilon L_f \tag{3-18}$$

where A_f is the area of the flange and L_f is the effective length of the yield zone in the flange. In equations (3-17)-(3-18), the relationship between stress σ and strain ε is dependent on temperature. Here, it is assumed to follow Eurocode 3 [21] for carbon steel at elevated temperature with 0.5% strength hardening.

The effective length of the yield zone depends on whether the beam flange is loaded in tension or compression. For the flange in tension, L_f is taken as the distance from the weld at the face of the column to the centerline of the bolts. For the flange in compression, L_f is based on the model by Yang et al. [25], which involves three stages, namely, the elastic stage, the strain hardening stage, and the local buckling stage. The effective length for the flange in compression during the elastic stage is calculated as

$$L_f = \gamma c + \xi c \tag{3-19}$$

where c is half of the flange width, and γ and ξ are coefficients to determine the dimensions of the yield line and plastic zone [25]. Local buckling was not observed in the finite element model of the WUF-B connection tested by Mao et al. [23]. Therefore, after yielding, strain hardening was assumed to occur until the limit on plastic deformation was achieved. The force-displacement relationship for the beam flange in compression is shown in Fig. 3.8.

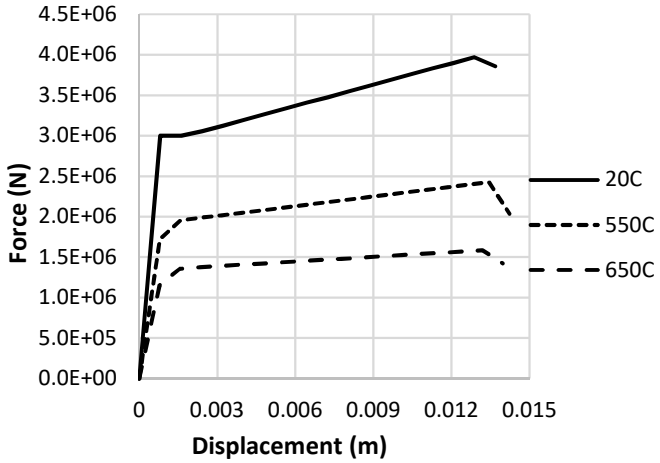

Fig. 3.8. *Force-displacement relationship for beam flange in compression*

The stiffness of springs K_7 follows the panel zone spring proposed in Khandelwal et al. [15] as following:

$$K_7 = K_{pz} = \frac{G\left(d_c - t_{cf}\right)t_{pz}}{\left(d_b - t_{bf}\right)\cos^2\theta} \tag{4-20}$$

$$f_{pz} = \frac{0.6F_y d_c t_{pz}}{\cos\theta}\left(1 + \frac{3b_{cf}t_{cf}^2}{d_b b_c t_{pz}}\right) \tag{4-21}$$

where K_{pz} and f_{pz} = stiffness and strength of panel zone spring; G = shear modulus of steel; F_y = yield strength of steel; t_{pz} = thickness of panel zone; d_b = depth of beam; d_c = depth of column; t_{bf} = thickness of beam flange; b_{cf}, t_{cf} = width and thickness of column flange; θ = angle between panel zone spring and horizontal line. G and F_y vary depending on temperature

In the macro model, it was assumed that the vertical shear deformation of the connection was negligible, which is consistent with the observations in experiments and FE models. The shear behavior was therefore assumed to be rigid.

3.3. Validation

3.3.1. Validation at room temperature

The subassembly tested at NIST by Sadek et al. [5] was simulated to verify the model's capability of simulating the behavior of a subframe undergoing column removal at ambient temperature. The subassembly was taken from an exterior moment-resisting frame in a building designed for seismic category D in the U.S. It consisted of three columns connected with two 6.1-meter-long beams, in which the middle column was removed, as shown in Fig. 3.9. The column removal effect was achieved by applying a vertical load on the middle column, which then redistributed to surrounding beams and columns, eventually leading to collapse. WUF-B connections were used at the joints between the beams and columns. At each connection, the beam web was connected to the shear tab by 25-mm-diameter ASTM A490 bolts, and the shear tab and the beam flanges were welded to the column flange, as shown in Fig. 3.4. ASTM A992 steel was used for all beams and columns while ASTM Grade 36 steel was used for shear tabs and continuity plates.

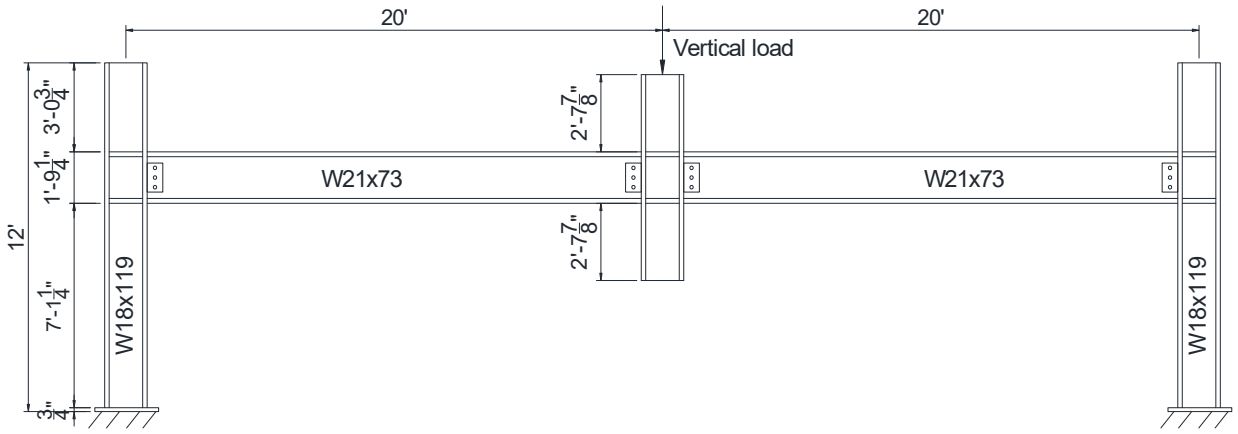

Fig. 3.9. *NIST test set-up (adapted from Sadek et al. [5])*

The high-resolution model described in Section 3.2.1 was used to model the response of the subassembly. The experimentally measured values for the material strengths were used in the model. Implicit and explicit models were run, and it was found that both models provided good agreement with the experimental data, as shown in Fig. 3.10. The implicit model terminated when the deflection reached 270 mm while the explicit model was able to simulate the response beyond 400mm deflection. Both models conservatively predicted the ultimate capacity of the sub-assembly.

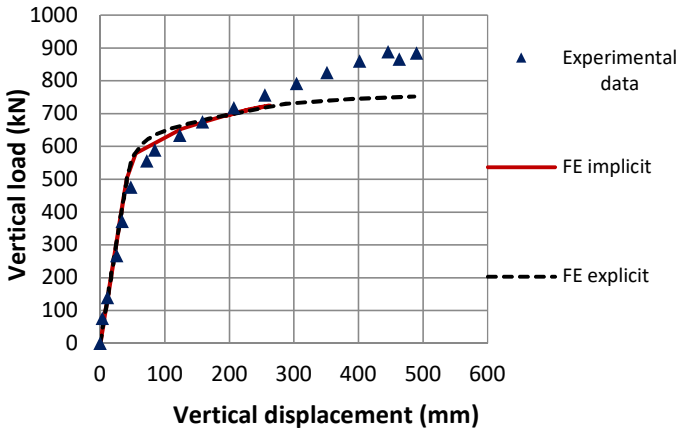

Fig. 3.10. *NIST test at ambient temperature*

3.3.2. Validation at elevated temperature

The subassembly tested by Mao et al. [23] was simulated to validate the high-resolution finite element model of the WUF-B connections at elevated temperature. The data by Mao et al. also provided a means for validating the component model described in Section 3.2.2. Figure 3.11 shows the subassembly, which consisted of a 4.35m column (H600x600x25x36) and a 3.1m beam (H600x300x12x25). The beam flanges were welded to the column flange and the beam web was connected through a bolted shear tab connection, as illustrated in Fig. 3.11. Five M22 F10T bolts were used. The rest of steel was ASTM A572 Gr.50. Three different cases were tested: (1) fixed temperature at 550°C and increasing load, (2) fixed temperature at 650°C and increasing load, and (3) constant load under the ISO 834 standard fire. In tests (1) and (2) the beam was loaded until failure while in test (3) a load of 34 tons was applied and kept constant during the entire test.

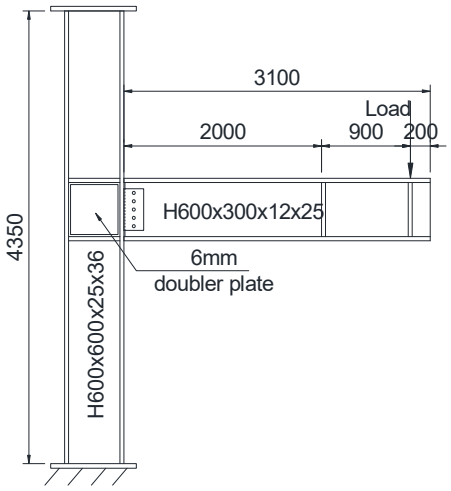

Fig. 3.11. *Setup for the Mao et al. tests (adapted from Mao et al. [23])*

The high-resolution model described in Section 3.2.1 was used to model the response of the subassembly. The relationship between the applied load and vertical displacement at the beam end is shown in Fig. 3.12 for the constant temperature tests. Furthermore, the displacement is plotted against temperature in Fig. 3.13 for the ISO 834 fire. It can be seen that the high-resolution model matches well with the experimental tests, with errors being conservative. This demonstrates that the Eurocode model for the material properties provides acceptable accuracy and that the assumptions embedded in the finite element model are accurate.

The macro-element model from Section 3.2.2 was developed where spring components were calibrated to high-resolution models of the WUF-B connection in Mao et al. Figures 3.12-3.13 show the results of the subassembly model utilizing beam-column elements for the beam and column and the macro-element model for the BC connection. It can be seen that the macro element model matches well with the high-resolution model's results and test data. This illustrates that the macro-element model is capable of simulating the response of WUF-B connections under fire. For more accurate conclusions, further work is recommended to fully validate the macro-element model, as the amount of experimental data is limited.

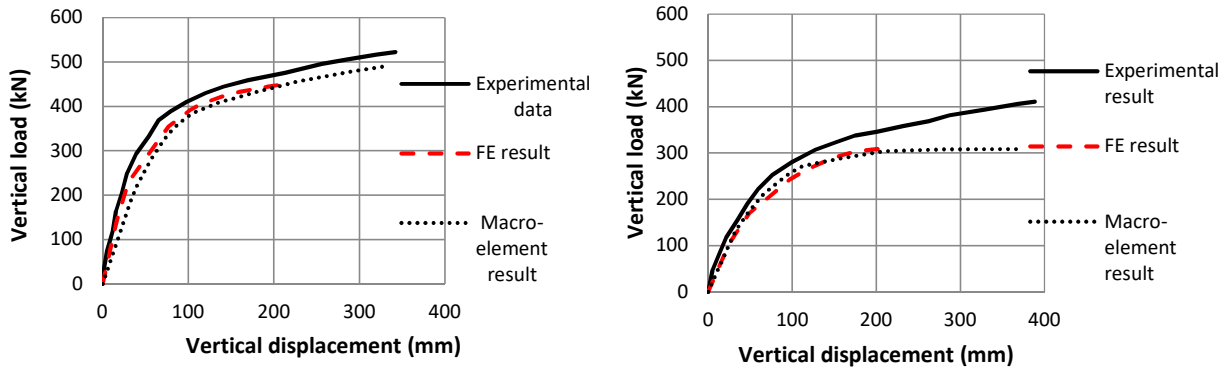

(a) *(b)*

Fig. 3.12. *Mao et al. test at constant temperature (a) at 550°C and (b) at 650°C*

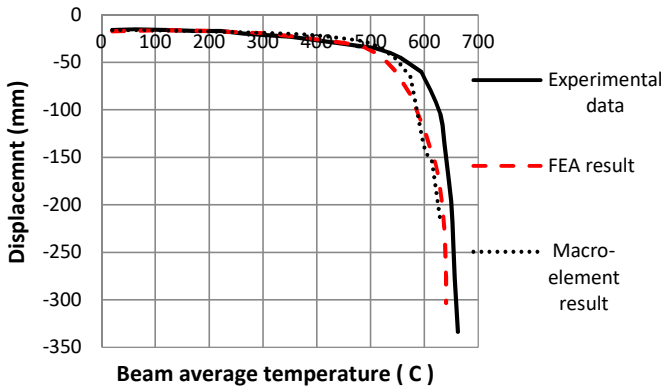

Fig. 3.13. *Mao et al. result in ISO 834 standard fire test.*

3.4. Column loss scenarios

The geometry of the frame shown in Fig. 3.9 was used as the basis for a numerical study into the collapse resistance of moment frames with WUF-B connections. The goal of the study was to evaluate the ability of the frame to redistribute loads at elevated temperatures, providing a means to resist fire-induced progressive collapse in the event of column loss. The study considered two cases of multi-hazard threats: (1) fixed load and increasing temperature, representing fire after column loss (e.g., due to blast or impact); and (2) fixed temperature and increasing load, representing the column loss during fire exposure.

3.4.1. Case 1: Fire following column loss (blast/impact scenario)

For the fixed load and increasing temperature case, the beams were protected for a one-hour fire resistance rating according to the ISO 834 standard, the columns were protected for a two-hour fire resistance rating, and a 200mm concrete slab was placed on top of the beam to simulate the heat sink effect of the slab. A heat transfer analysis was performed to determine the transient temperature distributions in the structure due to convection and radiation heat transfer associated with the standard fire exposure. Parameters for the heat transfer analysis were based on the Eurocode 1 [26] recommended values. The temperatures were inputted to the structural model as a predefined field, and the structural analysis was subsequently performed. Due to the long duration of heating, an implicit analysis with artificial damping was carried out. The modeling assumptions in Section 3.2 were used.

The load was applied to the center column and maintained until failure of the structural system. The magnitude of the load was varied between 0.3 and 0.6 of the ultimate load-bearing capacity of the subassembly at ambient temperature. It can be seen in the deflection-time plot (i.e., Fig. 3.14) that the frame has a shorter period of fire resistance with a larger ratio of applied load. At 0.3*P*, the frame is capable of withstanding fire for 100 min whereas at 0.6*P*, the frame is capable of withstanding fire for 40 min. This demonstrates that the system is capable of transferring load to adjacent columns at elevated temperature, provided the connections are designed to transfer the load at ambient temperature and the system is adequately protected against fire.

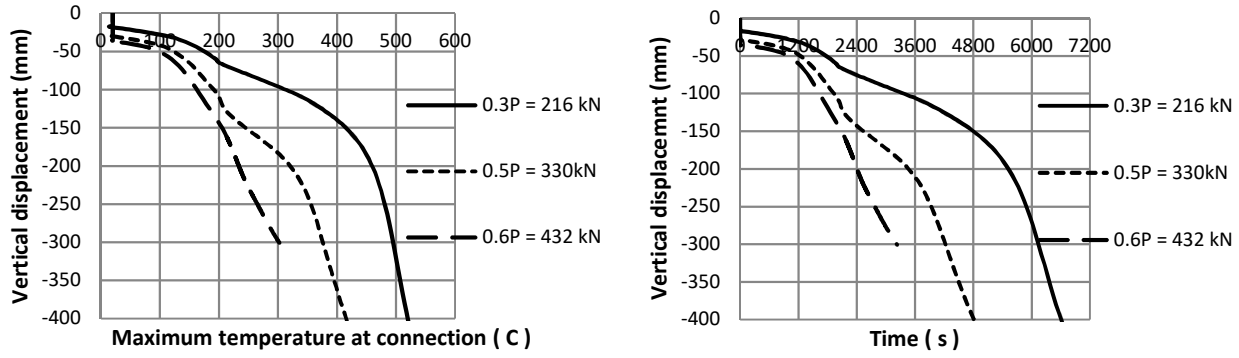

Fig. 3.14. *NIST test in fixed load - increasing temperature scenario*

3.4.2. Case 2: Column loss during fire

To simulate column loss during fire and to gain a better understanding of the mechanics of the subassembly at elevated temperature, the temperature was fixed while the load was increased to failure. The geometry was taken from Sadek et al. [5] and nominal strengths for the materials were used instead of experimentally measured values to provide generalized conclusions. Temperatures of 20°C, 400°C, 500°C, and 600°C were considered. Fracture was not explicitly simulated in the model. However, for the interpretation of the failure mechanisms of the subassembly, fracture was assumed to occur when the strain exceeded 2%.

Figure 3.15 shows the strain and stress contours for the subassembly at room temperature. The strain distribution is plotted in Fig. 3.15a, where gray color represents the regions with strain beyond 2%. The stress distribution is plotted in Fig. 3.15b. It can be seen that the subassembly fails at the connection. As reported by Sadek et al. [5], yielding and local buckling initiated in the top (compression) flange of the beam, followed by shearing of the bolts, and finally tensile fracture of the bottom flange at the central connection in the original experiment. Here, we are using nominal strengths of the materials rather than experimentally measured values. Therefore, the model predicts that yielding and local buckling initiate in the top flange, followed by fracture of the shear tab, and finally tensile fracture of the bottom flange. The same failure mechanism occurs at 400°C. At 500°C and 600°C, the connection fails by yielding and local buckling initiated in the top (compression) flange of the beam, followed by shearing of the bolts, and finally tensile fracture of the bottom flange. Thus, at 500°C and 600°C, shearing of the bolts occurs prior to fracture of the shear tab due to the degradation of strength at elevated temperature.

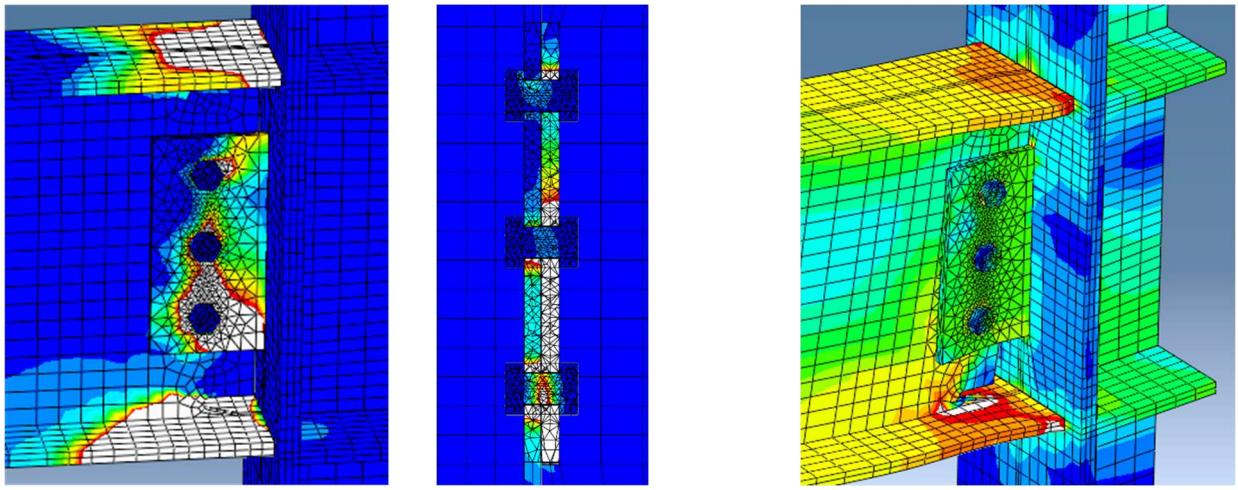

(a) Strain (grey color indicates $\varepsilon \geq 0.02$) *(b) Mises stresses*

Fig. 3.15. *Connection failure at 20°C*
Failure by local buckling in the compression (top) flange, fracture of the shear tab, and fracture in the tension (bottom) flange

A parametric study was performed to investigate the influence of various components on the connection's behavior. The parameters varied in the study are summarized in Table 3.4. Case 1 is the control case, in which the parameters were taken from Sadek et al. In Case 2, the thickness of the shear tab is increased. Case 3 considers a larger beam size. In Case 4, a strength of 450MPa is assumed for the beam. Cases 5 and 6 consider bolts that are have higher and lower strengths than the original strength of the bolts.

Table 3.4. *Parametric study*

Case	Shear tab thickness	Beam web thickness	Beam flange thickness	Beam material (A992)	Bolt material (A490)
1	12.7 mm (1/2")	11.6 mm (W21x73)	18.8 mm (W21x73)	345 MPa (50 ksi)	827 MPa (120 ksi)
2	**9.5 mm (3/8")**	11.6 mm (W21x73)	18.8 mm (W21x73)	345 MPa (50 ksi)	827 MPa (120 ksi)
4	12.7 mm (1/2")	**13.1 mm (W21x83)**	**21.2 mm (W21x83)**	345 MPa (50 ksi)	827 MPa (120 ksi)
5	12.7 mm (1/2")	11.6 mm (W21x73)	18.8 mm (W21x73)	**450 MPa (65 ksi)**	827 MPa (120 ksi)
6	12.7 mm (1/2")	11.6 mm (W21x73)	18.8 mm (W21x73)	345 MPa (50 ksi)	**950 MPa (138 ksi)**
7	12.7 mm (1/2")	11.6 mm (W21x73)	18.8 mm (W21x73)	345 MPa (50 ksi)	**586 MPa (85 ksi) A325**

In all cases, tensile fracture of the bottom flange of the beam at the central column was the dominant failure mode. Local buckling in the top flange occurred in all cases. Variations in parameters resulted in intermediate failures that consisted of fracture of the shear tab (as illustrated in Fig. 3.15), shearing of the bolts (as illustrated in Fig. 3.16), or bearing in the shear tab or beam web. Table 3.5 summarizes the intermediate failure mechanisms in different cases.

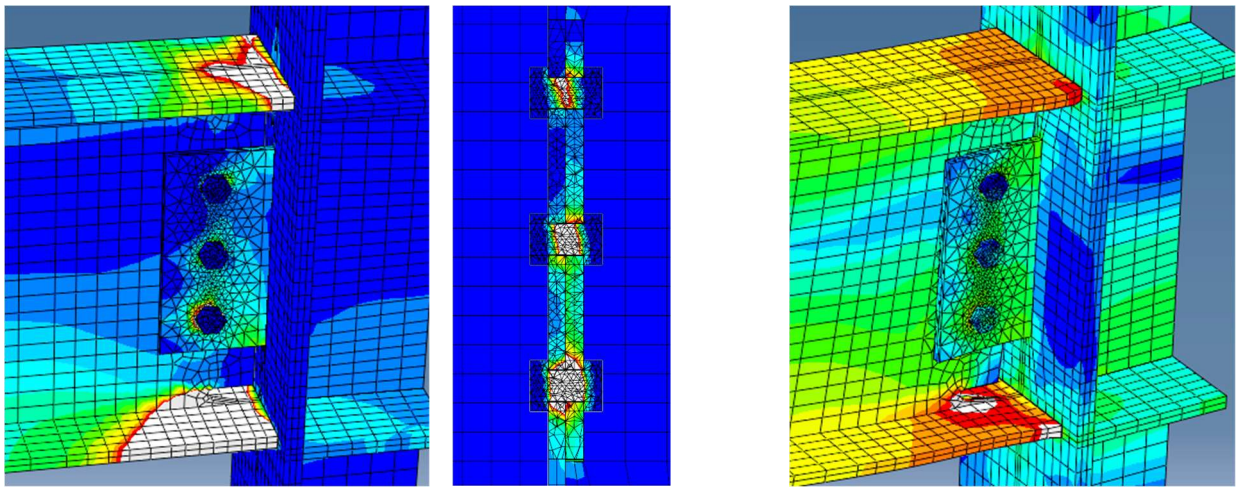

(a) Strain contour (grey color indicated $\varepsilon \geq 0.02$) *(b) Stress contour*

Fig. 3.16. *Case 7 - connection at 600°C*
Failure by local buckling in the compression (top) flange, shearing of the bolts, and fracture in the tension (bottom) flange

Table 3.5. *Intermediate failure mechanisms*

Case	Description	Temp. (°C)	Intermediate Failure Mechanism
1	Control case	20	Fracture of shear tab
		400	Fracture of shear tab
		500	Shear of 2 bolts
		600	Shear of 2 bolts
2	Thicker shear tab	20	Bearing of beam web
		400	Bearing of beam web
		500	Bearing of beam web
		600	Shear of 3 bolts
3		20	Fracture of shear tab

	Larger beam size	400	Fracture of shear tab
		500	Fracture of shear tab
		600	Shear of 3 bolts
4	Higher-strength beam	20	Fracture of shear tab
		400	Fracture of shear tab
		500	Fracture of shear tab
		600	Shear of 3 bolts
5	Higher-strength bolts	20	Fracture of shear tab
		400	Fracture of shear tab
		500	Bearing of shear tab
		600	Shear of 3 bolts
6	Lower-strength bolts	20	Shear of 2 bolts
		400	Shear of 2 bolts
		500	Shear of 3 bolts
		600	Shear of 3 bolts

The capacity of the sub-assembly in each case was also compared with that in the original case (Case 1) to study the influence of different parameters on the ultimate strength of the structure. Figures 3.17-3.21 show the load-displacement relationships at various temperatures for each of the parameters considered. Major findings can be concluded as follows:

- Increasing the thickness of the shear tab had a negligible effect on the capacity of the connection, as shown in Fig. 3.17 - comparison between Case 2 (thicker shear tab) and Case 1. This is because the response is dominated by yielding and fracture in the beam flanges.

- Increasing the dimensions of the beam increased the capacity of the connection, as shown in Fig. 3.18 - comparison between Case 3 (larger beam size) and Case 1. The possible reason is that the capacity of the connection was largely dependent on the strength of the beam flanges.

- Increasing the yield strength of the beam also greatly influenced the capacity, as shown in Fig. 3.19 - comparison between Case 4 (higher strength beam) and Case 1. It is because the capacity of the connection was largely dependent on the strength of the beam flanges.

- Increasing the strength of the bolts had no effect on the capacity of the connection, as shown in Fig. 3.20 - comparison between Case 5 (higher strength bolts) and Case 1. This is because the intermediate failure of the connection was due to fracture of the shear tab and not the shearing of the bolts. For this reason, another investigation (Case 6) was conducted to determine whether use of lower strength bolts influenced the capacity of the connection.

- Reducing the strength of the bolts changed the intermediate failure mode (from bearing in shear tab to shear in bolt) but did not change the overall capacity of the connection, as shown in Fig. 3.21 - comparison between Case 6 (lower strength bolt) and Case 1. This indicates a potential of utilizing lower strength bolts to reduce cost without compromising the capacity of the connections.

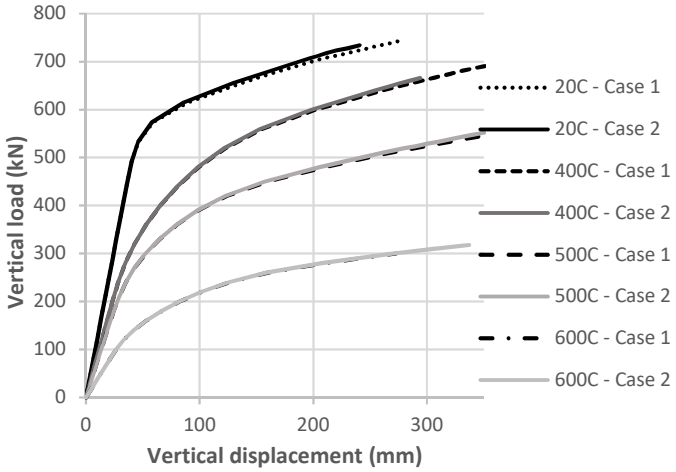

Fig. 3.17. *Load - displacement relationship in Case 2 (thicker shear tabs)*

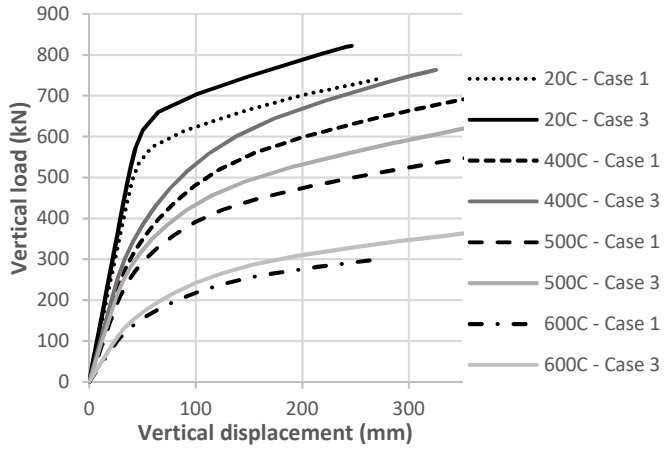

Fig. 3.18. *Load - displacement relationship in Case 3 (larger beam size)*

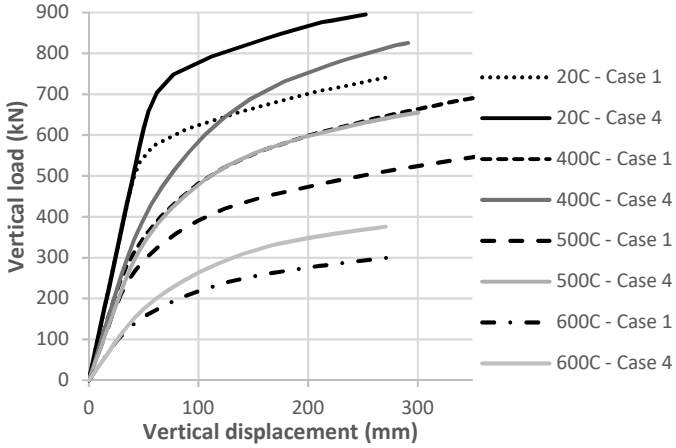

Fig. 3.19. *Load - displacement relationship in Case 4 (higher strength beam)*

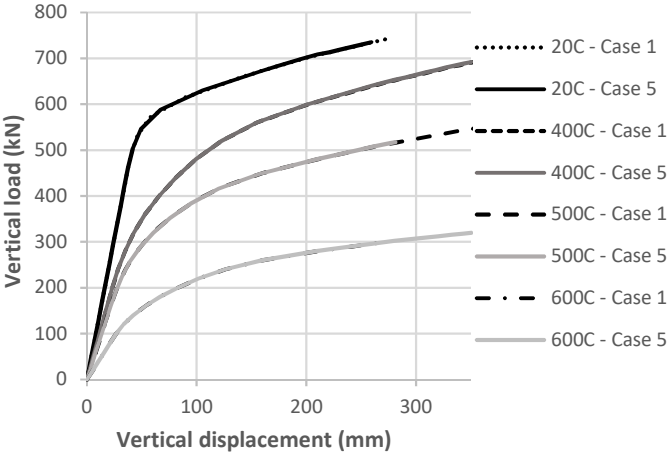

Fig. 3.20. *Load - displacement relationship in Case 5 (higher-strength bolts)*

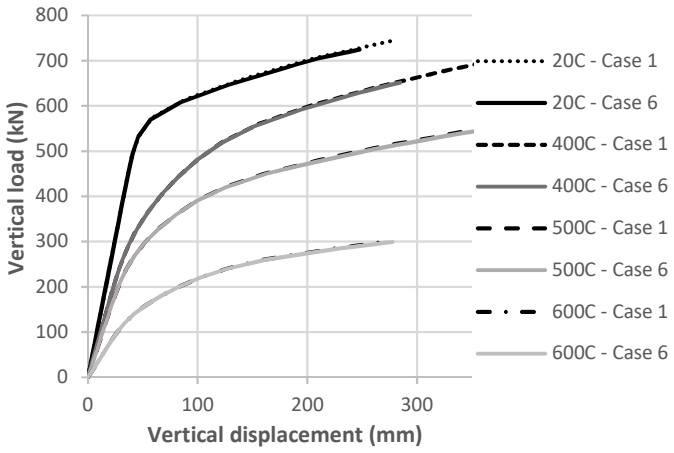

Fig. 3.21. *Load - displacement relationship in Case 6 (lower-strength bolts)*

3.5. Conclusions

This chapter proposes a macro-element model for WUF-B connections in order to provide an efficient and accurate means for analyzing large-scale structures under multi-hazard scenarios involving fire. The model was successfully validated against the high-resolution model and test data at room temperature and elevated temperatures. The model was then utilized to investigate the high-temperature response of steel frame subassemblies that use WUF-B connections. The goal is to determine the capabilities of the moment frame to redistribute loads during fire in the event of column loss, which may occur due to impact, blast, or fire. Two analysis approaches (i.e., explicit and implicit analysis) were adopted and it was found that both approaches provided good agreement. Explicit models offer improved stability in the simulation of structures under fixed-temperature increased-load (e.g., column loss during fire), whereas implicit models offer efficiency in analyzing structures under fixed-load increased-temperature (e.g., column loss followed by fire).

The failure mechanisms of WUF-B connections at elevated temperature are similar to the response at ambient temperature. Failure initiates with yielding and/or local buckling in the compression flange; followed by fracture of the shear tab, shearing of the bolts, or bearing in the shear tab or beam web; followed by fracture of the tension flange. The intermediate failure depends on the geometry and material strengths of the components in the connection. Because the response is dominated by fracture of the tension flange, the capacity of the connection was significantly influenced by the size and strength of the beam. Considering only failure due to column loss under

fire, cost-savings may be achieved with the use of lower strength bolts. Weld fracture was not considered, which is consistent with the findings of Sadek et al. [4] and Mao et al. [22].

The research demonstrates that WUF-B connections may provide suitable robustness against fire-induced progressive collapse, as the connections are capable of transferring the load in the situation of column loss at extreme temperature. However, it is important that the connections are properly detailed and that the members are adequately protected against fire.

There are several limitations to the study presented herein. Additional experimental research is recommended to verify the findings of this research because there is presently limited data regarding the performance of WUF-B connections under fire, particularly concerning the redistribution of forces under column loss. The models presented here did not consider high-temperature creep, which may have influence on the response of steel structures under long duration fires. The research also did not take into account the integrity of the fireproofing. Because deformations were found to be large, it is important for future research to ensure that fire protection materials maintain integrity under large deformations and under potential dynamic effects that may exist in a frame experiencing sudden loss of a column (e.g., due to blast or impact).

The model considered yielding but no local buckling in the compression flange of the beam. Local buckling in the compression flange was not observed in the experimental tests by Mao et al. [23] but in some simulations of WUF-B connections detailed to U.S. standards. Thus, the component model should be extended to include local buckling in the compression flange. The model also did not consider vertical shear deformation.

Reference

[1] Nguyen, H., Jeffers, A., Kodur, V. (2015). "Computational Simulation of Steel Moment Frame to Resist Progressive Collapse in Fire." *J. Structural Fire Engineering*, v 7 (4), 286-305.

[2] Burgess, I., Davison, J. (2012). "Briefing: Role of Connections in Preventing Steel Frame Collapse in Fire." *Engineering and Computational Mechanics, Proc. the Institution of Civil Engineers*, v 165, Iss. EM4, 219-221.

[3] Bailey, C. G., Lennon, T., Moore, D. B. (1999). "the Behavior of Full-Scale Steel-Framed Buildings Subjected to Compartment Fires." *The Structural Engineer*, v 77 (8), 15-21.

[4] Wald, F., Silva, L., Moore, D., Lennon, T., Chladna, M., Santiago, A., Benes, M., Borges, L. (2006). "Experimental Behavior of a Steel Structure under Natural Fire." *Fire Safety Journal*, 41, 509-522.

[5] Sadek, F., Main, J., Lew, H., Robert, S., Chiarito, V., El-Tawil, S. (2010). "An Experimental and Computational Study of Steel Moment Connections under a Column Removal Scenario." NIST Technical Note 1669, *National Institute of Standards and Technology*, Gaithersburg, MD.

[6] Elghazouli, A., Izzuddin, B. (2004). "Realistic Modeling of Composite and Reinforced Concrete Floor Slabs under Extreme Loading. II: Verification and Application" *J. Structural Engineering*, v 130 (12), 1985-1996.

[7] Foster., S., Chladna, M., Hsieh, C., Burgess, I., Plank, R. (2007). "Thermal and Structural Behavior of a Full-scale Composite Building Subject to a Severe Compartment Fire." *Fire Safety Journal*, v 42, 183-199.

[8] Garlock, M., Quiel, S. (2007). The Behavior of Steel Perimeter Columns in a High-Rise Building under Fire, Eng. J. AISC, 359-372.

[9] Quiel, S., Marjanishvili, S. (2012). Fire Resistance of a Damaged Steel Building Frame Designed to Resist Progressive Collapse, J. Perform. Constr. Fac., 26, 402-409.

[10] Neal, M., Garlock, M., Quiel, S., Marjanishvili, S. (2012). Effects of Fire on a Tall Steel Building Designed to Resist Progressive Collapse, *ASCE* Structures Congress, Chicago, IL.

[11] Sarraj, M., Burgess, I.W., Davidson, J.B., Plank, R.J. (2007). "Finite Element Modeling of Steel Fin Plate Connections in Fire." *Fire Safety Journal*, v 42, 408-415.

[12] Khandelwal, K., El-Tawil, S. (2007). "Collapse Behavior of Steel Special Moment Resisting Frame Connections." *ASCE J. Structural Engineering*, v 133 (5), 646-655

[13] Dai, X.H., Wang, Y.C., Bailey. C.G. (2010). "Numerical Modeling of Structural Fire Behavior of Restrained Steel Beam-column Assemblies Using Typical Joint Types." *Engineering Structures*, v 32, 2337-2351.

[14] Sarraj, M. (2007). The Behavior of Steel Fin Plate Connection in Fire, Ph.D. Thesis, Department of Civil and Structural Engineering, *University of Sheffield*, UK.

[15] Khandelwal K., El-Tawil S., Kunnath S., Lew H. (2008). "Macromodel-Based Simulation of Progressive Collapse: Steel Frame Structures." *Structural Engineering*, 134(7), 1070-1078.

[16] Yu, H., Burgess, I.W., Davidson, J.B., Plank, R.J (2009). "Tying Capacity of Web Cleat Connections in Fire, Part 2: Development of Component-based Model." *Engineering Structures*, v 31, 697-708.

[17] Alashker, Y., Li H., El-Tawil S. (2011). "Approximations in Progressive Collapse Modelling." *Structural Engineering*, v 137 (9), 914-924.

[18] Agarwal, A., Varma, A. (2014). "Fire Induced Progressive Collapse of Steel Building Structures: The Role of Interior Gravity Columns." *Engineering Structures*, v 58, 129-140.

[19] Wang, W., Li, G., Dong, Y. (2007). "Experimental Study and Spring-Component Modelling of Extended End-Plate Joints in Fire." *J. Constructional Steel Research*, v 63, 1127-1137.

[20] ABAQUS, v. 6.11 (2011). *Dassault Systemes*, Providence, RI.

[21] Eurocode 3 (2005). "Design of Steel Structures, Part 1.2: General Rules for Structural Fire Design." *Commission of European Communities*, Brussels.

[22] ABAQUS Analysis User's Manual version 6.12. (2014). *ABAQUS Inc.*

[23] Mao, C., Chiou, Y., Hsiao, P., Ho, M. (2009). "Fire Response of Steel Semi-Rigid Beam-Column Moment Connections." *J. Constructional Steel Research*, v 65, 1290-1303.

[24] Yang, K-C., Chen, S-J., Ho, M-C. (2009). "Behavior of Beam-to-Column Moment Connections under Fire Load." *J. Constructional Steel Research*, 65, 1520-1527.

[25] Yang, B., Tan, K., Xiong, J. (2015). "Behaviour of Composite Beam–Column Joints under a Middle-Column-Removal Scenario: Component-based Modelling." *J. Constructional Steel Research*, 104, 137-154.

[26] Eurocode 1. (2002). "Actions on Structures, Part 1-2: General Actions - Actions on Structures Exposed to Fire." Commission of European Communities, Brussels, Belgium.

CHAPTER 4. 2D ANALYSIS FOR MOMENT-RESISTING FRAME IN FIRE-INDUCED PROGRESSIVE COLLAPSE

Chapter 4 presents 2D analyses of moment resisting frames in resistance to fire-induced progressive collapse. It provides insights into the failure mechanisms, the critical fire case for progressive collapse design, and an estimate of the time limit of the structure in various fire scenarios. The three criteria for quantifying structural robustness (described in Chapter 2) were applied to evaluate the performance of a 2D moment frame. The 2D analyses also adopted the macro-element connection model (presented in Chapter 3) to ensure an accurate prediction at a reasonable computational cost.

4.1. Introduction

4.1.1. Research background

As described in Section 1.1, multiple studies on structural performance in fire have proved the cause-effect relationship between long duration fires and progressive collapse. More specifically, during a long fire, significant thermal expansion followed by sudden contraction of the heated floor system during fire can produce significant lateral deflections in columns, which can then lead to global collapse of the building. Examples of those studies are Lange et al. [1] (i.e., a 12-story steel building subjected to fire on three consecutive floors), Garlock and Quiel [2] (i.e., a 38-story steel building exposed to a vertically developing fire), and Agarwal and Varma [3] (i.e., two 10-story buildings subjected to corner fires on the fifth floor). Therefore, when designing medium- and high-rise buildings, there is a need to understand structures subjected to the loss of a column during fire, which could lead to disproportionate collapse.

Progressive collapse at room temperature has long been studied in scientific research and has been adopted in design guidelines [4-6]. In the United States, guidelines for progressive collapse resistant design at room temperature are provided by the General Service Administration (GSA) [5] and the Unified Facility Criteria (UFC) [6]. Among the two approaches, namely Direct Design (e.g., Alternate Path method) and Indirect Design (e.g., Tie Forces method), research mostly focuses on the Alternate Path method with the column removal scenario. In this method, the structure is required to bridge the loss of a column by redistributing the load to the surrounding elements. Sadek et al. [7] carried out an experiment and structural analysis of a steel sub-assembly where the middle column was removed at room temperature. Both the experiment and FE analysis found that the sub-assembly failed around the region of beam-to-column connection, and the failure mechanisms of the connection included shear failure of bolts, bearing failure of shear tab and beam web, and tension failure of beam flange [7]. A larger scale FE analysis was presented in Khandelwal et al. [8], where 2D ten-story steel frames experienced a sudden loss of an interior column on the first floor. With FE analyses of two types of structure, i.e., intermediate moment frame (IMF) and special moment frame (SMF), Khandelwal et al. [8] found that catenary action developed in the gravity bay after large deformation occurred, providing additional resistance against progressive collapse. SMF was also found to be more robust against progressive collapse than IMF because of its higher stiffness (i.e., having more moment connections and fewer shear connections) [8]. Alashker et al. [9] studied progressive collapse at a higher level of complication, i.e., 3D FE analyses of a ten-story composite building subjected to the loss of a perimeter column. Compared to the 2D model, the 3D model was more realistic because of capturing the effect of composite floors; the 3D model tended to predict a potential of system-wide collapse while the 2D model tended to localize the collapse [9]. The slab also reduced the deformations and redistributed load from the removed column to the adjacent columns [9].

Despite being thoroughly studied and understood at room temperature, the threat of progressive collapse at elevated temperature (e.g., in fire) has been far less investigated in research and is not addressed in design guidelines. Some recent research has addressed this issue by studying fire-induced collapse mechanisms and the effect of different factors on the structural behavior. Porcari et al. [10] summarized recent findings on the mechanisms related to fire-induced progressive collapse, including the effect of restraint, stiffness, and bracing. Some highlights are: (1) local yielding and buckling of structural members during fire can improve the overall resistance to

progressive collapse in fire; (2) catenary forces in composite floor system cause the columns to lose lateral supports, which may initiate progressive collapse; (3) larger cross section members are better at resisting failure than the smaller/slender one; (4) beam-to-column connections should be particularly considered to ensure an adequate ability of load redistribution; (5) braced frames are more resilient against progressive collapse and a combination of hat truss bracing system and vertical bracing system can be the most effective in mitigating progressive collapse [16]. On the other hand, when analyzing a ten-story building subjected to corner fire, Agarwal and Varma [9] found that reinforcement in the floor system could help to evenly redistribute the load from the removed column to the adjacent columns, improving the resistance against fire-induced progressive collapse. Jiang et al. [11] studied mechanisms of fire-induced progressive collapse using OpenSees, an open-source FE software for seismic analysis. It was found that the collapse is mostly triggered by the buckling of the heated columns, and significantly affected by the thermal expansion (at early heating stage) and catenary action (at high temperature) of heated beams [11]. Another conclusion is that the common collapse modes were the lateral drift of the frames above the heated floor in association with the downward collapse of frames on the heated floor [11].

Quiel and Marjanishvili [12] studied fire following an extreme event (i.e., blast or impact) that causes failure of a perimeter column in a steel building frame. Using SAFIR software with 2D fiber-beam elements and ASTM E119 standard fire curve, the authors estimated the collapse time and the influence of fire protection [12]. It was found that with no fire proofing, the structure remained stable for 11 min; whereas with fire proofing, the structure remains stable for 30 min to 90 min depending on the level of fire protection [12]. A study done by Neal et al. [13] showed that meeting progressive collapse design requirements was insufficient to prevent buildings from collapse in fire. The presented scenario was that although the structure could sustain localized damage, the nearby fire protection was damaged or removed, resulting in progressive collapse under fire-following-column-loss [13]. Using SAFIR software and 2D FE models to analyze a 38-story building, the authors further discussed the effect of different parameters including fire protection (i.e., the existence of fire protection determined collapse and no collapse in fire), fire type (i.e., fire with cooling phase resulted in a longer time limit than that without cooling phase), and location of fire-blast event (i.e., upper-floor fire resulted in a shorter time limit than lower-floor fire, and the collapse mechanisms were different between upper- and lower-floor fire) [13].

In summary, there are multiple studies and well-established guidelines for evaluating structural robustness at room temperature. However, these guidelines have not been applied to structures threatened by fire hazards, and most of research on progressive collapse in fire focus on qualitative aspects (e.g., failure mechanisms and influence of different factors). Some important factors for structural fire engineering have not been addressed such as how deformation limits should be imposed to prevent damage to fire insulation materials, and how to determine the time limit before the structural collapse in fire. This chapter seeks to address these concerns by developing 2D analyses of steel frames in exposure to progressive collapse in fire, and applying the method presented in Section 2.3 to quantitatively assess the structural robustness. This serves as a practical guideline for design in extreme hazards including fire and progressive collapse.

4.1.2. Research objectives

The study presented here aims to investigate the structural performance of medium- and high-rise buildings in multi-hazard scenarios involving fire and progressive collapse. In the context of progressive collapse, the Alternate Path method with the column removal scenario was applied, as illustrated in Fig. 4.1.

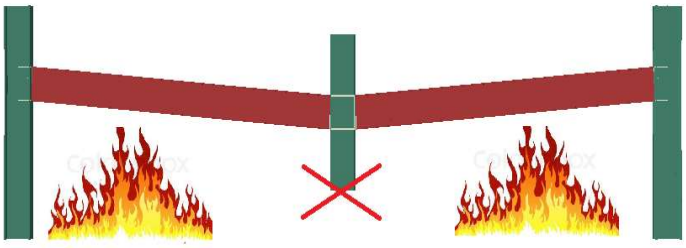

Fig. 4.1. *Column removal scenario for simultaneously fire and progressive collapse event*

There are two types of progressive collapse scenarios involving fire:

(1) Type 1 - Column removal after fire exposure: During a fire, the thermal expansion of the heated floor system can lead to significant lateral displacements and instability in column(s); thus, it is reasonable to consider removing the unstable column(s) from the global structural system. In this scenario, the appropriate simulation condition is fixed temperature (at elevated temperature) and increasing load (gradually from zero to service load). It is assumed that after the long period of fire, the temperatures of fire-affected

members have reached a stable state (i.e., fixed temperature) and the column is gradually removed from the system due to instability, causing load redistribution to the remaining structure (i.e., increasing load).

(2) Type 2 - Fire following sudden column removal: Following a dramatic impact (e.g., bomb attack, vehicle crash, or blast), a column may be suddenly damaged, followed by fire ignition. A case in point is the collapse of the World Trade Center buildings after the airplane attack in 2001. In this scenario, the appropriate simulation condition is fixed load (at service load) and increasing temperature (as a fire curve). The assumption is that the load is completely distributed to the remaining structure before the fire reaches flashover.

This research focuses on Type 1, i.e., column removal after fire exposure, which is referred as fire-induced progressive collapse. The structure under study is a moment resisting frame, using steel-reinforced concrete composite floor system. The novelty of this chapter is primarily a computationally efficient model for simulating framed structures in fire, in which the important role of the beam-to-column connections are taken into account by using a 2D macro-element model calibrated for the structure studied.

Important questions addressed in this study are as follows:

- What are the failure mechanisms in structures under the fire-induced progressive collapse hazard?
- How is structural performance evaluated under this scenario? What are appropriate limits?
- What is the critical scenario of fire-induced column removal?
- How do various factors affect the structural response? Specifically:
    - Location of column removal (i.e., perimeter column vs. corner column)
    - Amount of insulation on columns
    - Location of fire (i.e., lower floor, middle floor, or top floor)
    - Scale of fire (fire on one floor vs. fire on multiple consecutive floors)

4.2. Methodology

To investigate the structural performance of buildings (i.e., steel frames and composite frames) in fire-induced progressive collapse hazard, the finite element (FE) method was adopted. Four major components should be highlighted in the computational analysis. They are summarized below and described in detail in the following subsections.

(1) *Thermal analysis for structural elements*: based on the principles of heat transfer (i.e., radiation, convection, and conduction) and the atmospheric temperature of the fire, the temperature of structural members is calculated. These members' temperatures are the inputs in the structural analysis. The thermal analysis is carried out in ABAQUS.

(2) *Macro-element model for structural analysis*: for reasonable accuracy and computational efficiency, the 2D structural model includes the macro-element beam-to-column connection model (presented by Nguyen et al. [14] and described in Chapter 3). Here, analyses are carried out in ABAQUS.

(3) *Loading for fire-induced progressive collapse scenario*: following UFC guideline for progressive collapse resistance design [6], applied loads include gravity and lateral loads. The two different approaches (i.e., the nonlinear static approach and the nonlinear dynamic approach) are described in Section 4.2.3.

(4) *Criteria for quantifying structural robustness*: the level of performance depends on the design objectives of the building, which are identified as immediate occupancy (IO), life-safety (LS), or collapse prevention (CP). Structural robustness is based on three criteria, namely insulation, integrity, and stability.

4.2.1. Thermal analysis for structural elements

The thermal analysis is used to determine the temperature of structural members, given the atmospheric temperature and the duration of the fire. It is based on the principles of heat transfer, including radiation, convection, and conduction. In this study, two assumptions are adopted:

(1) The fire protection layer remains effective during the entire fire duration. To ensure this, the strain in steel is limited to prevent deformation that would lead to damage in the insulation.

(2) Members are heated uniformly along the length. The purpose is to simplify the thermal loading, where the temperature gradients are only considered through the cross-section. This assumption is widely used in computational studies [2-3,12-13] on structural response in fire.

The thermal analysis involves convection and radiation heat transfer from the atmosphere to the surface of the member (beam or column). The atmospheric temperature is assumed to be uniform, which is a reasonable assumption for a post-flashover fire. It is noted that for the perimeter frame, only one side of the structural member is exposed to fire while the other side is exposed to room temperature (i.e., open air), as illustrated in Fig. 4.2. The emissivity coefficient for steel and concrete is taken as 0.8 on the fire-exposed side and 0.6 on the unexposed side; the coefficient of convection is assumed to be 25 W/m^{2}K for standard fire, 35 W/m^{2}K for natural fire, and 10 W/m^{2}K on the unexposed side [15]. The material properties (i.e., density, thermal conductivity, and specific heat) at elevated temperature for steel, concrete, and fire insulation material follow Eurocode 4 [16], as detailed in Section 5.2.1.

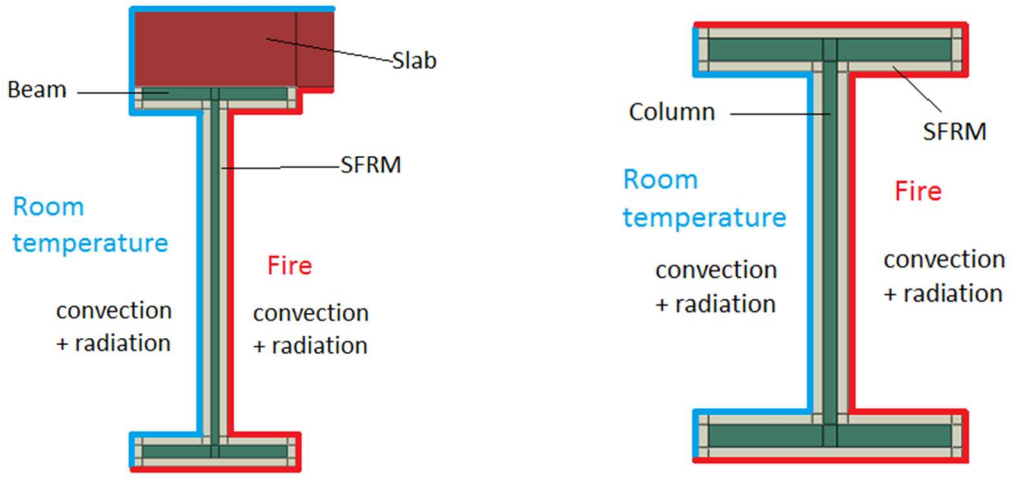

Fig. 4.2. *Thermal analysis of (a) insulated perimeter beam, and (b) insulated perimeter column*

The important output of the thermal analysis is the temperature in the steel, which is then used as input in the structural analysis. Fig. 4.3 illustrates the distribution of nodal temperatures within a

steel beam and column. Because in the component-based structural analysis, beam elements are used for beams and columns, not all nodal temperatures are needed. The model in ABAQUS [17] uses three temperature points for beam in 2D plane, as shown in Fig. 4.4.

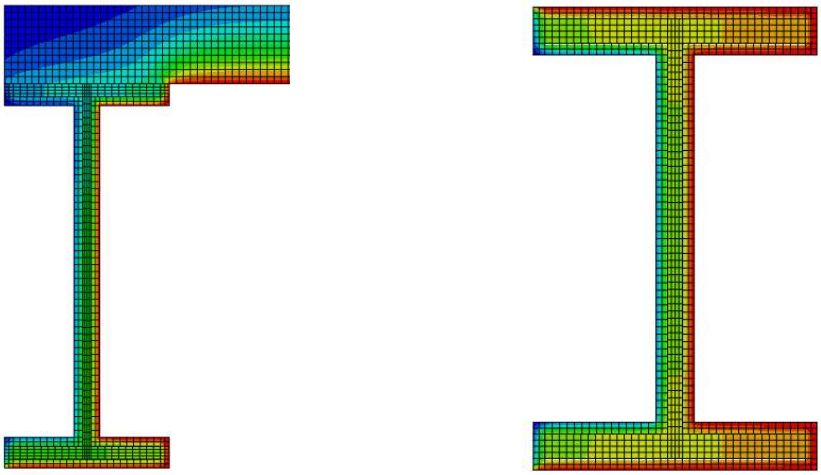

Fig. 4.3. *Nodal temperature profile in (a) perimeter beam, and (b) perimeter column*

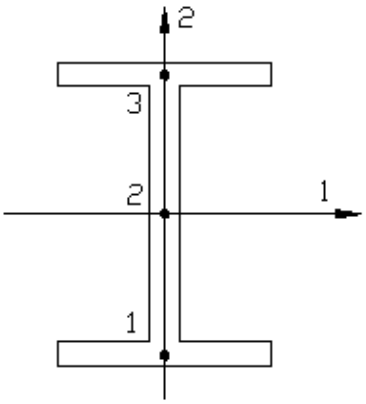

Fig. 4.4. *Temperature points for beam in 2D plane*

4.2.2. Macro-element structural model

Due to the thermal expansion and capacity degradation of beam-to-column connections at elevated temperature, it is necessary to treat beam-to-column connections as special elements in the structural system rather than ideally pinned or fixed joints. For computational efficiency, macro-element model is used to simulate connection behavior, as described in Chapter 3. In this model, beams and columns are modeled as beam elements. Beam-to-column connections can be modeled

as connector elements (i.e., Cartesian translational and rotational type in ABAQUS) whose force-deformation relationship is dependent on temperature. The concept is to use a system of springs and rigid links to model the connection between the beam and column, as shown in Fig. 3.5 with details presented in Chapter 3 (or in Nguyen et al. [14]). The macro-element model for WUF-B connection was validated against high-resolution FE models and experimental data at room temperature (from Sadek et al. [7]) and elevated temperatures (from Mao et al. [18]). Similar expressions can be derived for other types of connections using the same procedure.

Temperature-dependent stress-strain relationships were obtained from Eurocode 4 [16], as detailed in Section 5.2.2.

4.2.3. Loading for fire-induced progressive collapse scenario

In the presented research, the UFC [6] Alternate Path method was utilized in the analysis of a steel frame at elevated temperature. In this method, gravity loads and lateral loads are simultaneously applied to the structure. The structure is then subjected to the sudden removal of a column. Two acceptable approaches are nonlinear static analysis and nonlinear dynamic analysis. For nonlinear static analysis, the gravity load is artificially increased on the floor areas above the removed column to simulate the dynamic effect. The UFC [6] provides formulae to determine the magnitudes of applied loads, which are presented here for clarity. Because the load factors are consistent with the extreme load condition, they are deemed to be appropriate for fire-induced collapse analysis.

Nonlinear static analysis

In the nonlinear static analysis, the increased gravity loads for floor areas above removed column are given in UFC [6] as

$$G_N = \Omega_N\left[\left(0.9\,or\,1.2\right)D+\left(0.5L\,or\,0.2S\right)\right] \tag{4-1}$$

where G_N = increased gravity load; D = dead load; L = live load; S = snow load; Ω_N = dynamic increase factor for nonlinear static analysis, depending on structure type and acceptance criteria.

The gravity loads for floor areas away from the removed column are calculated as

$$G = \left(0.9\,or\,1.2\right)D+\left(0.5L\,or\,0.2S\right) \tag{4-2}$$

where G = gravity load.

The lateral loads for each floor are applied according to the following equation:

$$L_{LAT} = 0.002\sum P \tag{4-3}$$

where L_{LAT} = lateral load; $\sum P$ = sum of gravity loads acting on only that floor. Note that dynamic increase factors are not applied for the determination of *P*.

In the nonlinear static approach, the column is removed at the start of the analysis. Then the loads given in Eqs. (4-1)-(4-3) are applied to the structure, and an incremental, iterative analysis is performed. The dynamic effect of the column removal is represented by factor G_N, applied on floor areas above the removed column. ABAQUS/Standard was used in the case study that follows.

Nonlinear dynamic analysis

In the nonlinear dynamic analysis, the gravity loads for the entire structure are calculated as [6]

$$G_{ND} = (0.9\,or\,1.2)D + (0.5L\,or\,0.2S) \tag{4-4}$$

where G_{ND} = gravity load used in the nonlinear dynamic analysis.

The lateral loads for each floor are calculated in the same manner as in the nonlinear static approach, i.e., Eqn. (4-3).

In the nonlinear dynamic approach, the loads given in Eqs. (4-3)-(4-4) are gradually applied to the structure (i.e., ramped slowly and then maintained for a period of time to minimize dynamic effects) until the structure stabilized. The column is then suddenly removed. A dynamic analysis is performed (e.g., using ABAQUS/Explicit) to determine forces and deformations.

Global damping is applied in the nonlinear dynamic analysis in order to minimize oscillations in the structural response. The appropriate magnitude of the damping factor can be determined based on the critical damping coefficient and trial-and-error. As suggested in the LS-DYNA user's manual [19], the critical mass damping coefficient is calculated as follows:

$$\beta_{cr} = \frac{4\pi}{T} = 2\omega = 2\sqrt{\lambda} \tag{4-5}$$

where β_{cr} = the critical mass damping coefficient; T, ω , and λ = the period, frequency, and eigenvalue of the first mode.

Based on the findings, the nonlinear static analysis with dynamic amplification of the gravity load tends to be more conservative and computationally efficient compared to the nonlinear dynamic analysis.

4.2.4. Criteria for quantifying structural robustness

To quantify structural robustness in fire, three criteria (i.e., insulation, integrity, and stability), as described in Section 2.3, are adopted. This method is the combination of Acceptance Criteria (provided by UFC [6] and ASCE/SEI 41-06 [20]), Fire Protection Criteria (provided by ASTM E119 [21]), Garlock and Quiel [2]'s proposed method of calculating capacity of heated members, and research findings [22-23] on the failure of fire insulation material in extreme load.

In performance-based structural design, there are three main levels of performance, based on the objectives of the design. They are Immediate Occupancy (IO), Life Safety (LS), and Collapse Prevention (CP). LS is the performance level typically sought in structural fire engineering.

Three criteria are as follows:

(1) Insulation: To prevent the failure of fire insulation materials, the deflections in beams shall not exceed L/40 and the lateral displacements in columns shall not exceed 120 mm.

(2) Integrity: To prevent the formation of openings through which flames and hot gases can pass, deflections in beams are not allowed to exceed L/20 and rotations at BC connections cannot exceed $6\theta_y$ (θ_y is the yield rotation), assuming LS performance.

(3) Stability: To prevent the loss of load-bearing capacity of structural assemblies, the Demand over Capacity Ratio (DCR) cannot exceed 1.

Details on three criteria are presented in Section 2.3. For the global structure, the term "time limit" is defined as the maximum duration of ISO 834 standard fire exposure that the structure can

withstand before failure (i.e., when the elements exceed the limit state). Even for the same structure, the time limit varies depending on the severity of fire, the location of column loss, and other factors, as discussed further in the case study.

4.3. Case study

4.3.1. Building and fire setup

A ten-story steel framed building appearing in Sadek et al. [7] was analyzed in this research, as shown in Fig. 4.5. The building was designed for Seismic Design Category C (SDC C) which resulted in intermediate moment frames (IMFs) as defined in the AISC (2002) seismic provisions. The 2D frame under study was the exterior moment-resisting frame, shown in Fig. 4.5, which used shear tab connections for bays 1-3 and WUF-B moment connections in bays 3-6. All the interior frames are gravity frames, using bolted shear connections. Details for members are given in Table 4.1. Because the focus was on the moment resisting frame, only the right side of the frame, from column 3 to column 6, was studied for structural performance evaluation.

Table 4.1. *Member sizes of different floor levels*

Floor	Beam		Column	Shear tab
	Bay 1-3	Bay 3-6		
Floor 1-3	W16x26	W21x73	W18x119	1/2"x12"x6"
Floor 5-6	W16x26	W21x68	W18x97	1/2"x12"x6"
Floor 8-10	W16x26	W21x44	W18x55	3/8"x12"x6"

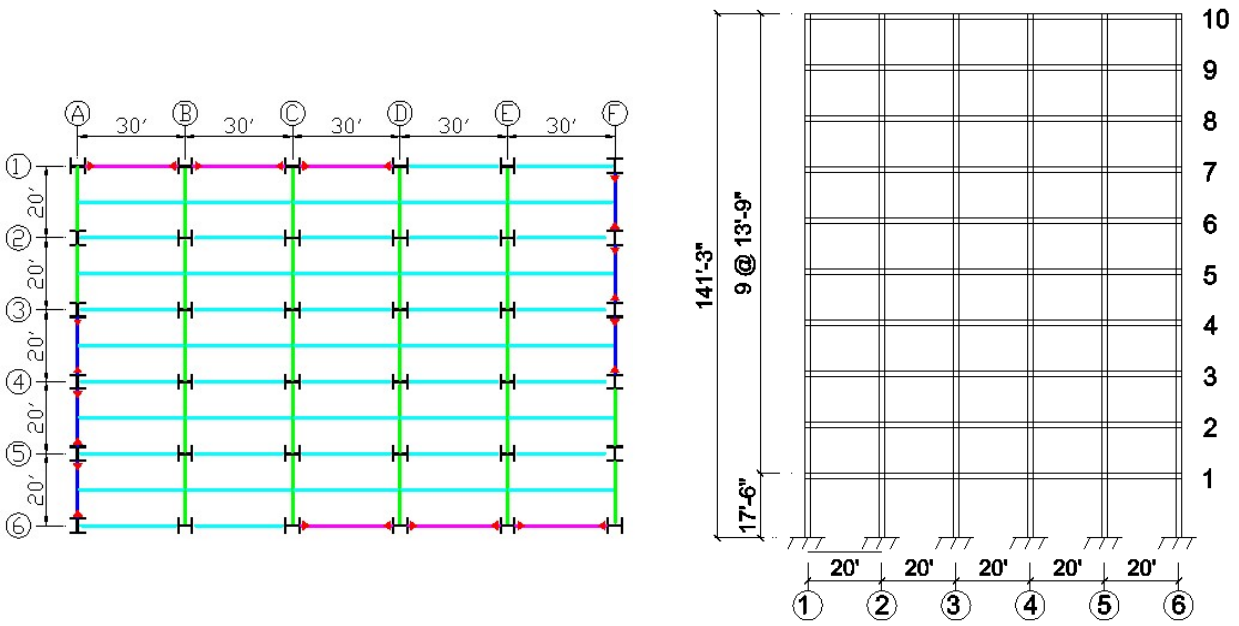

Fig. 4.5. *Floor plan and elevation view of the building*

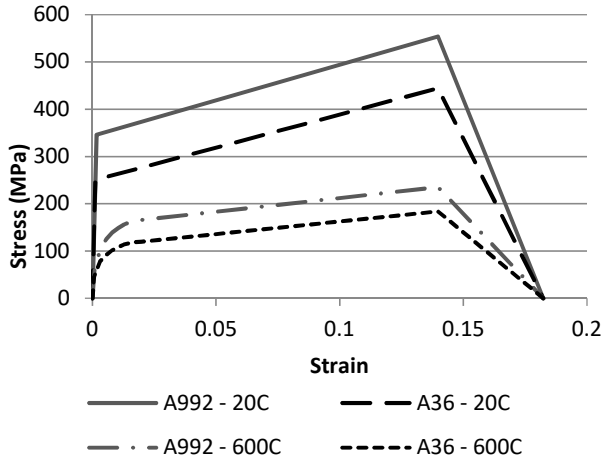

Fig. 4.6. *Stress-strain curves for structural steel*

ASTM A992 structural steel (f_y = 50 ksi = 345 MPa) was used in all beams, and columns. At beam-to-column connections, ASTM A36 steel (f_y = 36 ksi = 250 MPa) was used for the shear tabs and continuity plates, ASTM A490 high strength bolts were used, and welding requirements followed the recommendations in FEMA 353 (2000). The stress-strain curves for the various grades of steel at elevated temperature were assumed to follow Eurocode 3 [18] with 0.5% hardening strain, as illustrated in Fig. 4.6. For typical floors, the dead load was 76 psf (3.64 kN/m^2) and design live

load of 100 psf (4.79 kN/m^2). For the roof, the dead load was 56 psf (2.68 kN/m^2) and the design live load was 20 psf (0.96 kN/m^2).

Because the investigated scenario is fixed-temperature increased-load, only three-hour standard fire was considered, as shown in Fig. 4.7 along with time history of member temperatures.

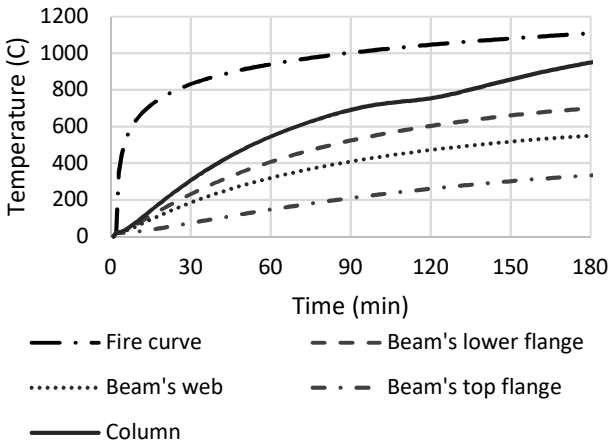

Fig. 4.7. *Time history of standard fire curve and member temperatures*

Following common practice on fire protection in buildings, all beams were insulated for one-hour fire rating. To investigate the opportunity of cost saving for fire protection material, the columns are insulated for one-hour or two-hour fire rating; the structural response corresponding to these two levels of fire protection, are discussed following the results in the parametric study.

Several questions to be addressed in this case study are as follows:

- Can the building resist progressive collapse under fire if it is designed to do that at room temperature? If so, for how long (i.e., what is the time limit)?
- What are the failure mechanisms of the building?
- How is structural response affected by following factors?
    - Structure-related factors: column-loss location (e.g., corner column vs. perimeter column), fire proofing level (e.g., two-hour rating vs. one-hour rating for column)
    - Fire-related factors: fire location (e.g., first story vs. middle story vs. top story), number of floors involved in fire

- Which case is the critical case? Can we design based on only the critical cases?

The influences of these different factors were investigated through a parametric study. For a one-floor fire, nine cases were considered, with one-hour fire protection for all beams and columns, varying locations of column loss (i.e., perimeter column 4, 5, or corner column 6), and varying locations of fire (i.e., fire on the first, fifth, or ninth floor), as described in Table 4.2. Among these nine cases, the ones that failed early (i.e., the time limit is less than the three-hour fire duration) were reinvestigated with two-hour fire protected columns. The purpose is to quantify how much robustness the additional one-hour insulation for columns added to the structure. Moreover, several cases where fire occurred on two consecutive floors and three consecutive floors were also studied to understand the impact of fire scale on this particular structure.

4.3.2. Analysis approach

The non-linear static approach was adopted to save computational time and provide conservative results, as mentioned in Section 4.2.3. The ABAQUS sequentially coupled thermal and structural analysis was used with the Standard/Implicit solver.

As explained in Section 4.2.4. for the structural performance evaluation, the variables to be computed in this case study are:

- For stability criterion: axial force and moments in columns and at BC connections
- For integrity criterion: maximum deflections in beams and rotations at BC connections
- For insulation criterion: maximum strains in all members

In the nonlinear static structural analysis, the first step was to apply the member temperatures (obtained from thermal analysis) and remove one column. In ABAQUS, temperatures are applied to members as “predefined fields”. Once temperatures were assigned, gravity and lateral loads were increased from zero to the magnitude given in Eqs. (4-1)-(4-3).

Criteria were compared to their limits to determine whether the structure can sustain the extreme load (i.e., fire-induced column loss) within the period of fire exposure.

4.3.3. Findings

Table 4.2 summarizes the time limit and failure mechanism of the framed structure with the single-floor fire and the one-hour fire protected beams and columns. With basic fire protection (i.e., one-hour rating) and design against progressive collapse at room temperature, the structure could withstand the fire-induced column loss for at least two hours. When fire occurs on the middle floor, the structure could maintain its robustness for three hours. The critical case was when fire occurred on the top floor and the corner column was removed.

When fire occurred on the lower floor, stability failure in column was dominating, whereas when fire occurred on the top floor, failure was governed by integrity criterion (i.e., failure in beam due to large deflection). It is possibly because the existence of many floors above the first floor creates a higher load to redistribute from the removed column to the adjacent column(s) and leaves a larger portion of structure to resist deformation.

Two-hour fire protection for columns were also investigated for the cases in which the time limit was less than three hours (i.e., Case 1, 3, 7, 8, and 9). It was found that increasing the fire rating to two hours extend the time limit of Case 1 and 3 by 10-20 min or 6-12%, which is not significant, considering the additional cost of the fire protection material. This increase in cost also provided no help in Case 7-9 when the fire occurred on top floor. Therefore, adding one-hour fire protection to the insulated columns is not suggested in this structure.

Table 4.2. *Time limit of the building subjected to fire-induce progressive collapse*

Case	Column loss	Floor	Time Limit (min)	Failure	Governing Failure Mechanism	Component's Failure			
						Column	Connection	Beam	SFRM
1	Col 4	1	170	Yes	Stability	Yes	No	No	No
2	Col 5	1	180	No	N/A	N/A	N/A	N/A	N/A
3	Col 6	1	160	Yes	Stability	Yes	No	No	No
4	Col 4	5	180	No	N/A	N/A	N/A	N/A	N/A
5	Col 5	5	180	No	N/A	N/A	N/A	N/A	N/A
6	Col 6	5	180	No	N/A	N/A	N/A	N/A	N/A
7	Col 4	9	135	Yes	Integrity	No	No	Yes	No

8	Col 5	9	135	Yes	Integrity	No	No	Yes	No
9	Col 6	9	120	Yes	Integrity	No	No	Yes	No

(Note: SFRM = spray-applied fire resistive material, the insulation material used in this study)

Table 4.3 describes the member temperatures corresponding to the time limits of the structure in various fire-induced column loss scenarios. They are relatively consistent with the critical temperature of steel provided in FEMA Appendix A [21]. (i.e., the critical temperature is 538°C (1000°F) for steel columns, and 593°C (1100°F) for steel beams and open web joists). In Case 7, 8, and 9, the failure was dominated by integrity (i.e., limiting deflections of beams and rotations at BC connections), thus the member temperatures were a bit lower than the critical temperature.

Table 4.3. *Member temperatures at time limit of the building*

Case	Column loss	Fire on Floor	Fire Duration (min)	Component's Temperature (°C)				
				Primary Beam			Connection	Column
				Lower Flange	Web	Upper Flange		
1	Col 4	1	170	653	554	385	554	589
2	Col 5	1	180	667	566	397	566	606
3	Col 6	1	160	637	541	372	541	570
4	Col 4	5	180	667	566	397	566	606
5	Col 5	5	180	667	566	397	566	606
6	Col 6	5	180	667	566	397	566	606
7	Col 4	9	135	588	502	334	502	516
8	Col 5	9	135	588	502	334	502	516
9	Col 6	9	120	557	477	311	477	482

The failure mechanism in the nine cases of single-floor fire is further explained in Table 4.4 and Table 4.5. In all cases, the internal force demands in the beam-to-column connections were lower than the capacities, thus there was no stability failure at the connections. On the other hand, the columns started to fail (i.e., stability failure) when the demand exceeded the capacity (i.e., DCR > 1), as illustrated in Fig. 4.8 for Case 3. In 9th-floor fire, the integrity failure in beam (due to large

deflection) was observed at time t = 135 min for Case 7 and 8, and at time t = 120 min for Case 9, as shown in Fig. 4.9.

Table 4.4. *Variables for stability criterion of the structure in a single-floor fire*

Case	Column loss	Fire on Floor	Fire Duration (min)	Stability Criterion (i.e., DCR ≤ 1)							
				Adjacent Column				Connection			
				N (kN)	M (kNm)	N/ N_{CL}	DCR	N (kN)	M (kNm)	N/ N_{CL}	M/ M_{CL}
1	Col 4	1	170	3660	29.0	0.93	0.97	194.4	126.1	0.10	0.28
2	Col 5	1	180	2976	31.0	0.83	0.89	168.1	107.4	0.09	0.26
3	Col 6	1	160	3988	14.7	0.91	0.93	22.5	184.1	0.01	0.39
4	Col 4	5	180	2070	14.6	0.72	0.75	189	120.6	0.10	0.29
5	Col 5	5	180	1683	15.6	0.64	0.68	171	109	0.09	0.26
6	Col 6	5	180	2311	16.6	0.80	0.83	27.4	169	0.01	0.40
7	Col 4	9	135	563.3	131.3	0.30	0.51	218	209	0.22	0.62
8	Col 5	9	135	585.8	83.0	0.31	0.45	175	211	0.18	0.63
9	Col 6	9	120	652.7	116.6	0.22	0.40	99.1	199.9	0.05	0.52

Table 4.5. *Variables for insulation and integrity criterion of the structure in a single-floor fire*

Case	Column loss	Fire on Floor	Fire Duration (min)	Insulation Criterion		Integrity Criterion			
				SFRM		Beam		Connection	
				Max Strain	$\varepsilon / \varepsilon_{limit}$	Displacement (m)	Δ / L	Rotation	θ / θ_y
1	Col 4	1	170	0.001	0.1	0.106	1/58	0.017	1.74
2	Col 5	1	180	0.0009	0.09	0.100	1/61	0.016	1.64
3	Col 6	1	160	0.0008	0.08	0.177	1/34	0.029	2.90
4	Col 4	5	180	0.0013	0.13	0.100	1/61	0.016	1.64
5	Col 5	5	180	0.0012	0.12	0.095	1/64	0.016	1.56
6	Col 6	5	180	0.0011	0.11	0.170	1/36	0.028	2.80
7	Col 4	9	135	0.0043	0.43	0.314	1/19	0.052	5.15

8	Col 5	9	135	0.0043	0.43	0.323	1/19	0.053	5.30
9	Col 6	9	120	0.0040	0.40	0.311	1/20	0.051	5.10

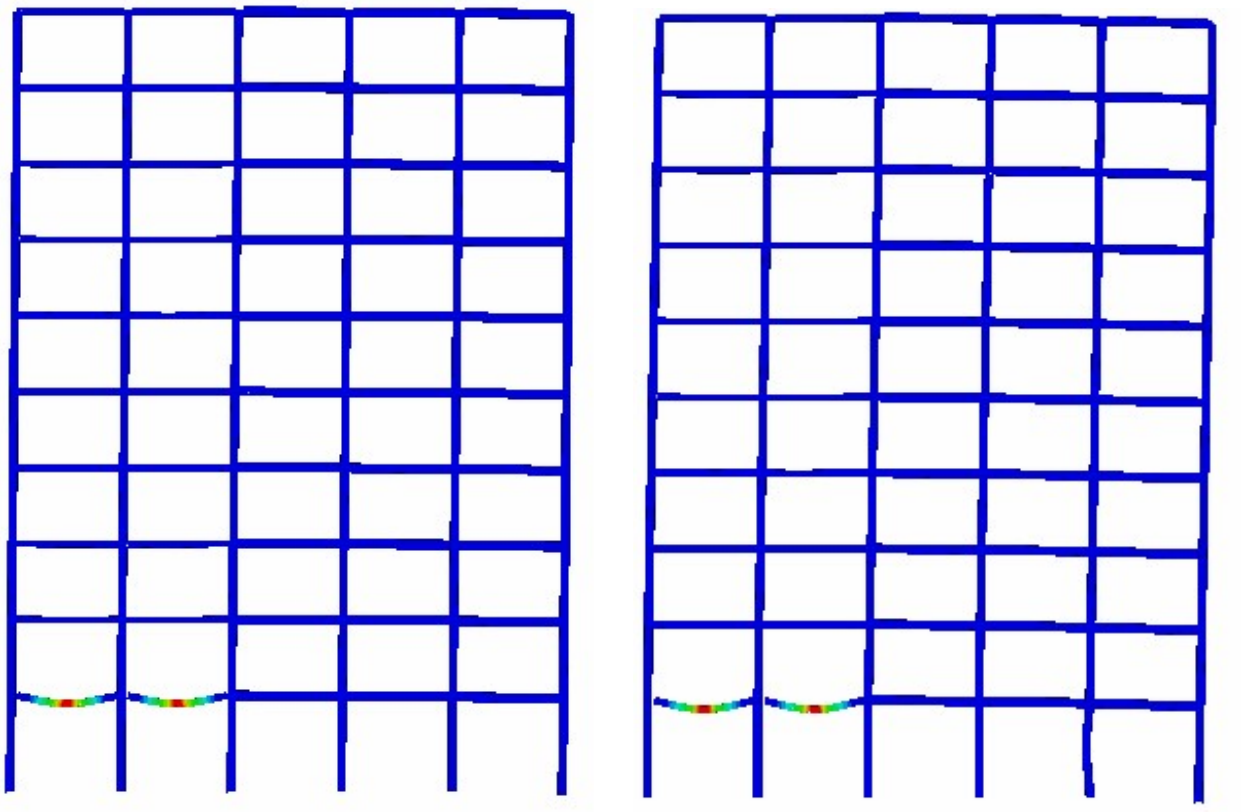

Fig. 4.8. *Case 3 (fire on 1st floor and column 6 is removed): stability failure in column*

(a) fire for 160 min (time limit, force ratio DCR = 0.93 < 1)

(b) fire for 165 min (beyond limit, force ratio DCR > 1 and the adjacent column buckles)

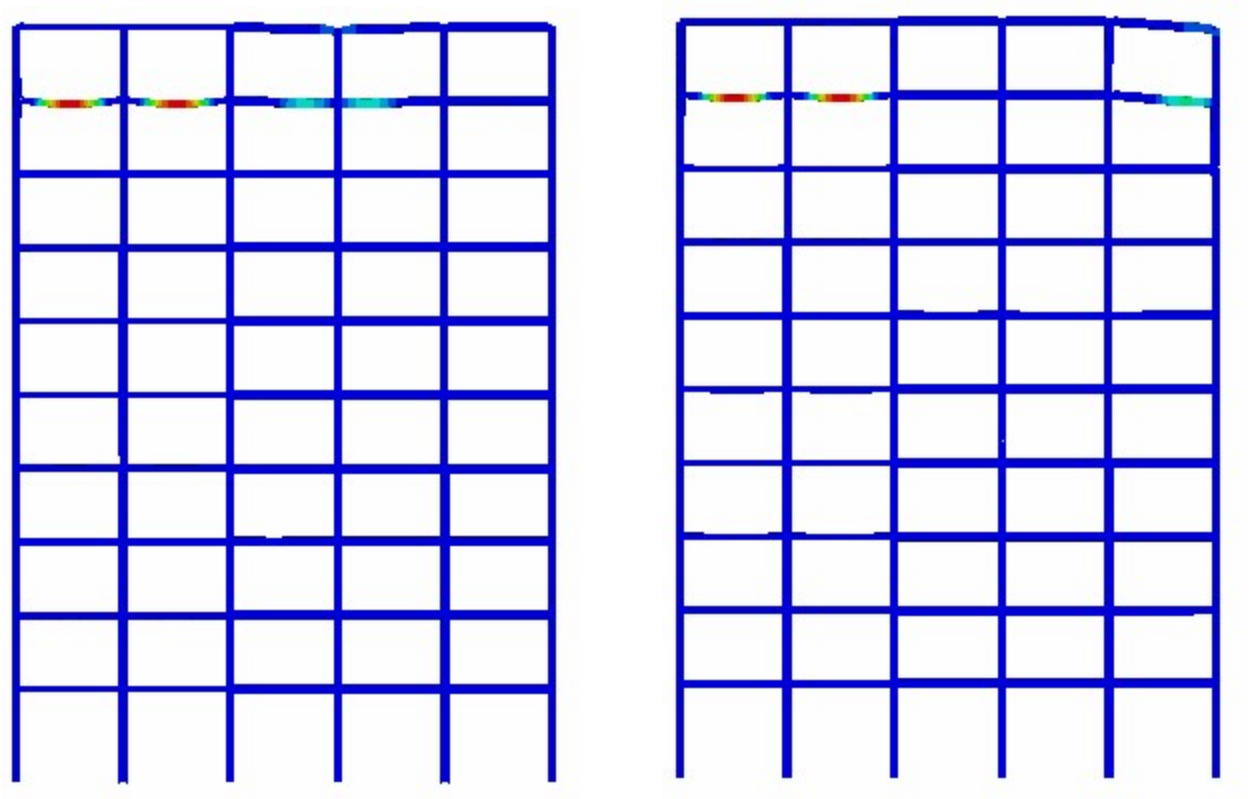

Fig. 4.9. *Integrity failure (due to large deflections in beams) in 9th-floor fire*

(a) 135-min fire in Case 7 (column 3 is removed)
(b) 120-min fire in Case 9 (column 6 is removed)

The case study also investigated the scenarios when fire spread on multiple floors. Table 4.6 describes the time limit of the structure when fire occurred on one floor, two consecutive floors, and three consecutive floors. Generally, multi-floor fire observed the same failure mechanism in the structure as single-floor fire but with lower time limit. When fire occurred on lower floor(s), stability failure (in columns) determined the time limit, whereas when fire occurred on middle or upper floor(s), integrity failure (in beams) determined the time limit. In the most severe case (i.e., when fire occurred on the three top floors), the structure could remain robust for 90 min. Fig. 4.10 describes the deformed shape with strain distribution in the frame when fire spreads on two and three consecutive floors.

Table 4.6. *Time limit of the structure in multi-floor fire*

Floor	Critical Failure Mechanism	Time limit (min) for fire on		
		1 floor	2 floors	3 floors
First	Stability failure in column	160	140	140
Fifth	Integrity failure in beam	> 180	150	120
Ninth	Integrity failure in beam	120	90	90

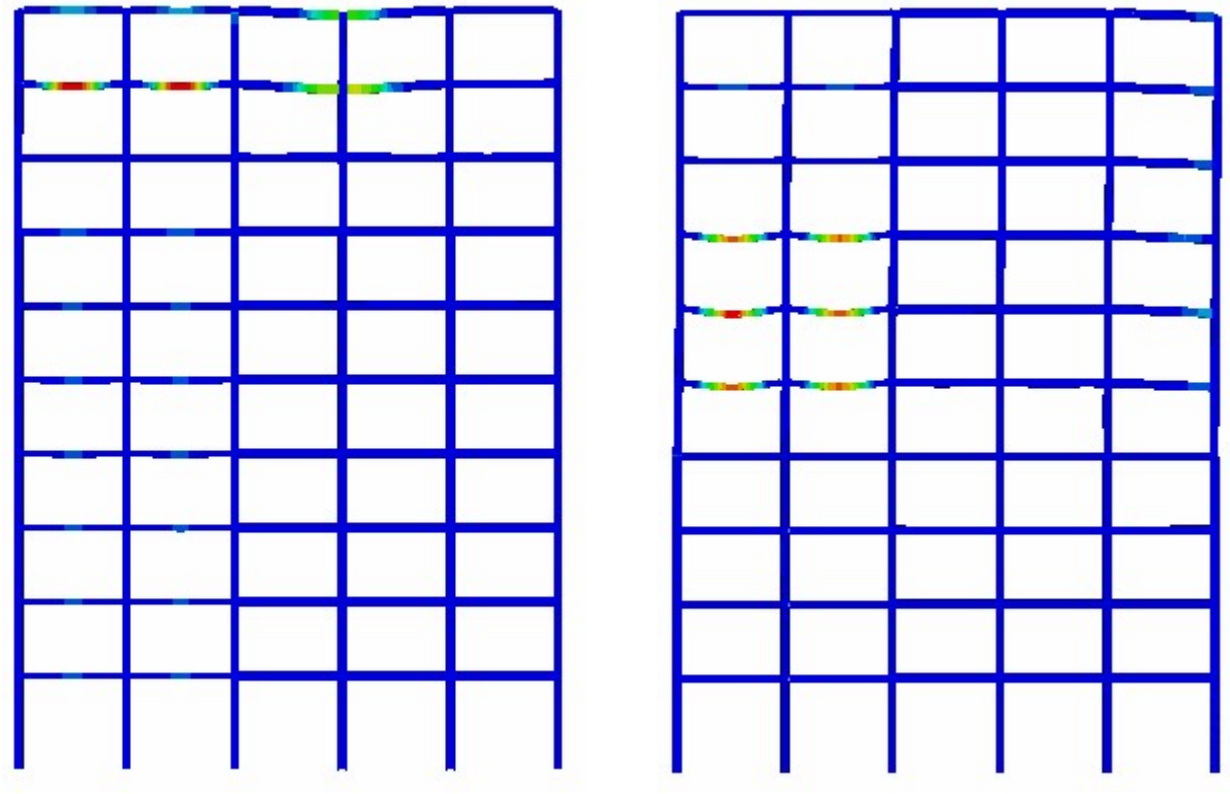

Fig. 4.10. *Integrity failure (due to large deflections in beams) in multi-floor fire*

(a) 100-min fire on 9^{th} and 10^{th} floors; column 4 is removed
(b) 120-min fire on 5^{th}, 6^{th}, and 7^{th} floors; column 6 is removed

4.4. Conclusions and limitations

4.4.1. Conclusions

The study investigates the response of a 2D steel moment resisting frame against fire-induced progressive collapse. A comprehensive method of quantifying the structural robustness in fire is also applied to measure the maximum time that the frame can withstand before failure, based on three criteria (i.e., stability, integrity, and insulation). Major conclusions are summarized as follows:

- The first step of quantifying the structural robustness is to identify the performance objective, namely immediate occupancy, life safety, or collapse prevention. Each level requires different limits for the three criteria.

- To assess robustness, the general principle for all three criteria is to compare the measures in structural members (i.e., internal forces, displacements, strains caused by the extreme loads) with the allowable limits. The allowable limits can be dependent on temperature (e.g., capacity of members), type of insulation material (e.g., strain limit), type of member (e.g., rotation limit), and performance level. For the stability criterion, the measures are internal forces in columns and beams and at BC connections; for the integrity criterion, the measures are deflections of beams and rotations at BC connections; and for the insulation criterion, the measures are the strains in all members.

- The fire-induced progressive collapse hazard is simulated by fixed-temperature increased-load scenario in 2D FE analysis. It is also recommended that a non-linear static approach be used for conservative results and computational efficiency.

- In the structure considered here, one-hour rated fire protection for beams and columns was sufficient and cost-effective for the structure to withstand progressive collapse for at least 90 min (for fire on three consecutive floors) or 120 min (for fire on a single floor). It was assumed that the structure was appropriately designed against progressive collapse at room temperature.

- In fire on the lower floor, the time limit was determined by stability failure in columns (i.e., when DCR > 1); whereas in fire on the middle and upper floor, the time limit was determined by integrity failure in beams (i.e., when deflections of beams exceed the limit).
- The critical case was the corner column being removed in fire on the top floor.

4.4.2. Limitations

The chapter only presents the analysis of a 2D steel moment-resisting frame with assumption of fire spreading on the entire floor. Research has shown that consideration of a 2D frame is insufficient for understanding the collapse resistance of the entire structural system. Moreover, the positive impact of composite floor system on the overall structural performance in fire was not considered in the analysis. This issue is addressed in the next chapters (Chapter 5 and 6) with complex 3D analyses for the building, which takes into account the effect of composite slab. However, the findings of the 2D analysis on the failure mechanisms are valuable for understanding the performance of building structures in fire.

In this study, the deflection limit for slabs was assumed to be $L_{span}/20$. Because there is in fact no established guideline for specific values of deflection limit for slab (in fire), further research may be needed to obtain the proper values of this limit.

Additionally, the analysis was based on uniform heating under standard fire exposure. Further research with different fire curves and non-uniform heating can be conducted to provide prediction with more realistic fire scenarios.

References

[1] Lange, D., Roben, C., Usmani, A. (2012). "Tall Building Collapse Mechanisms initiated by Fire: Mechanisms and Design Methodology." *Engineering Structures*, 36, 90-103.

[2] Garlock, M., Quiel, S. (2007). "The Behavior of Steel Perimeter Columns in a High-Rise Building under Fire." Engineering Journal, 44(4), 359-372.

[3] Agarwal, A., Varma, A. (2014). "Fire Induced Progressive Collapse of Steel Building Structures: The Role of Interior Gravity Columns." *Engineering Structures*, 58, 129-140.

[4] Standards ASCE/SEI 7. (2013). "Minimum Design Loads for Buildings and Other Structures." *American Society of Civil Engineers (ASCE)*, Reston, VA.

[5] U.S. General Service Administration. (2003). "Progressive Collapse Analysis and Design Guidelines for New Federal Office Buildings and Major Modernization Projects." Washington, D.C.

[6] Unified Facilities Criteria. (2009). "Design of Buildings to Resist Progressive Collapse. Department of Defense." Washington, D.C.

[7] Sadek, F., Main, J., Lew, H., Robert, S., Chiarito, V., El-Tawil, S. (2010). "An Experimental and Computational Study of Steel Moment Connections under a Column Removal Scenario." NIST Technical Note 1669, National Institute of Standards and Technology, Gaithersburg, MD.

[8] Khandelwal, K., El-Tawil, S., Kunnath, S., Lew, H. (2008). "Macromodel-Based Simulation of Progressive Collapse: Steel Frame Structures." *Structural Engineering*, 134(7), 1070-1078.

[9] Alashker, Y., Li, H., El-Tawil, S. (2011). "Approximations in Progressive Collapse Modelling." *Structural Engineering*, 137(9), 914-924.

[10] Porcari, G., Zalok, E., Mekky, W. (2015). "Fire Induced Progressive Collapse of Steel Building Structures: A Review of the Mechanisms." *Engineering Structures*, 82, 261-267.

[11] Jiang, J., Li, G-Q., Usmani, A. (2014). "Progressive Collapse Mechanisms of Steel Frames Exposed to Fire." *Advances in Structural Engineering,* 17(3), 381-398.

[12] Quiel, S., Marjanishvili, S. (2012) "Fire Resistance of a Damaged Steel Building Frame Designed to Resist Progressive Collapse." *J. Performance of Constructed Facilities*, 26(4), 402-409.

[13] Neal, M., Garlock, M., Quiel, S., Marjanishvili, S. (2012). "Effects of Fire on a Tall Steel Building Designed to Resist Progressive Collapse." *Proc., 2012 Structures Congress*, ASCE, Chicago, IL, 246-256.

[14] Nguyen, H., Jeffers, A., Kodur, V. (2015). “Computational Simulation of Steel Moment Frame to Resist Progressive Collapse in Fire.” *J. Structural Fire Engineering,* 7(4), 286-305.

[15] Eurocode 1. (2002). “Actions on Structures, Part 1-2: General Actions - Actions on Structures Exposed to Fire.” *Commission of European Communities*, Brussels, Belgium.

[16] Eurocode 4. (2005). “Design of Composite Steel and Concrete Structures, Part 1-2: General Rules - Structural Fire Design.” *Commission of European Communities*, Brussels, Belgium.

[17] ABAQUS v. 6.14. (2014). “Analysis User’s Guide - Elements: Beam Elements.”

[18] Mao, C., Chiou, Y., Hsia, P., Ho, M. (2009). “Fire Response of Steel Semi-Rigid Beam-Column Moment Connections.” *J. Constructional Steel Research*, 65, 1290-1303.

[19] LS-DYNA Support. “How to - General: Damping.” <http://www.dynasupport.com/howtos/general/damping> (Mar. 1, 2017).

[20] ASCE/SEI 41-06. (2007). “Seismic Rehabilitation of Existing Buildings.” *American Society of Civil Engineers (ASCE)*, Reston, VA.

[21] ASTM. (2000). “Standard Test Methods for Fire Tests of Building Construction and Materials.” ASTM E119, American Society for Testing and Materials, West Conshohocken, PA.

[22] Braxtan, N., Pessiki, S. (2011)."Bond Performance of SFRM on Steel Plates Subjected to Tensile Yielding." *J. Fire Protection Engineering,* 21(1), 37-55.

[23] Arablouei, A., Kodur, V. (2015). "Critical Factors Governing Crack Propagation at the Interface of Fire Insulation and Slender Steel Trusses." *ASCE J. Structural Engineering,* 141(12).

CHAPTER 5. METHODOLOGY OF 3D ANALYSIS FOR FIRE-INDUCED PROGRESSIVE COLLAPSE

Chapter 5 presents the complete methodology of using 3D macro-element model to analyze composite buildings under fire-induced progressive collapse threats. It describes the major components of the analysis, including the thermal analysis, the structural analysis with the loading for fire-induced progressive collapse scenario, and the method of quantifying structural robustness in fire. A 3D macro-element model is constructed using beam and shell elements. The model is validated against the Cardington corner test [1].

5.1. Introduction

5.1.1. Motivation

As described in Section 1.1, it is important to investigate the performance of buildings in resistance to fire-induced progressive collapse, especially high- and middle-rise buildings. Chapter 4 presents the 2D analysis for steel frames under this multi-hazard threat. By using macro elements (i.e., beam-column elements for beams and columns, and spring elements for beam-to-column connections), the 2D model can assess the performance of the structure (i.e., 2D frame) at a reasonable computational cost. However, it is not accurate to use a 2D frame for predicting the response of an entire 3D building subjected to extreme loads (i.e., fire and progressive collapse). The major reasons are:

- The 2D model does not consider the beneficial effects of composite floors on the global structural response in fire. Research [1,2] has proved that the membrane action developed in the composite slab during fire plays a big role in redistributing loads from the failed component to adjacent members, thereby improving structural redundancy. However, the composite slab cannot be included in the 2D model

- Even when subjected to the same time-temperature relationship for the fire, the temperatures in a 2D frame are different from the temperatures obtained from a 3D analysis, leading to different responses between the 2D and 3D structural analyses. For example, in the frame under consideration, the perimeter frame was determined to be critical because of its role in carrying lateral forces. However, the perimeter frame has one side exposed to fire and another side unexposed. Therefore, the 2D perimeter frame has a lower average temperature than the interior frame, but greater temperature difference between two sides (i.e., exposed and unexposed side). This can lead to different capacity due to strength degradation and different demand due to thermal expansion between the perimeter frame and the remaining structure. As a result, the fire performance of the 2D perimeter frame cannot represent that of the 3D building.

- The stiffness of the 2D frame is different from the entire 3D structure, resulting in a different resistance against progressive collapse. This is because of different connection types used in the building (e.g., the 2D perimeter frame uses moment connections while the interior frames use shear connections), different member sizes, and the consideration of lateral restraints (e.g., composite floor) in the structural analysis. Research [3] has shown the influence of stiffness on the structural robustness in fire-induced progressive collapse.

- The 2D model cannot accommodate buildings that have complicated plan layouts or combinations of different types of structure (e.g., rigid core with gravity perimeter frame, and "tube in tube" structures). With this type of building, a 3D analysis is necessary to accurately predict the global behavior in extreme loading conditions.

- The 2D model cannot analyze the building under a real fire such as a compartment fire (e.g., fire constrained in a room) and a spreading fire (e.g., fire spreading from room to room, from story to story through time).

In brief, a 3D model is necessary for accurate structural evaluation, especially for complicated structures subjected to extreme loads. As the buildings utilize steel-concrete composite floor systems, the focus is on modeling such floor systems using beam and shell elements.

5.1.2. Literature review

One of the most influential studies on composite building structures in fire is the series of large-scale fire tests (also known as the Cardington Fire Tests) [1], which were carried out on an 8-story composite frame at the BRE Cardington facility in England during the mid-1990s. The Cardington Fire Tests included four full-scale fire tests carried out by British Steel (i.e., the 1D restrained plane beam test, the 2D plane frame test, the corner compartment test, and the office fire demonstration test) and two additional fire tests carried out by Building Research Establishment (BRE). It was observed from the Cardington tests that the global performance of structure was different from that shown in standard fire test of a single structural component [2]. Local buckling was seen to occur primarily in the heated steel beams in the proximity of connections [2], and thus Bailey et al. [2] suggested to assume connections to be pinned in fire design. The Cardington Fire Tests also indicated the benefits of composite floors to the global structural performance, which came from the tensile membrane capacity of the slabs [2]. In fact, the membrane action in the Cardington tests was double that calculated using normal yield-line theory and the mode of failure was similar to that experienced in small-scale fire tests (i.e., large crack forming across the shorter span of the slab) [3].

After the Cardington Fire Tests, many studies focused on investigating the membrane action which developed in composite floor systems under fire conditions. Bailey (2001) [3] presented a simplified method of predicting the membrane behavior of simply-supported composite slabs in fire. The proposed theory used the equilibrium method and yield-line theory with the assumption that cracks formed at the center of slab across the shorter span. It was valid for both square and rectangular slab, and correlated well with Cardington test data [3]. Basically, the capacity enhancement created by membrane action consists of two parts: (1) in-plane tensile stresses developing at the center of slab, and (2) yield moment in the outer regions of slab, where compressive stresses occur (as shown in Fig. 5.1). According to Bailey [3], it was also observed in real fires (e.g., Broadgate and Basingstoke) that steel decks detached from the concrete slab due to the steam released at high temperatures. Bailey (2004) [4] extended the simplified method [3] to include the composite action of steel beams in composite floor systems. It was derived from the Cardington Fire Tests that despite no fire protection on internal secondary beams (i.e., the temperature reached above 1150°C) and large deflections, no structural collapse occurred [4].

Bailey argued that in order to fully utilize the membrane action of the composite floor system, no plastic hinge should be formed in the edge beams [4]. If such hinges develop in the beams, a folding mechanism will occur instead of membrane action [4]. If no hinge forms and vertical support on the perimeter of the slab is provided, membrane action will occur [4]. It was also found that the primary beams (i.e., the edge beams of slabs) are crucial for the mobilization of the membrane action, especially when the slab is horizontally unrestrained [4].

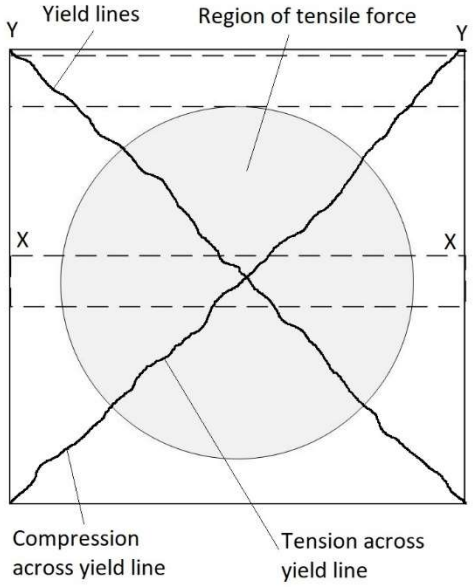

Fig. 5.1. *Bailey (2001) [3] - in-plane membrane forces in slab with no in-plane restraint*

In addition to understanding the mechanisms of membrane action in composite floor systems, many other studies have investigated the effect of different factors (e.g., shear studs, steel deck, and reinforcement) on the floor performance. Alashker et al. [5] found that the steel deck was the most influential component in resisting collapse (i.e., the steel deck accounts for 60% of overall floor capacity and doubling the thickness of steel deck could increase the overall floor capacity by 37%), while increasing slab reinforcement and shear tab strength provided small effect. Agarwal and Varma [6] found that reinforcement in the floor system could help to evenly redistribute the load from the removed column to the adjacent columns, improving the resistance against fire-induced progressive collapse. Huang et al. [7] explored the influence of composite interaction (between steel beams and concrete slabs) on the floor resistance in fire. Comparing different models with full-, partial-, and zero-interaction, Huang et al. [7] concluded that before the failure of shear studs, there was little difference between full- and partial-interaction behavior. The effect

of stud failure on continuous structure systems was more gradual than that on simply supported beams, and the partial-interaction model provided a closer match with experimental data.

In terms of modeling the concrete slab of composite floor system, the typical approach is to use flat shell element with uniform thickness; for slabs with profiled steel decks, the equivalent uniform thickness is equal to the average of the upper continuous portion and rib depth of the slab. The studies that apply this method include Agarwal and Varma [6], Huang et al. [7], Lamont and Usmani [8], McAllister et al. [9] among others. Additionally, few other studies have proposed different methods of modeling concrete slab. Elghazouli and Izzuddin [10] developed a new 2D shell element with the actual geometry of the composite slab using ADAPTIC software. The authors studied the membrane action of composite floor system under extreme loads including fire and the influence of planar restraint condition. With good validation against fire experiments, the study found that with full planar restraint, the slab reinforcement acted as a hanging tensile net at large deflection, adding to the floor capacity, and for simply supported slabs, membrane actions depended on geometric and material properties [10]. In the 3D analysis by Alashker et al. [5], the concrete slab was modeled by brick elements, the steel deck and shear tabs were modeled by shell elements, and the shear studs were modeled by beam elements [5]. The model was used to study the robustness of composite floor systems with shear tab connections against progressive collapse at room temperature, with validation against test data. Sadek et al. [11] also used brick elements to model a composite slab, where all components of the composite floor system (i.e., steel beams, metal deck, concrete slab, shear studs, and steel mesh) were considered in the simulation. The study investigated the robustness of composite floors at room temperature with validation against experimental data. One thing to note is that the studies that do not use shell elements to simulate slab behavior only focused on single floor systems rather than an entire building. A possible reason for this is the high computational cost associated with high-resolution slab models.

There have been a few studies which utilize 3D models with composite floor systems to analyze the performance of entire buildings under fire-induced progressive collapse. Agarwal and Varma [6] investigated two 10-story composite buildings of identical plan layout (i.e., one with rigid core in the center and the other with perimeter moment resisting frame), which were subjected to a fifth-floor compartment fire in the corner. The analysis adopted sequentially coupled thermal (transient) and structural analysis (explicit dynamic) in ABAQUS [6]. The simulated structure consisted of 2-

node beam-column elements (B31) for beams and columns, 4-node uniform-thickness shell elements (S4R) for concrete slabs, rigid constraints for composite action between concrete slabs and steel beams, and nonlinear spring elements for shear tab connections [6]. The results showed that both structures experienced column failures during fire: buckling of the perimeter columns in the structure with the interior rigid core, and buckling of the interior column in the structure with the perimeter moment frame [6]. McAllister et al. [9] conducted a computational study on fire-induce progressive collapse of the World Trade Center Building 7. This investigation developed a series of FE analyses, including (1) fire dynamics analysis to model the growth and spread of fire, (2) thermal analysis to predict temperature distribution in the structure, and (3) structural analysis to simulate the collapse of the building in fire [9]. The structural analysis used 3D macro-element models and consisted of two phases, as shown in Fig. 5.2: (a) Phase 1 - the structural response to elevated temperatures before collapse initiation, using ANSYS pseudo-static implicit analysis; and (b) Phase 2 - the sequence of subsequent structural failures from collapse initiation to total collapse of the building, using LS-DYNA dynamic explicit analysis [9]. Phase 1 accounted for temperature-dependent material degradation and component failure modes. Phase 2 accounted for component failures, buckling of columns due to loss of lateral supports, dynamic effects associated with structural failures, and debris impact of falling floors [9]. The fire-induced damage and material properties at the time of phase transition were input into Phase 2 as initial condition, as described in Fig. 5.1. When a component failed, it was numerically softened or removed from the structural system to prevent extreme impedance of analysis convergence [9]. The simulated structure included 3D linear beam elements (BEAM188) representing beams and columns, and 4-node shell elements (SHELL181) representing slabs [9]. The connection models were developed as a combination of spring elements, rigid beam elements, contact elements, control elements, and user-defined break elements (to model component failure). The analysis also included material and geometric nonlinearity, failure criteria for connections and shear studs, and buckling instability of beams and slabs [9]. Three temperature cases which had similar patterns but shifted in time were simulated. Regarding computational cost, the Phase 1 (pseudo-static) analysis modeled 16 stories with around 101,000 elements and required 6 months at a 64-bit work station for a single analysis simulating 4 hours of heating; the Phase 2 (dynamic) analysis modeled 47 stories with around 3.6 million elements and required 8 weeks at high-speed Linux computer clusters for a single global analysis simulating the structural response over 15 s [9]. McAllister et al.'s analysis provided good

correlation with the real sequence of WTC 7 collapse and four major findings [9]: (1) the failures for three thermal cases were similar in location and extent but shifted in time; (2) the dynamic analysis with fire-induced damage at 3.5 h stabilized after some local failures, whereas the analysis with fire-induced damage at 4.0 h progressed to global collapse; (3) the debris-impact damage resulting from the collapse of WTC 1 was not a primary contributor to the collapse; and (4) the uncertainty in the dynamic analyses increased with the failure sequence progression.

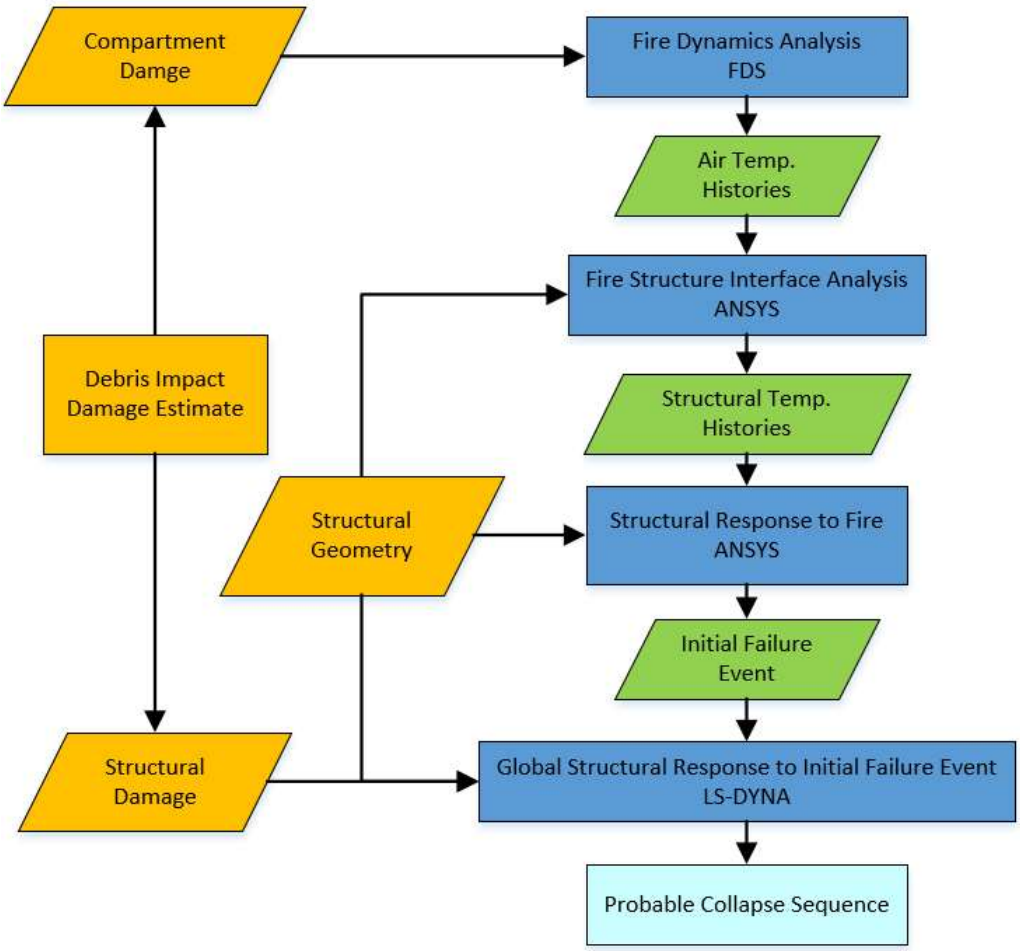

Fig. 5.2. *McAllister et al. [9] WTC 7 analysis sequence*

Some other studies used 3D macro-element models to investigate structures at room temperature. Alashker et al. [6] analyzed a ten-story composite building subjected to the loss of a perimeter column. Two types of 3D models were developed: (1) M1 using shell elements for all structural members, where the shear tab connection was modeled as a single row of shell elements whose thickness and stress-strain characteristics were derived from the strength and deformation of the

connection, and (2) M2 using beam-column elements, where the shear tab was modeled using a single beam element and a binding spring representing the contact between the beam flange and column flange. The macro-element model was found to significantly reduced the computational time (i.e., M2 ran 230 times faster than M1) [6].

Overall, the 3D macro-element model can provide a realistic and accurate prediction of structural performance in extreme loads, primarily because of considering the composite floor and the 3D effect in the analysis. The studies which employ the 3D model for large-scale analysis share a common modeling approach, that is using beam-column elements for the beams and columns, shell elements for the slabs, and spring elements for the connections. Those investigating structures against fire-induced progressive collapse often adopt dynamic explicit analysis, mostly because the explicit analysis can capture the dynamic effect of progressive collapse and fire growth, and overcome numerical instability. The shortcoming of the 3D model is high computational cost, particularly the processing time due to the large number of degrees of freedom. As indicated in McAllister et al. [9], the pseudo-static analysis required 6 months to simulate 4-hour fire and the explicit dynamic analysis required 8 weeks on high-speed Linux computer clusters.

This chapter presents a practical procedure of using 3D model to analyze the structural robustness of composite buildings subjected to fire-induced progressive collapse. It combines good practice in prior research to provide a comprehensive guideline for cost-effective design in this multi-hazard threat.

5.2. Methodology

To investigate the structural robustness of buildings (i.e., composite frames) in resistance to fire-induced progressive collapse, finite element (FE) method, sequentially coupling thermal analysis and structural analysis in ABAQUS, is adopted. Three major components should be noted in the computational analysis, as summarized below.

(1) *Thermal analysis*: based on the principles of heat transfer (i.e., radiation, convection, and conduction) and the atmospheric temperature of the fire, the thermal analysis calculates the transient temperatures of structural members, which develop during the fire. These members' temperatures are then input into the structural analysis. The thermal analysis is

carried out in ABAQUS heat transfer. Section 5.2.1 describes the thermal analysis for structural components.

(2) *Structural analysis - macro-element model*: for computational efficiency and realistic prediction, the 3D macro-element model of the composite floor system is employed in analyzing the structure exposed to fire. Here, structural analyses are carried out in ABAQUS explicit dynamic. Loading for fire-induced progressive collapse hazard is based on the nonlinear dynamic analysis procedure in the UFC guideline [13]. Section 5.2.2 describes the 3D structural analysis for composite buildings subjected to fire-induced progressive collapse.

(3) *Evaluation of structural robustness in fire*: the method of quantifying structural robustness in fire, that was detailed in Chapter 2, is used to quantify the performance. It includes three criteria, namely insulation, integrity, and stability. The requirements for each criterion can be different depending on different performance level, i.e., immediate occupancy (IO), life-safety (LS), and collapse prevention (CP). As the approach was described in detail in Chapter 2, it is not presented here.

Based on the result of structural robustness evaluation (i.e., satisfied or unsatisfied), the structural design can be kept unchanged or adjusted. The goal of design is likely to find the most cost-effective design which meets the desired performance. The strategies for adjusting the structural design may include changing member sizes, changing the level of fire protection, and changing the entire structural system. Iteration may be carried out until an optimal solution is obtained. Fig. 5.3. summarizes the design process, including thermal analysis, structural analysis, robustness evaluation, and design adjustment (or improvement). A case study is presented in Section 6.3 to show the design adjustment procedure.

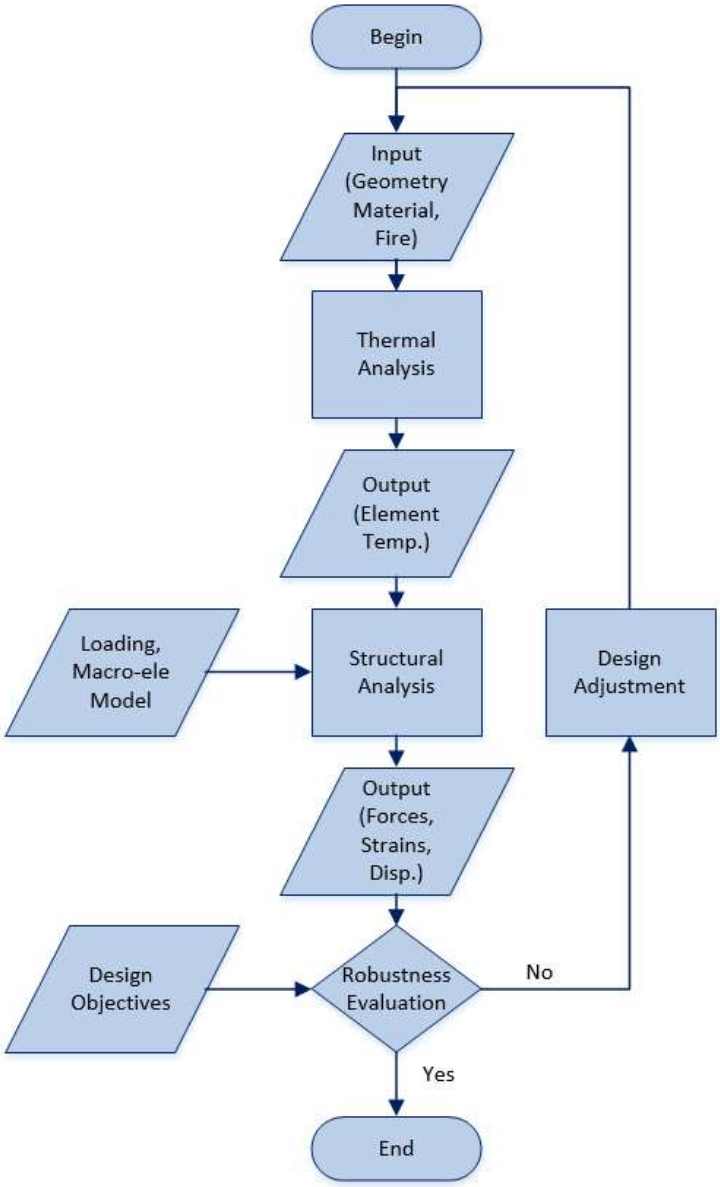

Fig. 5.3. *Structural design process*

5.2.1. Thermal analysis

The thermal analysis is used to determine the transient temperature distribution of structural members (e.g., beams, columns, and slabs). Given the atmospheric temperature and the duration of the fire, the analysis is based on the principles of heat transfer, by radiation, convection, and conduction. In this study, ABAQUS Standard / Heat Transfer is employed and two assumptions are adopted:

(1) Fire protection layer on steel members remains effective during the entire fire period. This entails limiting the strain in steel to prevent large deformations that would lead to damage in the insulation.

(2) Members are heated uniformly along the length. Thus, temperatures vary over cross-sections only. This assumption is applicable to compartment fire, which are the focus of this study.

The thermal properties (i.e., thermal conductivity and specific heat) for the composite steel and concrete structure follow Eurocode 4 [14], which are the same as Eurocode 3 [15] for steel and Eurocode 2 [16] for concrete. The thermal properties for fire insulation material (i.e., spray-applied fire resistive material or SFRM in this study) are taken from the product specifications provided by the manufacturer. The properties of steel, concrete, and SFRM are given below.

The specific heat of carbon steel (i.e., structural steel and steel reinforcement) c_s at temperature θ should be determined as follows [14,15]:

$$c_s = 425 + 7.73\times10^{-1}\theta - 1.69\times10^{-3}\theta^2 + 2.22\times10^{-6}\theta^3 \quad \text{(J/kgK)}, \ 20°\text{C} \le \theta < 600°\text{C} \qquad (5\text{-}1)$$

$$c_s = 666 + \frac{13002}{738-\theta} \quad \text{(J/kgK)}, \ 600°\text{C} \le \theta < 735°\text{C} \qquad (5\text{-}2)$$

$$c_s = 545 + \frac{17820}{\theta-731} \quad \text{(J/kgK)}, \ 735°\text{C} \le \theta < 900°\text{C} \qquad (5\text{-}3)$$

$$c_s = 650 \quad \text{(J/kgK)}, \ 900°\text{C} \le \theta \le 1200°\text{C} \qquad (5\text{-}4)$$

The specific heat of dry normal concrete (i.e., siliceous and calcareous aggregates) c_c at elevated temperature θ should be determined as follows [14,16]:

$$c_c = 900 \quad \text{(J/kgK)}, \ 20°\text{C} \le \theta \le 100°\text{C} \qquad (5\text{-}5)$$

$$c_c = 900 + (\theta - 100) \quad \text{(J/kgK)}, \ 100°\text{C} < \theta \le 200°\text{C} \qquad (5\text{-}6)$$

$$c_c = 1000 + (\theta - 200)/2 \quad \text{(J/kgK)}, \ 200°\text{C} < \theta \le 400°\text{C} \qquad (5\text{-}7)$$

$$c_c = 1100 \quad \text{(J/kgK)}, 400°C < \theta \leq 1200°C \qquad (5\text{-}8)$$

Based on Eurocode 4, the specific heat of lightweight concrete may be considered to be independent of the concrete temperature: c_c = 840 J/kgK. Fig. 5.4 shows the variation with temperature of the specific heat of carbon steel, normal concrete, and lightweight concrete.

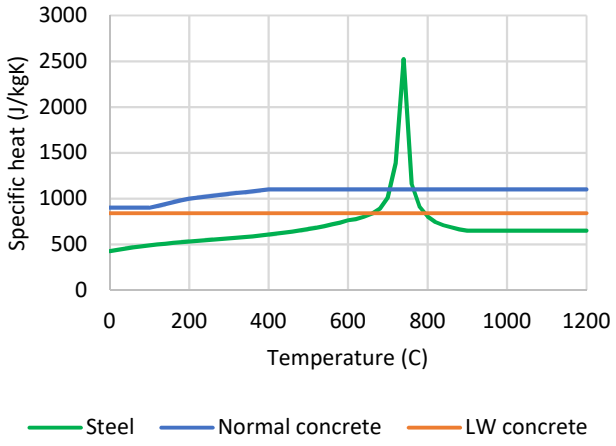

Fig. 5.4. *Specific heat of steel, normal concrete, and lightweight (LW) concrete*

The specific heat of SFRM is assumed to be independent of temperature [17], i.e., c_{ins} =1200 (J/kgK). The density of SFRM is 240 kg/m^3 [17].

The thermal conductivity of steel λ_s at temperature θ should be determined as follows [14,15]:

$$\lambda_s = 54 - 3.33\times10^{-2}\theta \quad \text{(W/mK)}, 20°C \leq \theta < 800°C \qquad (5\text{-}9)$$

$$\lambda_s = 27.3 \quad \text{(W/mK)}, 800°C \leq \theta \leq 1200°C \qquad (5\text{-}10)$$

The thermal conductivity of normal concrete λ_c at temperature θ may be determined between lower and upper limit, as follows [14,16]:

- Upper limit: $\lambda_s = 2 - 0.2451(\theta/100) + 0.0107(\theta/100)^2$ (W/mK), $20°C \leq \theta \leq 1200°C$ (5-11)

- Lower limit: $\lambda_s = 1.36 - 0.136(\theta/100) + 0.0057(\theta/100)^2$ (W/mK), $20°C \leq \theta \leq 1200°C$ (5-12)

For simple calculations, the thermal conductivity of normal concrete λ_c may be assumed to be independent of the concrete temperature, i.e., $\lambda_s = 1.60$(W/mK).

The thermal conductivity of lightweight concrete λ_c at temperature θ may be determined as follows [14]:

$$\lambda_c = 1.0 - (\theta/1600) \quad \text{(W/mK)}, \ 20°\text{C} \le \theta \le 800°\text{C} \qquad (5\text{-}13)$$

$$\lambda_c = 0.5 \quad \text{(W/mK)}, \ \theta > 800°\text{C} \qquad (5\text{-}14)$$

The thermal conductivity of SFRM is assumed to be independent of temperature [17], i.e., $\lambda_{ins} = 0.078$(W/mK).

Fig. 5.5 shows the variation with temperature of the thermal conductivity of carbon steel, normal concrete, and lightweight concrete.

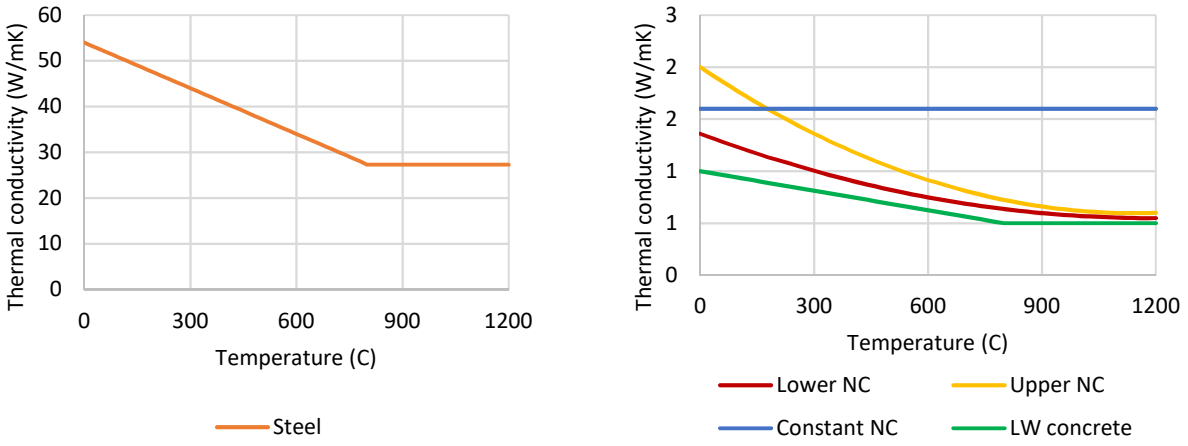

Fig. 5.5. *Thermal conductivity of steel, normal concrete (NC), and LW concrete*

The thermal analysis involves convection and radiation heat transfer from the surrounding gas (assumed to be uniform in temperature) to the surface of the member. For interior members, all sides are exposed to fire; whereas for exterior members, only one side is exposed to fire while the other side is exposed to room temperature (i.e., open air), as illustrated in Fig. 5.6 and Fig. 5.7. The emissivity of steel and concrete is taken as 0.8 on the fire-exposed side and 0.6 on the

unexposed side; the coefficient of convection is assumed to be 25 W/m^{2}K for standard fire, 35 W/m^{2}K for natural fire, and 10 W/m^{2}K on the unexposed side, according to Eurocode 1 [18].

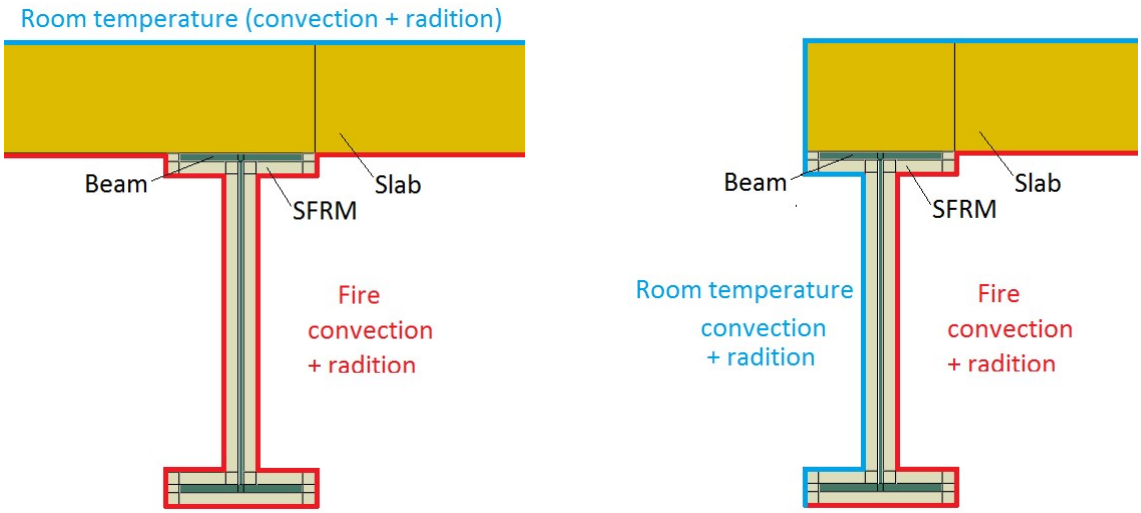

Fig. 5.6. *Thermal analysis of (a) insulated interior beam, and (b) insulated perimeter beam*

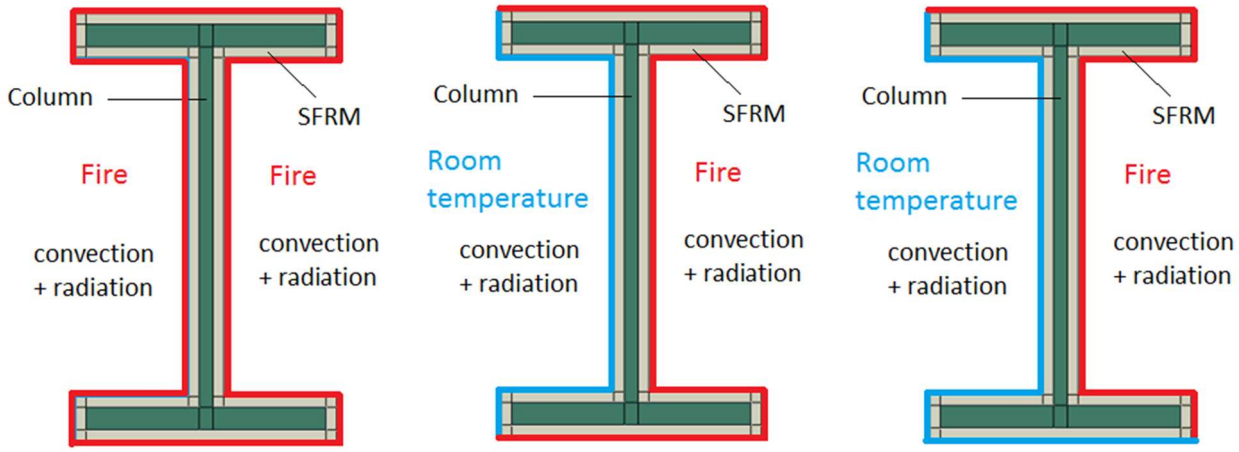

Fig. 5.7. *Thermal analysis of (a) interior column, (b) exterior column, and (c) corner column*

The important output of the thermal analysis is the temperature in the steel, which is then used as input in the structural analysis. Fig. 5.8 illustrates the distribution of nodal temperatures within a perimeter beam and perimeter column. Because beam elements are used for beams and columns, not all nodal temperatures are needed. The recommendation by ABAQUS [19] is to use five temperature points for 3D beam elements, as shown in Fig. 5.9.

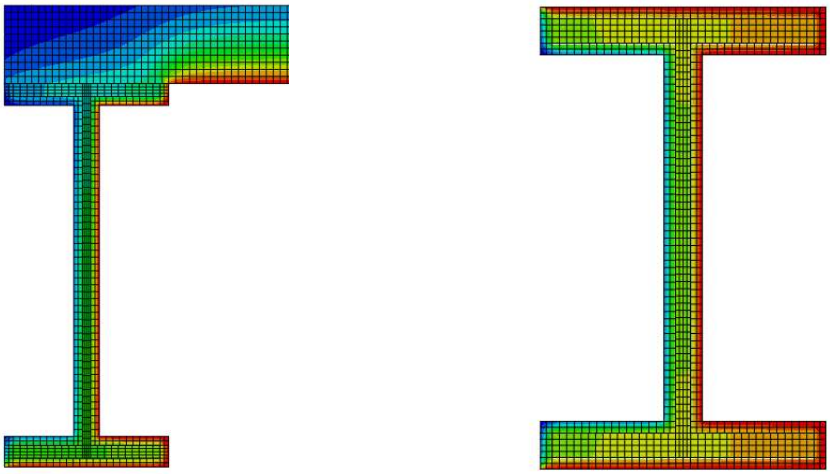

Fig. 5.8. *Temperature distribution in (a) perimeter beam, and (b) perimeter column*

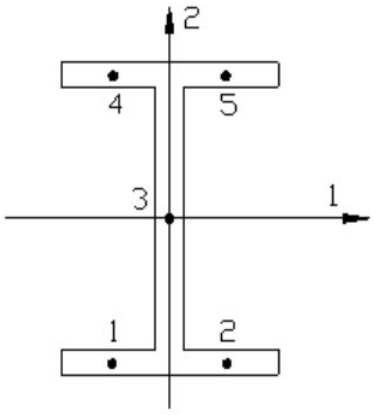

Fig. 5.9. *Temperature points for 3D beam element*

Because the structural model for the profiled concrete slab uses flat shell elements of uniform thickness with three layers (i.e., lower concrete layer, reinforcement layer, and upper concrete layer, as shown in Table 5.1), only five temperature points are needed for slab shell elements. The levels to determine temperature points are shown in Fig. 5.10, where N3 (i.e., temperature point for reinforcement layer) is taken at the real level of reinforcement, N1 (i.e., temperature point for the bottom of lower layer) is taken at the level of equivalent uniform thickness. The equivalent uniform thickness is calculated as the average thickness of the upper continuous portion and rib depth of the slab, as follows:

$$d = a + b/2 \tag{5-15}$$

where d = the equivalent thickness of the flat shell element, a = the thickness of the upper concrete portion above steel deck, b = the depth of metal deck, as shown in Fig. 5.10.

The temperature points for three layers of shell elements are described in Table 5.1.

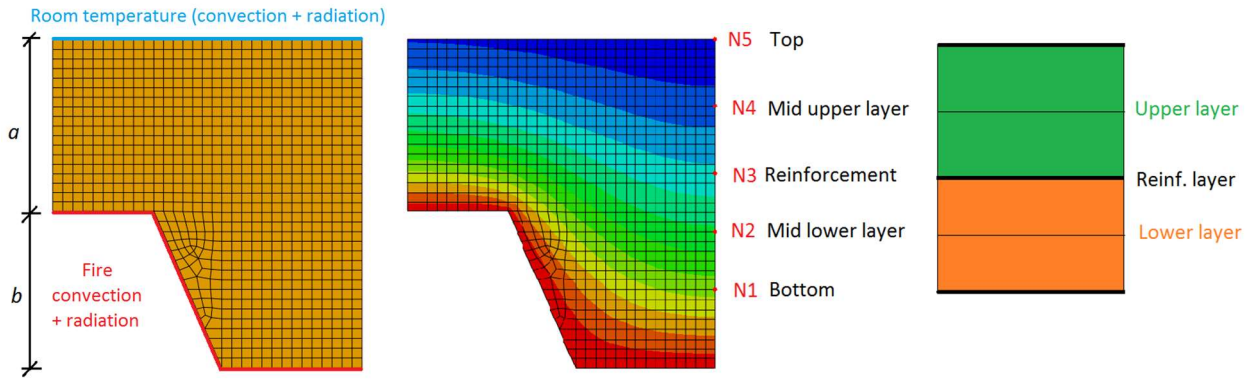

Fig. 5.10. *Half-model of slab: thermal boundary condition and temperature distribution*

Table 5.1. *Three layers of uniform-thickness composite shell elements*

Layer	Material	Temperature points
Lower layer	Concrete	3 points: N1, N2, N3
Reinforcement layer	Steel	1 point: N3
Upper layer	Concrete	3 points: N3, N4, N5

5.2.2. Structural analysis

The structural analysis is used to predict the force-deformation response of building structures under combined fire and progressive collapse. The loads in the structural analysis include the gravity loads and lateral loads. The fire load is applied on the structure in the form of elevated temperatures in the structural members (i.e., the output data of the thermal analysis).

Both material and geometric non-linearities are considered in the structural analyses. The concrete damaged-plasticity model available in ABAQUS was used to represent the inelastic behavior of concrete, while the classical metal plasticity model available in ABAQUS, using the von Mises yield criterion, was used to represent the plasticity of structural steel (for beams and columns) and steel mesh (in slabs). ABAQUS uses the true stresses and strains (i.e., true plastic strain for steel,

and true inelastic strain for compressive behavior of concrete), which can be converted from nominal stresses and strains, as follows:

$$\sigma_{tru} = \sigma_{nom}(1+\varepsilon_{nom}) \tag{5-17}$$

$$\varepsilon_{tru} = ln(1+\varepsilon_{nom}) \tag{5-18}$$

$$\varepsilon_{pl} = \varepsilon_{tru} - \frac{\sigma_{tru}}{E}, \text{ where } E = \frac{\sigma_p}{\varepsilon_p} \tag{5-19}$$

$$\varepsilon_{inel} = \varepsilon_{tru} - \frac{\sigma_p}{E} \tag{5-20}$$

where σ_{tru} = true stress; σ_{nom} = nominal stress; ε_{tru} = true strain; ε_{nom} = nominal strain; ε_{pl} = true plastic strain; ε_{inel} = true inelastic strain; ε_{pl} = true elastic modulus; σ_p = true proportional/elastic stress = first nonzero true stress; ε_p = true proportional/elastic strain = first nonzero true strain.

Temperature-dependent stress-strain relationships (i.e., σ-ε-T constitutive model) of steel and concrete follow Eurocode 4 [14], which also appear in Eurocode 3 [15] for steel and Eurocode 2 [16] for concrete. The thermal expansion of steel and concrete are also taken from Eurocode 4 [14].

More specifically, the temperature-dependent stress-strain relationship of steel is shown in Fig. 5.11, and Table 5.2 and 5.3.

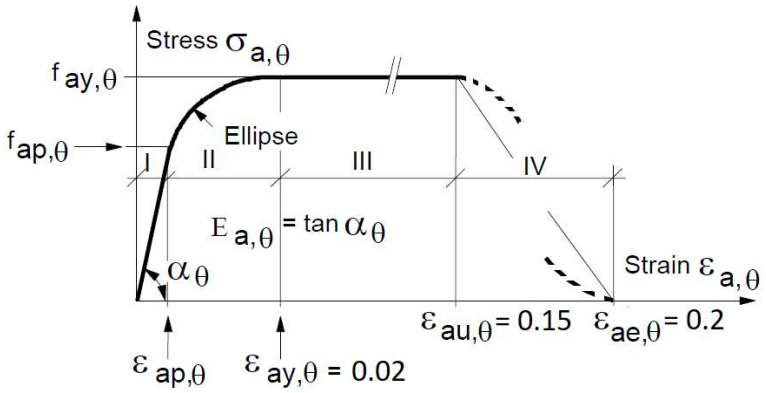

Fig. 5.11. *Stress-strain relationship of steel at elevated temperatures*

where $E_{a,\theta}$ = the slope of the linear elastic range; $f_{ap,\theta}$ = the proportional limit; $f_{ay,\theta}$ = the maximum stress level or effective yield strength.

Table 5.2. *Relation between the parameters of the model in Fig. 5.12*

Strain range	Stress	Tangent modulus
I. Elastic $\varepsilon \le \varepsilon_{ap,\theta}$	$E_{a,\theta}\varepsilon_{a,\theta}$	$E_{a,\theta}$
II. Transit elliptical $\varepsilon_{ap,\theta} \le \varepsilon \le \varepsilon_{ay,\theta}$	$\left(f_{ap,\theta}-c\right)+\frac{b}{a}\sqrt{a^2-\left(\varepsilon_{ay,\theta}-\varepsilon_{a,\theta}\right)^2}$ where $a^2=\left(\varepsilon_{ay,\theta}-\varepsilon_{ap,\theta}\right)\left(\varepsilon_{ay,\theta}-\varepsilon_{ap,\theta}+c/E_{a,\theta}\right)$ $b^2=E_{a,\theta}\left(\varepsilon_{ay,\theta}-\varepsilon_{ap,\theta}\right)c+c^2$ $c=\frac{\left(f_{ay,\theta}-f_{ap,\theta}\right)^2}{E_{a,\theta}\left(\varepsilon_{ay,\theta}-\varepsilon_{ap,\theta}\right)-2\left(f_{ay,\theta}-f_{ap,\theta}\right)}$	$\frac{b\left(\varepsilon_{ay,\theta}-\varepsilon_{a,\theta}\right)}{a\sqrt{a^2-\left(\varepsilon_{ay,\theta}-\varepsilon_{a,\theta}\right)^2}}$
III. Plastic $\varepsilon_{ay,\theta} \le \varepsilon \le \varepsilon_{au,\theta}$	$f_{ay,\theta}$	0

Table 5.3. *Reduction factor for stress-strain relationship of steel at elevated temperatures*

Steel temperature θ_a (°C)	$k_{E,\theta}=\frac{E_{a,\theta}}{E_a}$	$k_{p,\theta}=\frac{f_{ap,\theta}}{f_{ay}}$	$k_{y,\theta}=\frac{f_{ay,\theta}}{f_{ay}}$
20	1.00	1.00	1.00
100	1.00	1.00	1.00
200	0.90	0.807	1.00
300	0.80	0.613	1.00
400	0.70	0.420	1.00
500	0.60	0.360	0.78
600	0.31	0.180	0.47

700	0.13	0.075	0.23
800	0.09	0.050	0.11
900	0.0675	0.0375	0.06
1000	0.0450	0.0250	0.04
1100	0.0225	0.0125	0.02
1200	0	0	0

The temperature-dependent stress-strain relationship of concrete in compression is shown in Fig. 5.12 and Table 5.4. The tensile strength of concrete is assumed to be a tenth of the compressive strength or conservatively, it can be assumed to be zero.

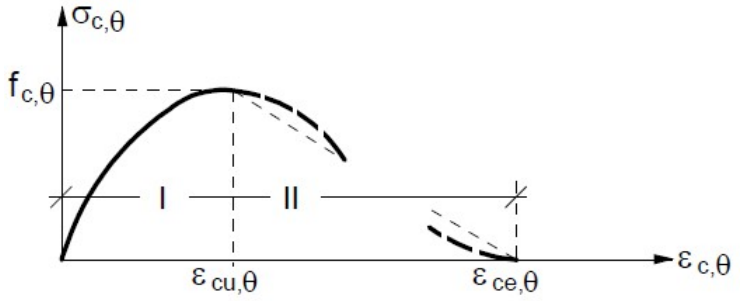

Fig. 5.12. *Stress-strain relationship of concrete under compression at elevated temperatures*

where Phase I (i.e., $\varepsilon_{c,\theta} \le \varepsilon_{cu,\theta}$), $\sigma_{c,\theta} = f_{c,\theta} \dfrac{3\left(\varepsilon_{c,\theta}/\varepsilon_{cu,\theta}\right)}{2+\left(\varepsilon_{c,\theta}/\varepsilon_{cu,\theta}\right)^3}$ (5-21)

Phase II (i.e., $\varepsilon_{cu,\theta} < \varepsilon_{c,\theta} \le \varepsilon_{ce,\theta}$) should be a descending branch for numerical purpose. In this study, a linear descending brand was adopted.

Table 5.4. *Parameters of the model in Fig. 5.12 for concrete at elevated temperatures*

Concrete temperature θ_a (°C)	$k_{p,\theta} = \dfrac{f_{ap,\theta}}{f_{ay}}$		$\varepsilon_{cu,\theta}.10^3$
	Normal concrete	Lightweight concrete	
20	1.00	1.00	2.5
100	1.00	1.00	4.0

200	0.95	1.00	5.5
300	0.85	1.00	7.0
400	0.75	0.88	10
500	0.60	0.76	15
600	0.45	0.64	25
700	0.30	0.52	25
800	0.15	0.40	25
900	0.08	0.28	25
1000	0.04	0.16	25
1100	0.01	0.04	25
1200	0	0	-

Fig. 5.13 illustrates the stress-strain relationship of steel ASTM A992 and lightweight concrete at 20°C, 400°C, and 600°C.

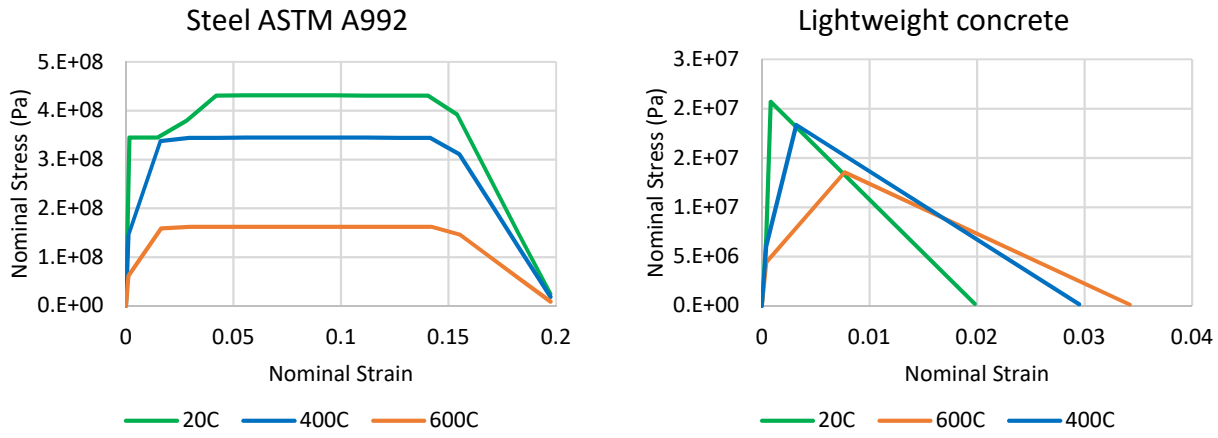

Fig. 5.13. *Stress-strain curves for structural steel ASTM A992 and lightweight concrete*

The thermal elongation of steel $\Delta l/l$ is determined as follows [14,15]:

$$\Delta l/l = 1.2\times10^{-5}\theta + 0.4\times10^{-8}\theta^2 - 2.416\times10^{-4},\ 20°C \le \theta < 750°C \quad (5\text{-}22)$$

$$\Delta l/l = 1.1\times10^{-2},\qquad 750°C \le \theta \le 860°C \quad (5\text{-}23)$$

$$\Delta l / l = 2\times10^{-5}\theta - 6.2\times10^{-3}, \qquad 860°C < \theta \le 1200°C \tag{5-24}$$

Similarly, the thermal elongation of normal concrete $\Delta l / l$ is determined as follows [14,16]:

$$\Delta l / l = 0.9\times10^{-5}\theta + 2.3\times10^{-11}\theta^3 - 1.8\times10^{-4}, \qquad 20°C \le \theta < 700°C \tag{5-25}$$

$$\Delta l / l = 1.4\times10^{-2}, \qquad 700°C \le \theta \le 1200°C \tag{5-26}$$

The thermal elongation of lightweight concrete $\Delta l / l$ is given as follows [14]:

$$\Delta l / l = 0.8\times10^{-5}(\theta - 20) \tag{5-27}$$

In Eqs. (5-21) – (5-26), l= the length at 20°C; Δl = the temperature-induced elongation; θ= the temperature of the material (°C). Fig. 5.14 shows the variation with temperature of the thermal elongation of steel, normal concrete, and lightweight concrete.

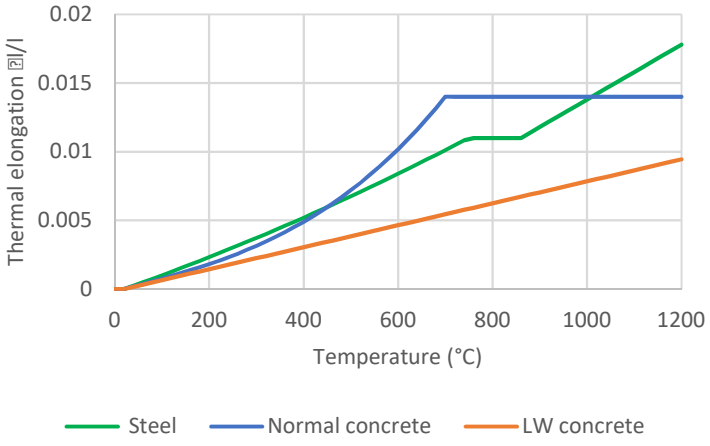

Fig. 5.14. *The thermal elongation of steel, normal concrete, and lightweight (LW) concrete*

The macro-element model for the 3D structural analysis follows a common approach used in prior studies on fire-induced progressive collapse. More specifically, the steel beams and columns are modeled with 3D 2-node linear beam-column elements (i.e., B31 type in ABAQUS); and the concrete slabs are modeled with linear 4-node doubly curved thin/thick shell elements (i.e., S4R type in ABAQUS) with composite layers. The 3D model for an entire framed building is illustrated in Fig. 5.15.

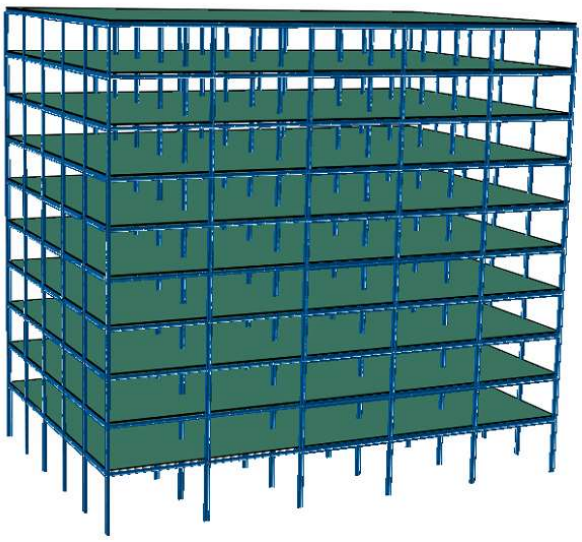

Fig. 5.15. *3D simulation model for a framed building*

The ribbed reinforced concrete slab is modeled as a flat shell whose thickness is equal to the average thickness of the upper continuous portion and rib depth of the slab, as detailed in Eqn. (5-15) and Fig. 5.16. The steel mesh in the floor slab is modeled as an equivalent smeared layer with thickness equal to the area of one reinforcing bar divided by its spacing, as follows:

$$t_{equiv.} = A_{mesh} / s \tag{5-28}$$

where $t_{equiv.}$ = equivalent thickness of the steel mesh layer; A_{mesh} = the cross-section area of steel mesh; s = the spacing between steel rebars. For example, mesh A185 (i.e., A_{mesh} = 185 mm^2/m) is equivalent to a layer with a thickness of 0.185 mm.

The steel deck of the composite slab was not modeled in the 3D analysis because of its insignificant contribution to the stiffness and load-bearing capacity of the floor system, and the observation from real fire events that steel deck tends to detach from concrete slab during fire [3].

Beam-to-column connections were modeled as simple joints (i.e., moment connections as fully fixed joints, and shear connections as pinned joints) using kinematic coupling constraints in ABAQUS for computational efficiency.

The composite interaction between the steel beams and concrete slabs was modeled as fully fixed. In ABAQUS, kinematic coupling constraints, where all 6 degrees of freedom are fixed, were used. Slabs were connected to beams at the location of studs, via node-to-node coupling constraints.

Some research investigated the effect of shear studs (e.g. Huang et al. [7]) using spring elements with finite stiffness to represent composite interaction between steel beam and concrete slab. Although a partial-interaction model can capture more accurately the floor response [7], the modeling approach requires significantly higher computational cost. Moreover, before shear studs fail (which is not as usual as failures around beam-to-column connection areas and stability failure in columns during fire), there is little difference in results between partial- and full-interaction model. Therefore, it is acceptable to consider the composite interaction between steel beams and concrete slabs as fully fixed constraints. It is noted that there is no interaction (or constraint) between steel columns and concrete slabs.

To preserve the moment of inertia of the composite section, the location of the top surface of the slab is preserved in this study, resulting in an offset between the slab and beam. Regarding the reference plane of beams (i.e., beam elements) and slabs (i.e., composite shell elements), an "interface" approach was used, in which the reference plane of slab and that of beam were placed at the top level of beam, as shown in Fig. 5.16.

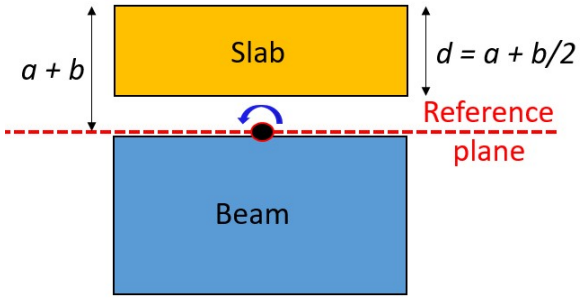

Fig. 5.16. *Reference plane of slab and beam. Note: a, b, and d are defined in Eqn. (5-15)*

An explicit dynamic analysis is used to model the structural response up to the point of global instability. The computational cost of an explicit dynamic analysis is significantly dependent on the number of degrees of freedom or the mesh size. The finer the mesh is, the higher the processing time is. For modeling the composite slab, it is the most accurate to divide the mesh of the slab at the locations of studs, where the slab connects with the steel beam. However, for better computational efficiency, it is acceptable to use a coarser mesh as long as the results are insignificantly affected, which is determined by a sensitivity analysis. It is noted that the best mesh size varies depending on the structure, the fire duration and the mass- and time-scaling factors for

explicit analysis. For the structures considered in this dissertation, a mesh size of 0.6-1.0 m, along with x10 mass-scaling and small time-scaling (i.e., 10 time units ~ 1 min of fire), was adequate.

Following the typical approach in progressive collapse design, this research uses the UFC [13] Alternate Path method to analyze a composite steel frame structure subjected to fire-induced progressive collapse hazard. In the Alternate Path method, the applied loads include gravity loads and lateral loads. Two acceptable approaches in the UFC [13] are the nonlinear static analysis and the nonlinear dynamic analysis. For the nonlinear static analysis, the gravity load is artificially increased on the floor areas above the removed column to simulate the dynamic effect. The UFC [13] provides formulae to determine the magnitudes of applied loads, which are presented here for clarity. Because the load factors are consistent with the extreme load condition, they are deemed to be appropriate for fire-induced collapse analysis.

In the 3D model, to capture the realistic effect of fire on the removal of column(s) as well as the progression of the structural response afterwards, the nonlinear dynamic analysis (using ABAQUS explicit dynamic analysis) is recommended. The scenario involves fixed-load increased-temperature.

The gravity loads for the entire structure are calculated as [13]

$$G_{ND} = (0.9\,or\,1.2)D + (0.5L\,or\,0.2S) \tag{5-29}$$

where G_{ND} = gravity load used in the nonlinear dynamic analysis; D = dead load; L = live load; S = snow load.

The lateral loads for each floor are applied according to the following equation:

$$L_{LAT} = 0.002\sum P \tag{5-30}$$

where L_{LAT} = lateral load; $\sum P$ = sum of gravity loads acting on only that floor.

In the nonlinear dynamic approach, Step 1 involves gradually applying the gravity and lateral loads, as given in Eqs. (5-29) and (5-30), to the structure at room temperature (i.e., ramped slowly and then maintained for a sufficiently long period to minimize dynamic effects) until the structure

stabilized. Step 2 involves applying elevated temperatures to structural members within the heated area using "predefined fields" in ABAQUS to simulate the effect of fire. These elevated temperatures are the outputs from the thermal analysis (described in Section 5.2.1). During Step 2, the heated columns which experience buckling instability are considered as removed columns. The buckling instability is quantitatively indicated in the time history of internal forces (i.e., the substantial decrease in axial forces of those columns, coupled with increase in axial forces of the adjacent columns) and lateral displacements of those columns, as illustrated in Fig. 5.17. Because the explicit dynamic analysis can numerically overcome local instability, the analysis continues to progress until excessive failures occur. It is important to note that the time when the analysis terminates may not be the time of building failure. The time of building failure, is determined based on three criteria (detailed in Section 2.3), which varies based on the performance level that the building is design for.

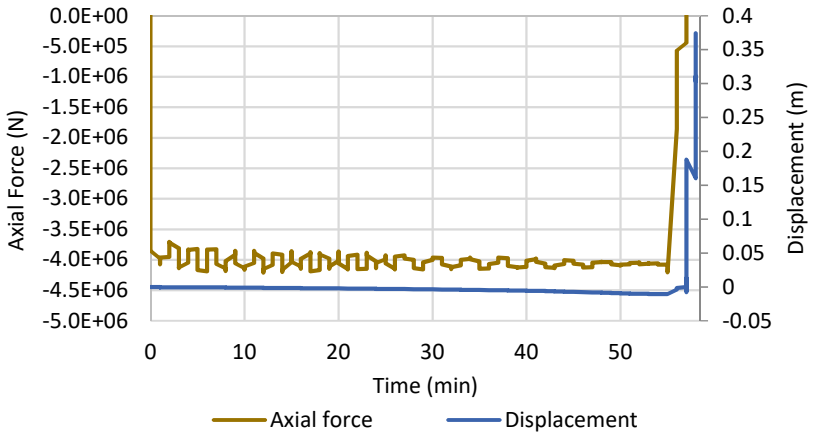

Fig. 5.17. *Axial force and lateral displacement of a removed column (illustration only)*

Unlike the 2D model where the failed column(s) is manually removed from the structure at a fixed elevated temperature, the 3D model with dynamic analysis allows the unstable columns to be automatically removed from the system and their loads to be redistributed to the adjacent columns. This is another advantage of the 3D model.

In terms of fire load, it is necessary to consider all possible fire scenarios in the building. Regarding the location of fire, both vertical location (i.e., lower floor, middle floor, upper floor) and horizontal location (i.e., which compartment on a single story is subjected to fire) are important.

Fig. 5.18 illustrates some different cases of fire location. Additionally, depending on the functionality of the building and other design objectives, different types of fire should be considered such as standard fire vs. parametric fire, or fire without cooling vs. fire with cooling phase. Eurocode 1 [18] provides details on calculating gas temperature for various fire curves.

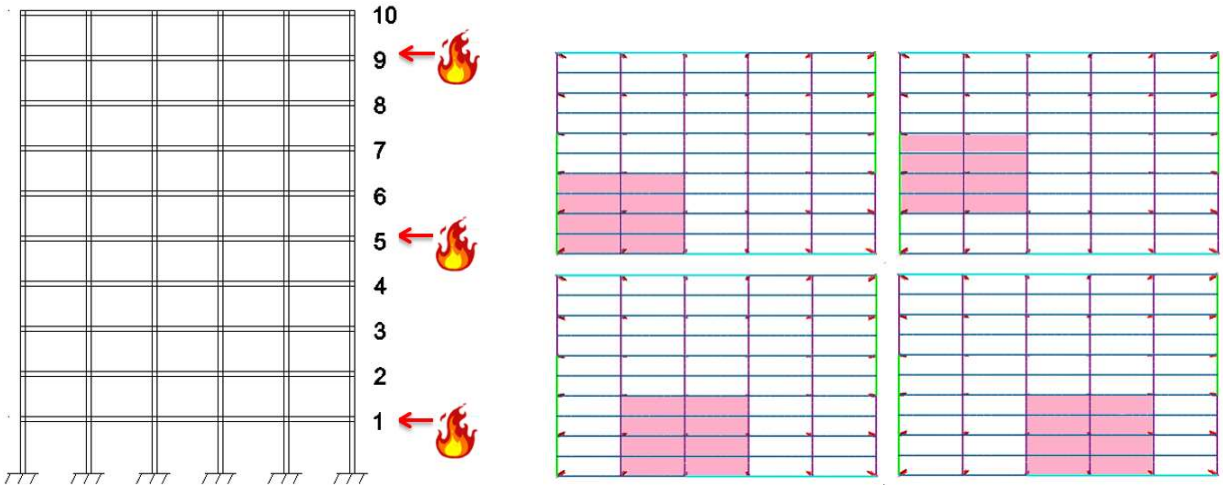

Fig. 5.18. *Cases of fire location in a building: (a) vertical location, and (b) horizontal location*

5.3. Validation

The Cardington corner compartment test (i.e., Cardington fire test 3) [1] was used to validate the 3D macro-element model for analyzing composite structures in fire.

5.3.1. Test set-up

The Cardington Fire Tests were carried out on an 8-story composite framed building. The corner compartment test was performed on the third floor, as shown in Fig. 5.19. Three sections were used for beams and two sections were used for columns. Steel grade S355 was used for columns while steel grade S275 and S355 were used for beams [19], as shown in Table 5.5. The slab was 70-mm lightweight concrete on top of 60-mm-high trapezoidal steel deck, and anti-cracking A142 steel mesh (i.e. 6mm- bars spacing 200mm) in both directions was used for reinforcement [10]. Table 5.6 describes the yield strength of materials, where test values were achieved from measurement in experiment and used in the computational analysis. The mechanical and thermal properties of materials at elevated temperatures follow Eurocode 4 [14].

The columns, beam-to-column connections, and edge beams were protected with 25-mm ceramic fiber, while the rest of steel work including beam-to-beam connections were left unprotected [10]. The design gravity load of 5.48 kN/m^2 were simulated by placing sandbags and spread evenly on the entire floor. Fig. 5.20 describes the gas temperature within the compartment fire.

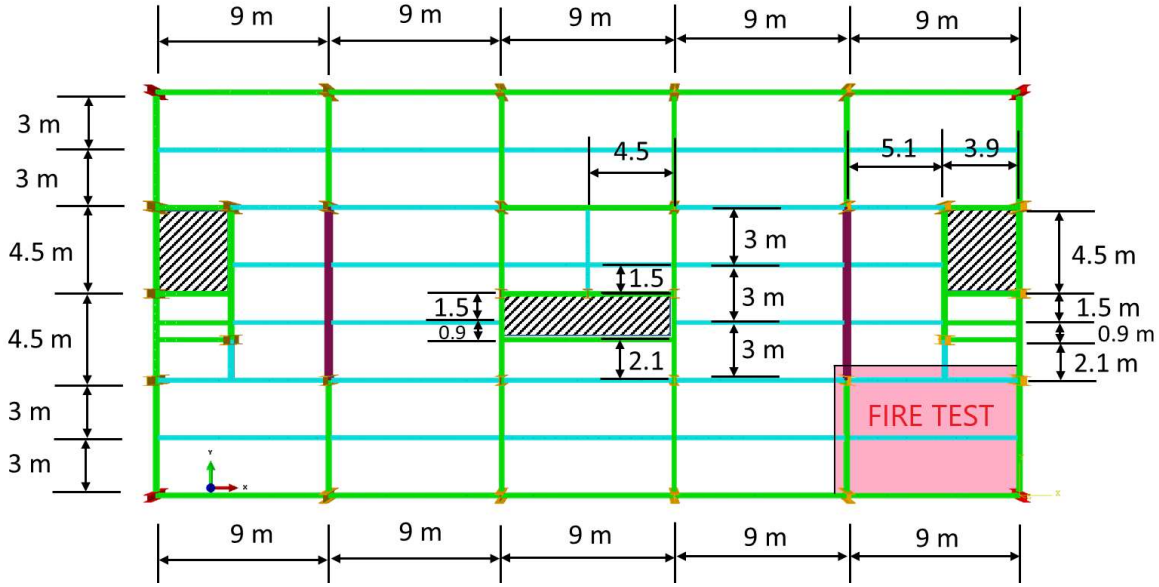

Fig. 5.19. *Floor layout and location of Cardington corner fire test*

Table 5.5. *Details of beams and columns in the Cardington test 3 (corner compartment test)*

	Beam			Column	
Color code	Green	Blue	Purple	Corner (Red)	Other (Orange)
Section size	356x171x51 UB	305x165x40 UB	610x229x101 UB	254x254x89 UC	305x305x137 UC
Steel grade	S355	S275	S275	S355	S355

Table 5.6. *Yielding strength (i.e., tension for steel and compression for concrete)*

	Tested Values (MPa)	Nominal Values (MPa)
Steel grade S275	308	275
Steel grade S355	390	355

Steel mesh	460	460
Concrete	35	35

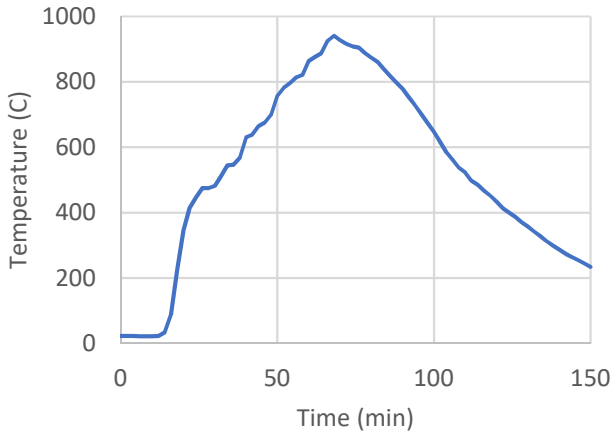

Fig. 5.20. *Gas temperature of the fire test*

5.3.2. Simulation and results

The simulation model follows the methodology presented in Section 5.2. A sequentially coupled thermal analysis and (explicit dynamic) structural analysis was adopted using ABAQUS. The experimental gas temperature was input into the thermal analysis to determine the temperatures in concrete slab, beams, and columns. These calculated temperatures were then input into the structural analysis as the "predefined fields" applied on structural members. Geometric and material nonlinearity was considered in the analysis. Because only a small part of the building (i.e., a corner compartment of the third floor) was on fire, the 3D model only included half of the third floor, which contains the heated compartment. 2-node beam elements (B31) represented beams and columns, 4-node shell elements (S4R) represented slabs, and kinematic coupling constraints represented the connections and composite interaction. The mesh size for slab was 0.3 m. The boundary conditions were applied to the bottom and top of all the columns, along the symmetric axis, and along the beams which connected to the rigid walls, as described in Fig. 5.21. Material properties were taken from Eurocode 4 [14].

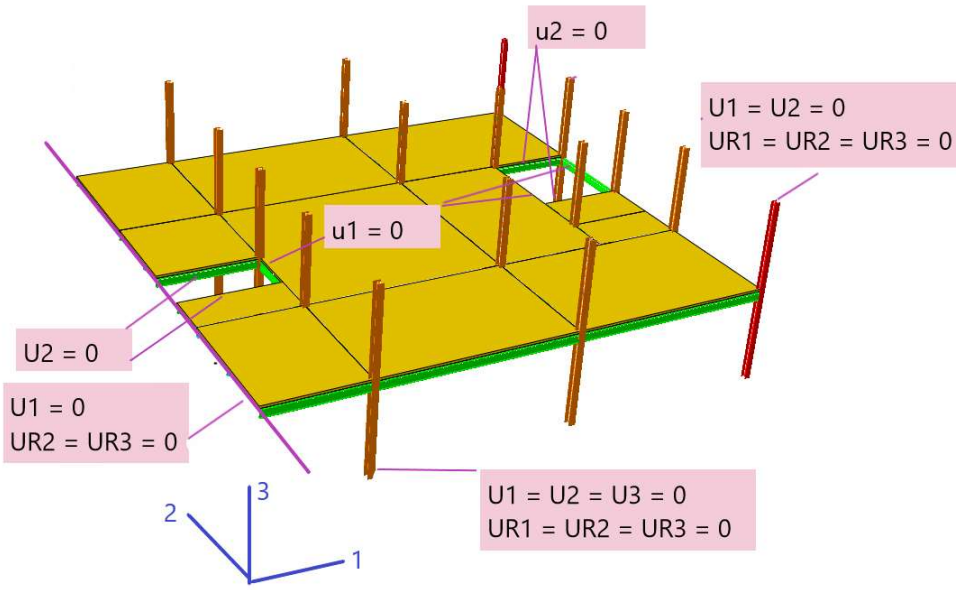

Fig. 5.21. *Boundary conditions for the Cardington model*

The validation was based on comparison between FE results and experimental data corresponding to member temperatures and displacements of the beams and slabs. As can be seen in Fig. 5.22 and Fig. 5.23, the thermal analysis provided a good correlation with the test data for beams and acceptable correlation for slab, where the peaks in calculated temperatures were higher than those measured in the experimental test by 50-200°C. The large difference in temperature in slabs between FE model and test data can come from several sources: (1) the thermal properties for concrete at elevated temperature following Eurocode were different from the test reality due to the evaporation of water in the concrete and the nature of concrete as a composite material; (2) the boundary conditions used in the thermal analysis may not be the same as what happened in the test.

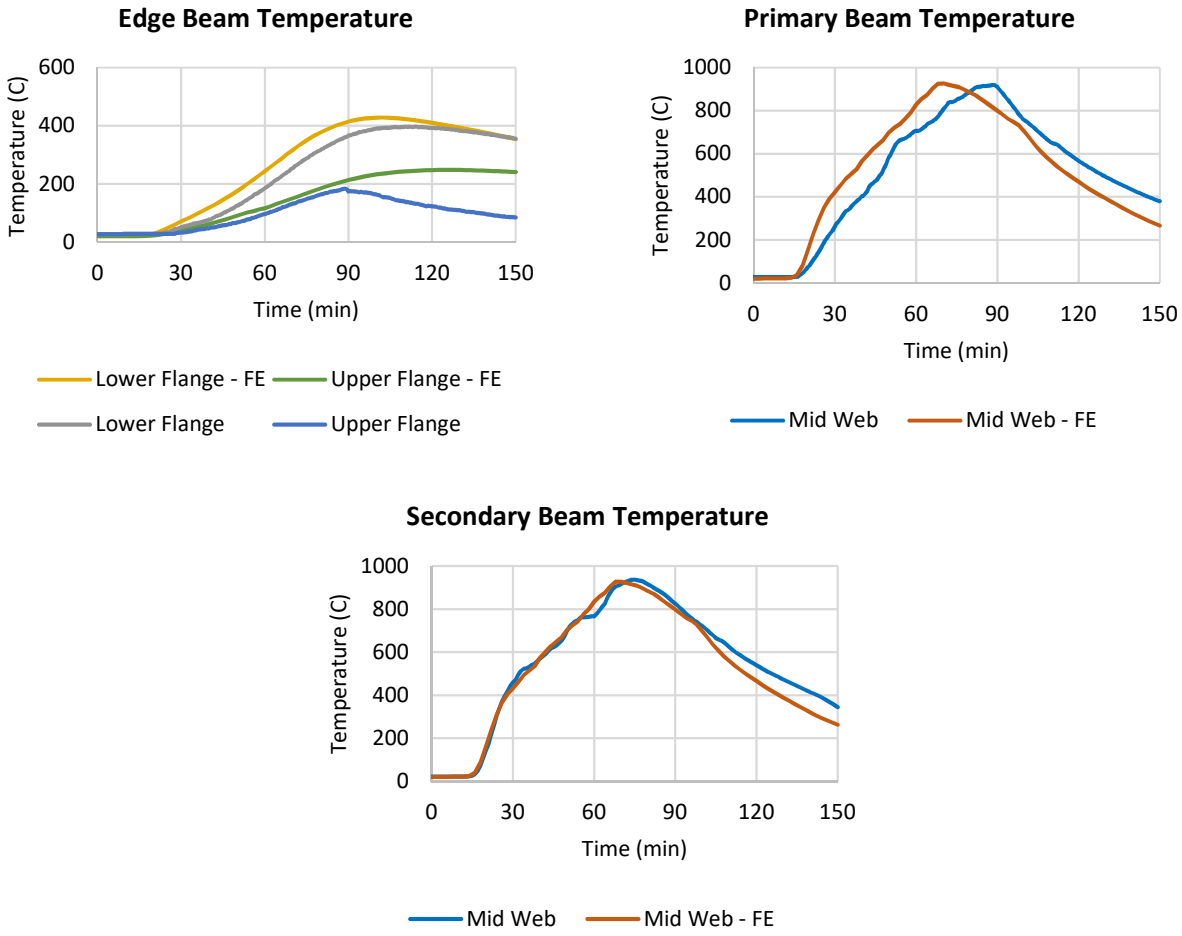

Fig. 5.22. *Temperature in beams (calculated values vs. test values)*

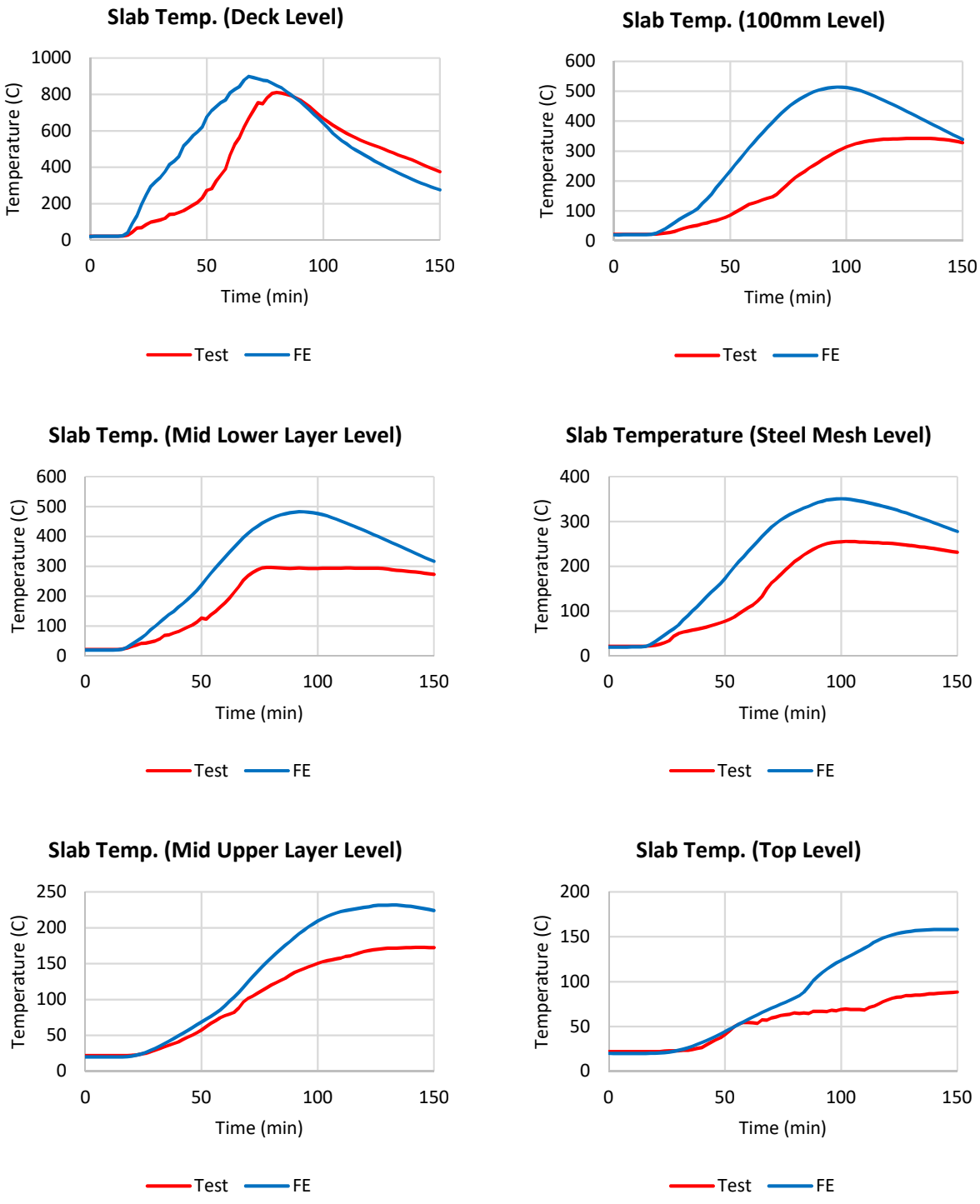

Fig. 5.23. *Temperatures in slabs (calculated values vs. test values)*

Regarding the structural analysis, Fig. 5.24 shows the deformed shape of the building with displacement contour. The correlation between the FE analysis and test data was indicated in Fig. 5.26, where the vertical displacements of the beams were plotted against time and maximum

temperatures in the beams, and in Fig. 5.27, where the vertical displacements of the slabs were plotted against time and temperature in the steel mesh of slabs.

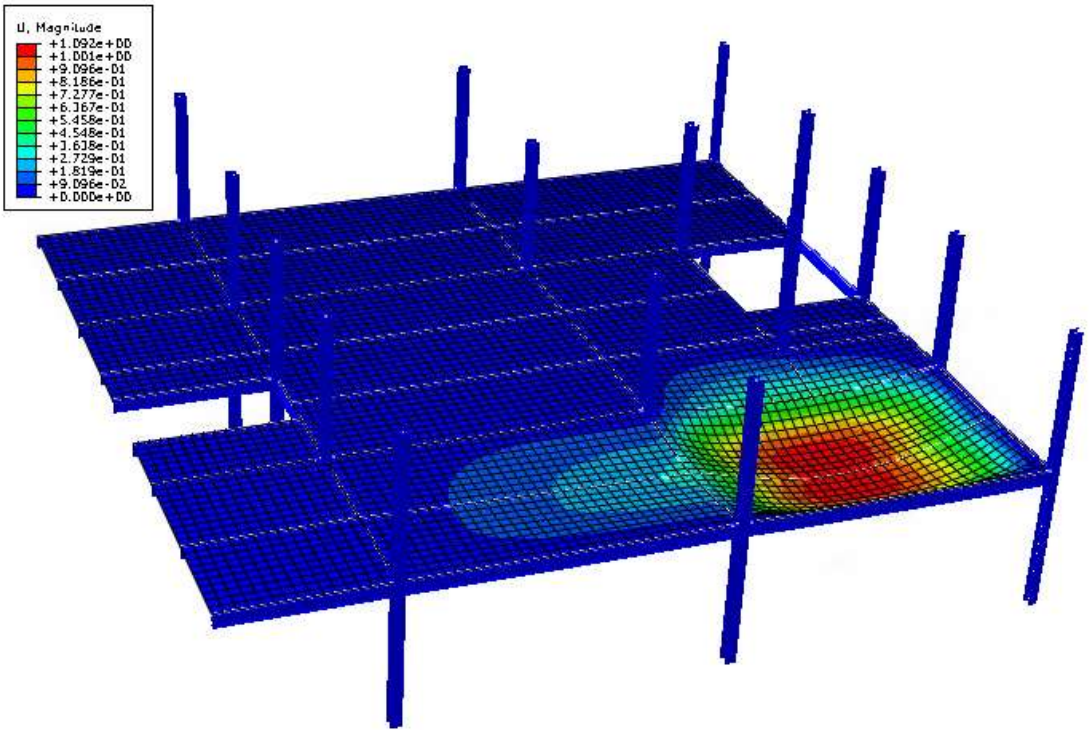

Fig. 5.24. *Deformed shape and displacement contour at the end of the structural analysis*

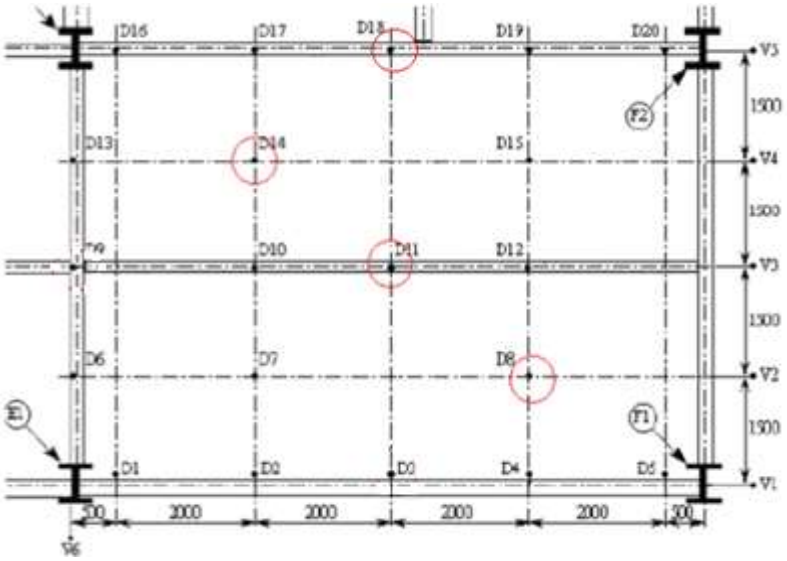

Fig. 5.25. *The location of displacement measurement in the corner test* [1]

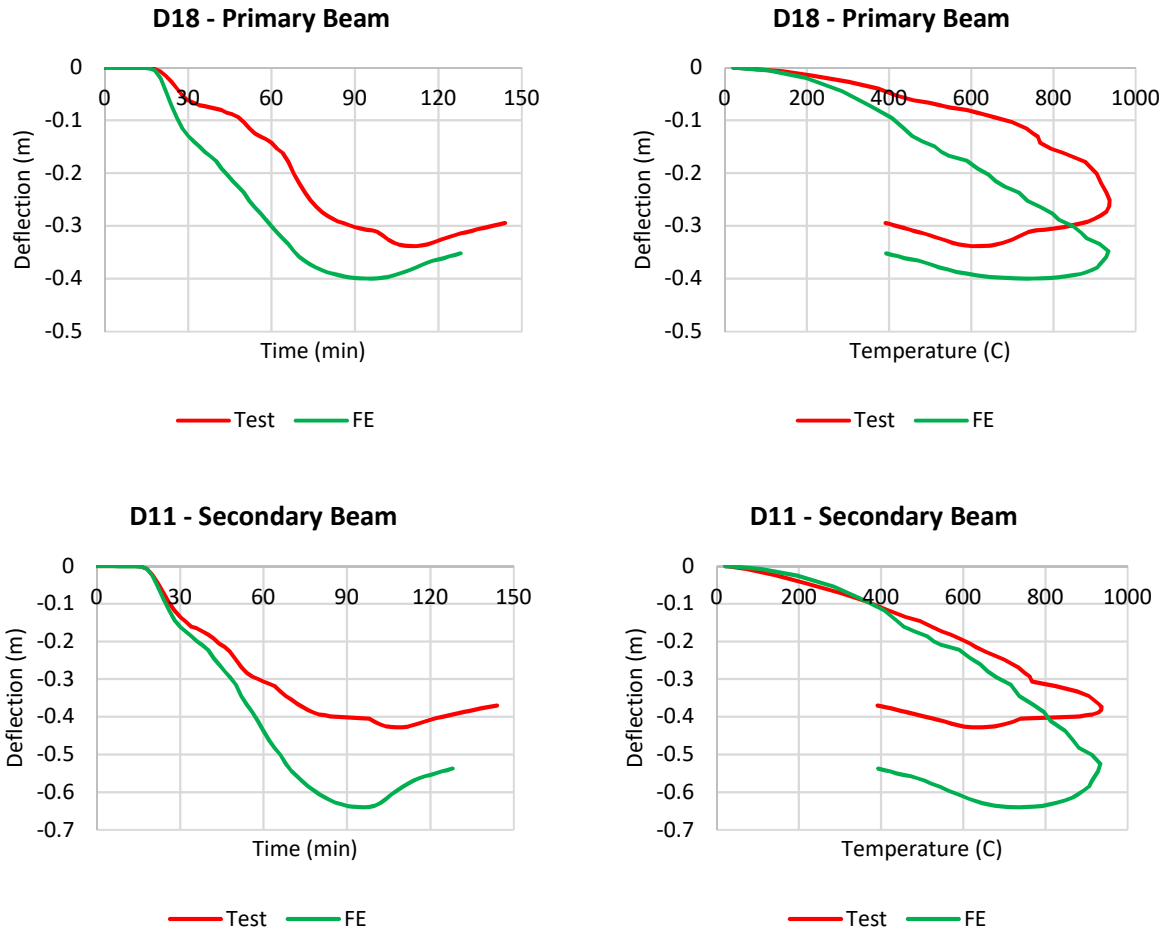

Fig. 5.26. *Beams: deflection vs. time and deflection vs. maximum temperature*

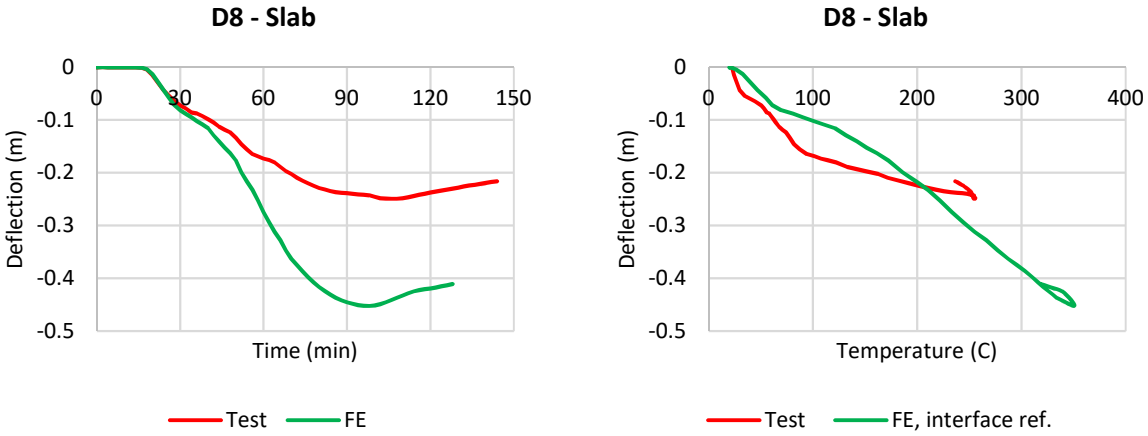

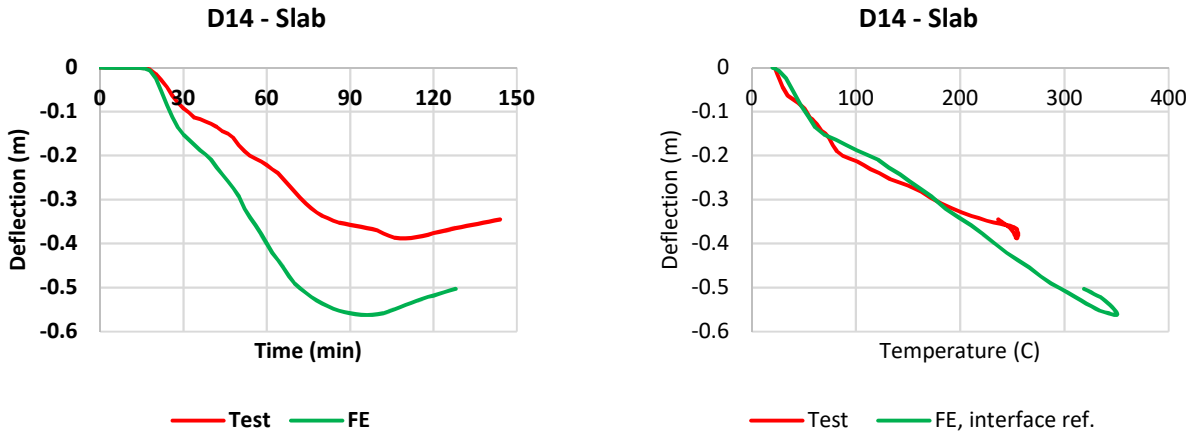

Fig. 5.27. *Slabs: deflection vs. time and deflection vs. temperature in steel mesh*

As can be seen in Fig. 5.26 and 5.27, the FE predicted higher deflections than the test data, and the plot of deflections against temperatures shows a better correlation than the plot of deflections against time. The possible reason is that the FE model used the calculated temperatures, which were higher than the tested temperatures and in the experiment, the room and structural members were not heated uniformly as assumed in the computational analysis. Thus, the FE model had a higher fire load, resulting in lower predicted robustness than the reality. However, it is acceptable in computational analysis that the FE results tend to be more conservative than the experimental data.

5.4. Conclusions and limitations

Chapter 5 presents the 3D macro-element model that is used to analyze and evaluate the structural performance of a composite building under fire-induced progressive collapse hazards. The 3D analysis uses beam-column elements to model the steel beams and columns, composite shell elements to model the reinforced concrete slabs, and kinematic coupling constraints to model the idealized connections and full composite interaction. The adopted approach uses a sequentially coupled thermal analysis to simulate fire-induced temperatures within structural members and a dynamic structural analysis to predict structural response to elevated temperatures and the loss of column. Explicit dynamic analysis in ABAQUS was used with consideration for material and geometric nonlinearity. Despite high computational cost, this method can provide more accurate and realistic prediction than a nonlinear static analysis. The simulation scenario involves fixed-load increased-temperature, and the loading is applied in two steps: (1) gravity loads are gradually

applied at room temperature and kept constant until the structure stabilizes, and (2) elevated temperatures are applied to structural members to simulate the dynamic effect of fire. During the second step, one or two columns start to buckle and the load is redistributed to the adjacent columns through the composite floor system.

It is noted that while the simplified beam-to-column connection model (using a system of nonlinear springs to represent components of connection) is a cost-effective method to accurately predict structural response in fire, it was not included in the 3D model due to high computational costs associated with the explicit dynamic model. Further 3D analyses with the macro-element connection model can be conducted in the future to provide more accurate prediction.

In nonlinear dynamic analysis used in 3D model, fixed-load increased-temperature scenario is adopted to simulate fire-induced progressive collapse events. The loss of a column happens automatically in the dynamic analysis during the growing progress of fire; whereas in the static analysis used in 2D model with fixed-temperature increased-load, the loss of a column is manually imposed on the structure. Therefore, 3D model can provide more realistic prediction than 2D model.

The appropriateness of the 3D model is proved via the good correlation between the computational results and experimental data of the Cardington fire test 3. It was also found that the consideration of latent heat of concrete had a significant effect on the predicted temperature of the upper part but insignificant effect on that of the lower part of concrete slab.

Reference

[1] SteelConstruction.info. “Cardington Fire Test Data.” <http://www.steelconstruction.info/Cardington_fire_test_data> (Jul. 1, 2017)

[2] Bailey, C. G., Lennon, T., Moore, D. B. (1999). “the Behavior of Full-Scale Steel-Framed Buildings Subjected to Compartment Fires.” *The Structural Engineer*, v 77 (8), 15-21.

[3] Bailey, C. G. (2001). “Membrane Action of Unrestrained Lightly Reinforced Concrete Slabs at Large Displacements.” *Engineering Structures*, v 23 (5), 470-483.

[4] Bailey, C.G. (2004). “Membrane Action of Slab/Beam Composite Floor Systems in Fire.” *Engineering Structures*, v 26 (12), 1691–1703.

[5] Alashker, Y., El-Tawil, S., Sadek, F. (2010) “Progressive Collapse Resistance of Steel-Concrete Composite Floors.” *J. Structural Engineering*, v 136 (10), 1187-1196.

[6] Agarwal, A., Varma, A. (2014). “Fire Induced Progressive Collapse of Steel Building Structures: The Role of Interior Gravity Columns.” *Engineering Structures*, *58,* 129-140.

[7] Huang, Z., Burgess, I., Plank, R. (1999). “The Influence of Shear Connectors on The Behavior of Composite Steel-Framed Buildings in Fire.” *J. Constructional Steel Research*, v 51, 219-237.

[8] Lamont, S., Usmani, A. S. (2003). “Possible ‘Panel Instability’ in Composite Deck Floor Systems under Fire.” *J. Constructional Steel Research*, v 59, 1397-1433.

[9] McAllister, T., MacNeill, R., Erbay, O., Sarawit, A., Zarghamee, M., Kirkpatrick, S., Gross, J. (2012). “Analysis of Structural Response of WTC 7 to Fire and Sequential Failures Leading to Collapse.” ASCE J. Structural Engineering, v 138(1), 109-117.

[10] Elghazouli, A., Izzuddin, B. (2004). “Realistic Modeling of Composite and Reinforced Concrete Floor Slabs under Extreme Loading. II: Verification and Application” *J. Structural Engineering*, v 130 (12), 1985-1996.

[11] Sadek, F., El-Tawil, S., Lew, H. S. (2008). “Robustness of Composite Floor Systems with Shear Connections: Modeling, Simulation, and Evaluation.” *J. Structural Engineering*, v 134 (11), 1717-1725.

[12] Alashker, Y., Li H., El-Tawil S. (2011). “Approximations in Progressive Collapse Modelling.” *Structural Engineering*, v 137 (9), 914-924.

[13] Unified Facilities Criteria. (2009). “Design of Buildings to Resist Progressive Collapse. Department of Defense.” Washington, D.C.

[14] Eurocode 4. (2005). “Design of Composite Steel and Concrete Structures, Part 1-2: General Rules - Structural Fire Design.” *Commission of European Communities*, Brussels, Belgium.

[15] Eurocode 3. (2005). “Design of Steel Structures, Part 1-2: General Rules for Structural Fire Design.” *Commission of European Communities*, Brussels, Belgium.

[16] Eurocode 2. (2004). “Design of Concrete Structures, Part 1-2: General Rules for Structural Fire Design.” *Commission of European Communities*, Brussels, Belgium.

[17] Promat. “CAFCO300. Vermiculite Gypsum Based Wet Mix Spray.”

[18] Eurocode 1. (2002). “Actions on Structures, Part 1-2: General Actions - Actions on Structures Exposed to Fire.” Commission of European Communities, Brussels, Belgium.

[19] ABAQUS v. 6.14. (2014). “Analysis User’s Guide - Elements: Beam Elements.”

[20] Huang, Z., Burgess, I., Plank, R. (2002). “Modeling of Six Full-Scale Fire Tests on a Composite Building.” *The Structural Engineer*, 30-37.

CHAPTER 6. CASE STUDY: 3D ANALYSIS AND DESIGN IMPROVEMENT FOR COMPOSITE BUILDINGS

Chapter 6 presents two examples of applying the 3D analysis method (described in Chapter 5) to evaluate the structural robustness of composite buildings. Two types of structures are studied and compared to each other in terms of their resistance against fire-induced progressive collapse. They are called as Structure A, which consists of perimeter moment frames with interior gravity frames, and Structure B, which consists of a central core and gravity frames. These structures are both ten stories high, and they use steel columns and composite floor systems (i.e., steel beams tied to reinforced concrete slabs). This chapter focuses primarily on Structure A, which is prototyped from the same building presented in Section 4.3 for the 2D analysis. The results from the analysis of Structure A are compared against the results in Section 4.3 to investigate the differences between the 2D and 3D analysis. Additionally, a parametric study is conducted to analyze the effectiveness of different strategies for design improvement.

6.1. Building prototypes

6.1.1. Structure A

Structure A is a ten-story composite framed building studied in Sadek et al. [1], as shown in Fig. 6.1. The building used intermediate moment frames (IMFs) for Seismic Design Category C. It consisted of perimeter moment-resisting frames using unreinforced welded-flange bolted-web connections and shear tab connections, and interior gravity frames using shear tab connections. The member sizes are given in Table 6.1.

ASTM A992 structural steel (σ_y = 50 ksi = 345 MPa) was used in all beams, and columns. At beam-to-column connections, ASTM A36 steel (σ_y = 36 ksi = 250 MPa) was used for the shear tabs and continuity plates, ASTM A490 high strength bolts were used, and welding requirements followed the recommendations in FEMA 353 [2]. The floor system consisted of 3 ¼ in. (83 mm) lightweight concrete (density = 110 pcf = 17.3 kN/m^3, compressive σ_y = 3 ksi = 21 MPa) topping on a 3 in. (76 mm) metal deck. Steel mesh in both directions were A185 (area = 185 mm^2/m) Grade 60 (σ_y = 60 ksi = 420 MPa). The slab acted compositely with the steel beams through shear studs.

The applied gravity load is equal to 1.2 D + 0.5 L. For typical floors, the dead load is 76 psf (3.64 kN/m^2) and design live load is 100 psf (4.79 kN/m^2). For the roof, the dead load is 56 psf (2.68 kN/m^2) and the design live load is 20 psf (0.96 kN/m^2).

As mentioned in Section 4.3.3, it was found from the 2D analysis that two-hour fire protection for the columns provided insignificant improvement to the global structural performance in fire compared to one-hour fire proofing. Therefore, in the 3D analysis, all beams and columns were insulated for a one-hour fire rating using CAFCO 300 with a thickness of 3/8 in. for beams and 1/2 in. for columns.

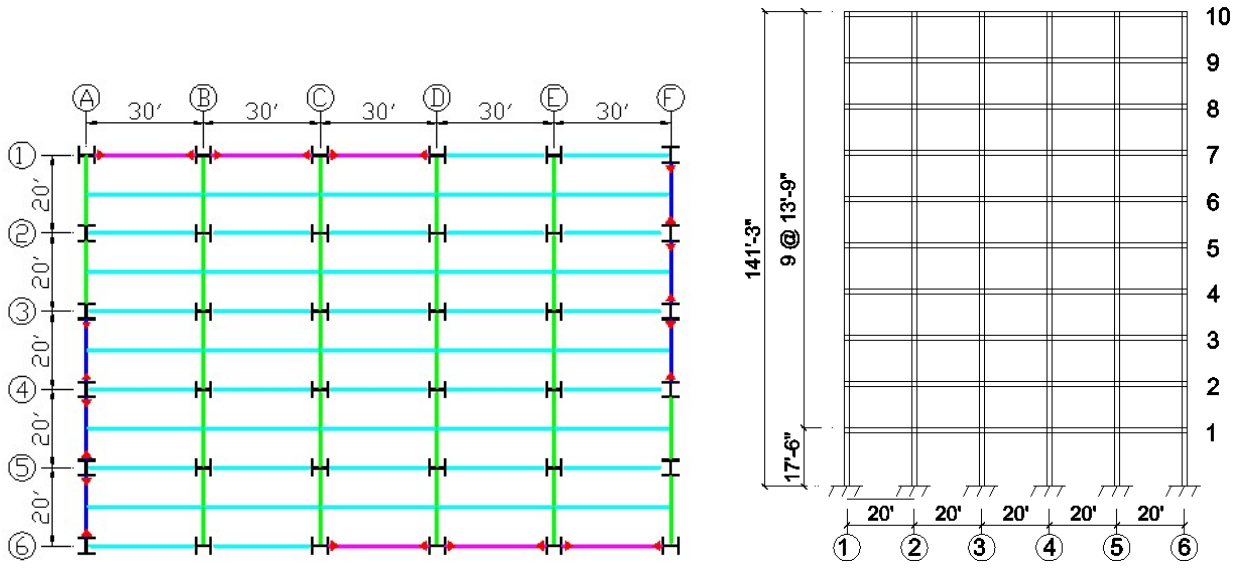

Fig. 6.1. *Floor plan and elevation view of Structure A (exterior moment frame)*

Table 6.1. *Member sizes of Structure A*

Floor	East-West Beam		North-South Beam		Column
	Moment (Purple)	Shear (Cyan)	Moment (Blue)	Shear (Green)	
1 - 3	W24x76	W14x22	W21x73	W16x26	W18x119
4	W24x76	W14x22	W21x68	W16x26	W18x119
5	W24x76	W14x22	W21x68	W16x26	W18x97
6	W24x62	W14x22	W21x68	W16x26	W18x97
7	W24x62	W14x22	W21x44	W16x26	W18x97
8 - 10	W21x50	W14x22	W21x44	W16x26	W18x55

6.1.2. Structure B

Structure B is a ten-story composite building studied in Agarwal and Varma [3], as shown in Fig. 6.2. The lateral load resisting system of Structure B (i.e., the rigid core in the center) was designed as an ordinary moment resisting frame for Seismic Design Category B. The rest of the building consisted of gravity frames that used shear tab connections. Each story was 3.65 m (12 ft.) high and the columns were 7.62 m (25 ft.) apart in both directions. Details of member sizes are given in Table 6.2.

ASTM A992 structural steel (σ_y = 50 ksi = 345 MPa) was used in all beams, and columns. At beam-to-column connections, ASTM A36 steel (σ_y = 36 ksi = 250 MPa) was used for the shear tabs, ASTM A325 bolts were used. The composite floor systems consist of 2.5 in. (65 mm) lightweight concrete (density = 118 pcf = 18.5 kN/m^3, compressive σ_y = 4 ksi = 28 MPa) topping on 3 in. (75 mm) ribbed deck. The steel mesh in both directions was A60 (area = 60 mm^2/m) Grade 60 steel (σ_y = 60 ksi = 420 MPa). The slab acted compositely with the steel beams through shear studs.

The applied gravity load is equal to 1.2D + 0.5L. On all floors, the nominal dead load was 65 psf (3.1 kN/m^2) and live load was 50 psf (2.4 kN/m^2). Like Structure A, all beams and columns of

Structure B were insulated with one-hour fire rating using CAFCO 300 with a thickness of 3/8 inch for beams and 1/2 inch for columns.

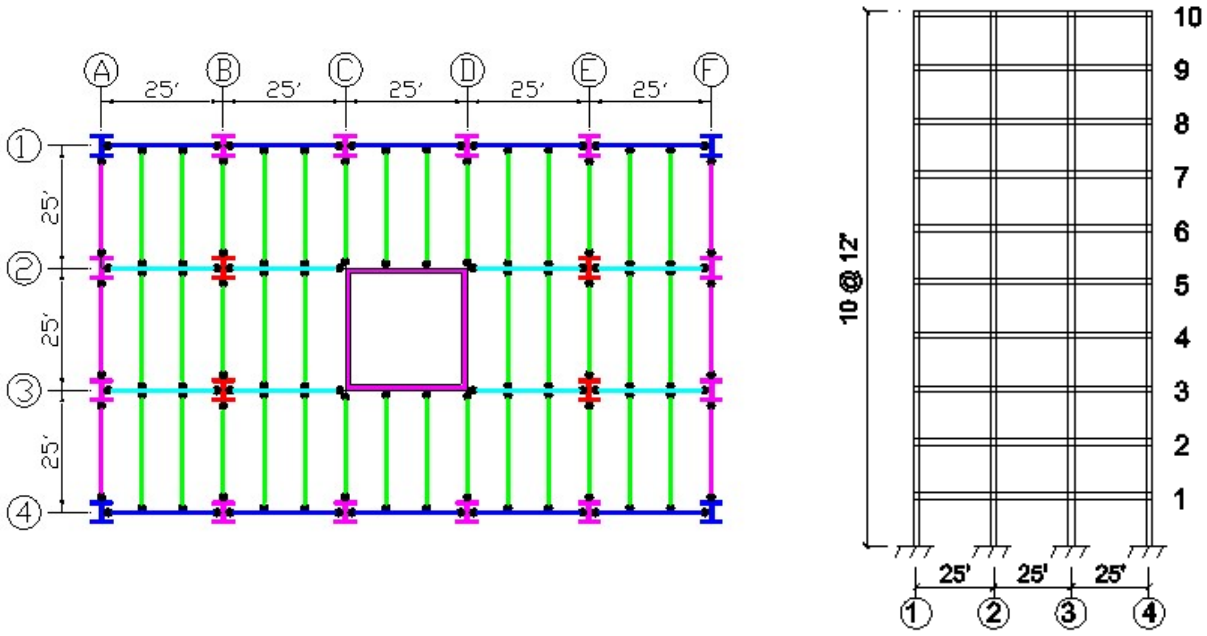

Fig. 6.2. *Floor plan and elevation view of Structure B (rigid core with gravity frame)*

Table 6.2. *Member sizes of Structure B*

Floor	Column			Beam			
	Interior	Corner	Edge	N-S Edge	N-S Int.	E-W Edge	E-W Int.
1, 2	W14x90	W10x33	W12x53	W12x16	W12x19	W14x22	W18x35
3, 4	W14x74	W8x24	W12x45				
5, 6	W12x58	W8x24	W10x39				
7, 8	W8x40	W6x15	W8x24				
9, 10	W8x24	W6x15	W6x15				

6.2. Fire scenarios

For standardized results, the ISO 834 standard fire with a duration of three hours was used in this study, which is shown in Fig. 6.3 along with time history of member temperatures for Structure A. The time history of gas temperature can be described following the Eurocode 1 [4] formula:

$$T_g = 20 + 345\log_{10}(8t + 1) \tag{6-1}$$

where T_g = gas temperature in the fire compartment (°C), and t = time (min)

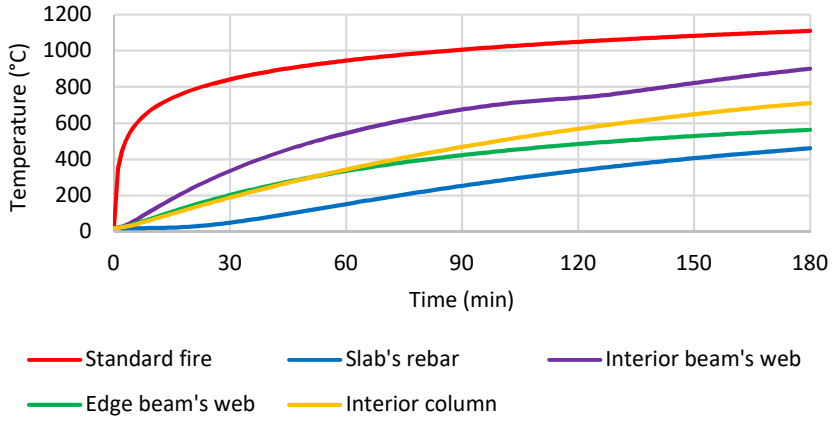

Fig. 6.3. *Time history of standard fire curve and member temperatures*

There are various parameters that may affect structural robustness in fire. They can be categorized into two groups, namely fire-related factors and structure-related factors. As summarized in Table 6.3, the case study in Section 6.3 focuses on fire-related factors to evaluate the structural robustness in different fire scenarios, whereas the design improvement in Section 6.5 focuses on structure-related factors to verify the effectiveness of different strategies on mitigating fire-induced progressive collapse of an existing design.

Table 6.3. *List of parameters that can affect structural robustness in fire*

	Category	Parameter	Consideration in the study
Case study (fire-related factors)	Location of fire	Vertical location (i.e., which floor is in fire)	1st, 5th, and 9th floor
		Horizontal location (i.e., which compartment is in fire)	12 fire cases for each floor
	Scale of fire	Number of floors in fire	Not considered i.e., fire on one floor only
		Number of compartments (within a floor) in fire	4 vs. 6 compartments in fire
	Type of fire	Standard fire vs. natural fire	Not considered i.e., standard fire only

		Fire with vs. without cooling	Not considered i.e., fire without cooling only
Design Improvement (structure-related factors)	Fire protection	Fire protection for columns	1 hr., 1.5 hr., and 2 hr. protection
		Fire protection for primary beams	1 hr. and 2 hr. protection
		Fire protection for secondary beams	1 hr. and 0 hr. protection
	Capacity of slab	Strength of concrete	3 ksi and 6 ksi concrete
		Strength of steel for steel mesh	Not considered i.e., Grade 60 (f_y = 60 ksi) only
		Size of steel mesh (or total area of steel mesh)	A185 and A370 mesh
	Capacity of beam	Size of beams	3 size groups for secondary beams
		Strength of steel for beams	Not considered i.e., A992 (f_y = 50 ksi) only
	Capacity of column	Size of columns	3 sizes for columns
		Strength of steel for columns	Not considered i.e., A992 (f_y = 50 ksi) only

In terms of fire location, twelve cases of different horizontal locations on one floor were investigated, as shown in Fig. 6.4 for Structure A and Fig. 6.5 for Structure B. Additionally, in Structure A, three different vertical locations of fire (i.e., the first, fifth, and ninth floor) were also considered to study the possible differences in the failure mechanisms and time limits. To save time, in the fifth-floor fire and ninth-floor fire, only four critical fire cases were explored instead of all 12 cases; these four cases were identified based on the analysis of the first-floor fire.

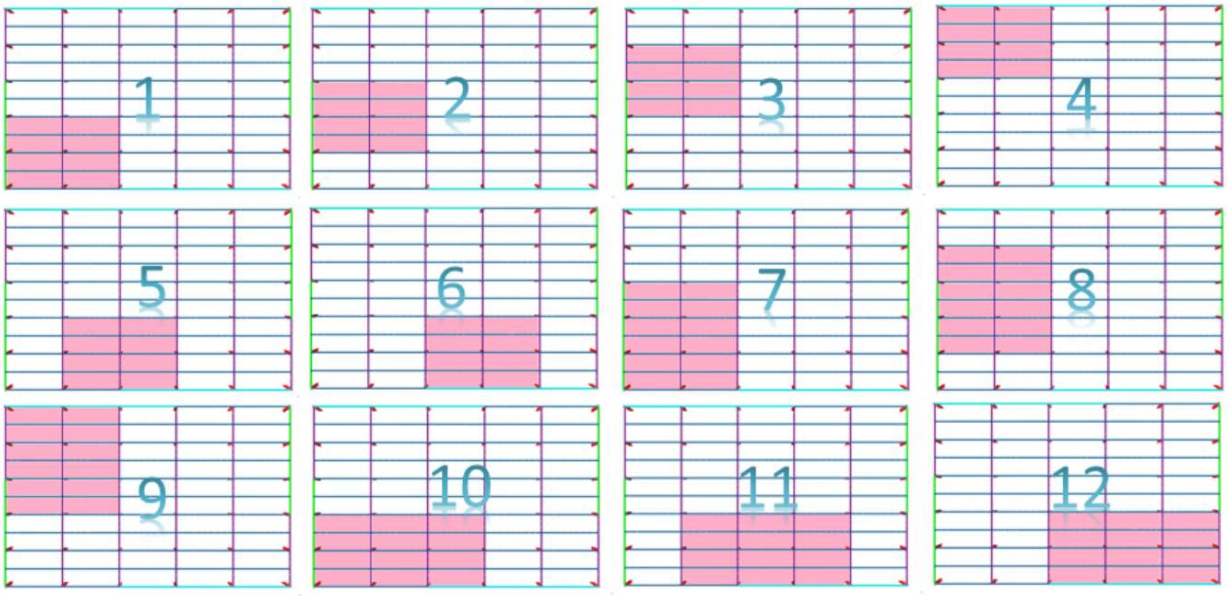

Fig. 6.4. *Structure A - 12 fire cases on each floor*

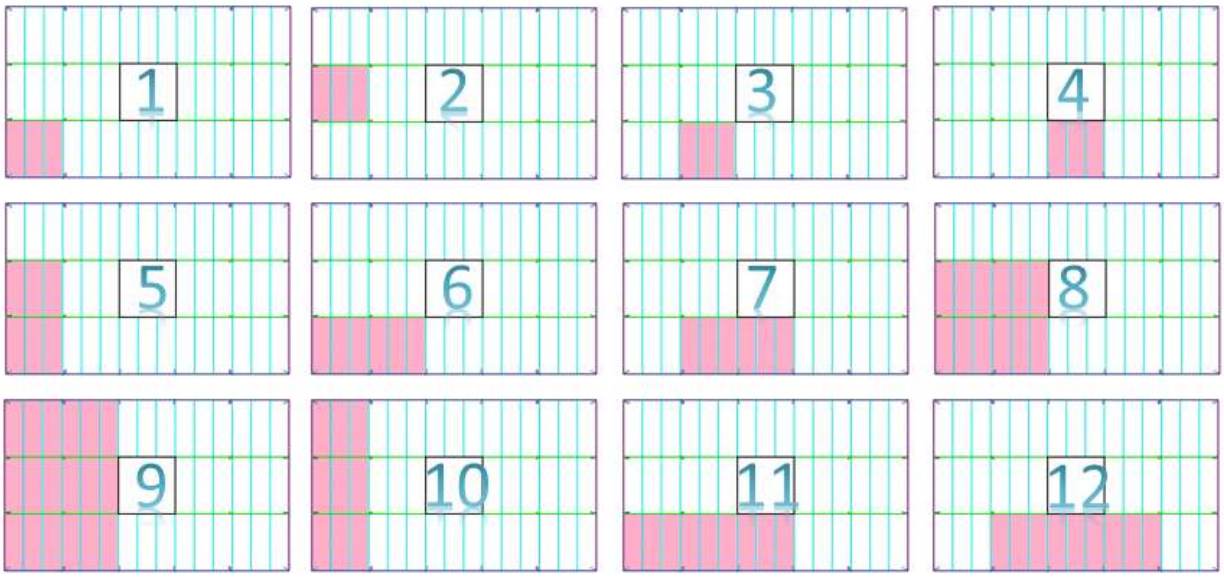

Fig. 6.5. *Structure B - 12 fire cases on each floor*

Based on the findings of the 2D analysis (shown in Section 4.3.3), the time limit of the structure under multi-floor fires is shorter than the time limit under single-floor fires of the same type. The focus of this study is on single-floor fire, under which the structures already collapsed after less than an hour of fire exposure (detailed in Section 6.3.2 and 6.3.3).

6.3. Case study

The case study and design improvement aim to address several important questions associating with structural evaluation in resistance to fire-induced progressive collapse, as follows:

- What is the time limit of the structures? (i.e., how long can they withstand the fire?)
- What are the failure mechanisms of the building?
- How is the structural response affected by different factors (as described in Table 6.3)?
- Which case is the critical fire case for design?

The final goal is to evaluate qualitatively and quantitatively the structural performance in fire.

6.3.1. Modeling approach

The analyses of the two building structures follow the methodology of the 3D analysis, which is described in Chapter 5. Steel beams and columns were modeled with 3D 2-node linear beam-column elements (i.e., B31 type in ABAQUS); concrete slabs were modeled with linear 4-node shell elements (i.e., S4R type in ABAQUS) of a uniform thickness with three layers, in which one layer represents the steel mesh. The steel deck of composite slab was not modeled. To preserve the moment of inertia of the composite section, the location of the top surface of the slab is preserved. The reference plane of slab and of beam were put at the top level of beam.

Beam-to-column connections were modeled as simple joints (i.e., kinematic coupling constraints in ABAQUS). The connection model (presented in Chapter 3) was not integrated into the 3D analysis due to the high computational cost. The composite interaction between the steel beams and concrete slabs was modeled as fully fixed using kinematic coupling constraints in ABAQUS. There was no interaction (or constraint) between the steel columns and concrete slabs.

The fixed-load increased-temperature scenario was adopted to simulate fire-induced progressive collapse events. The sequentially coupled thermal analysis and structural analysis in ABAQUS was employed for the study. The structural analysis used the explicit dynamic approach, in which gravity loads were applied at room temperature in the first analysis step, followed by elevated member temperatures applied in the second analysis step. To avoid unrealistic oscillations under

static gravity loads, the gravity load was gradually applied from zero to the service value and kept constant until the structure stabilized.

For computational efficiency, a mass scaling of factor 10 was applied. Based on my experience with modeling structures in ABAQUS, I assigned the duration of step 1 (or the loading step) as 10 units, and duration of step 2 (or the fire step) as 1800 units (i.e., 10 units for each minute of standard fire). In this study context, the 10-unit-long loading step with mass scaling of 10 was found to be sufficient for avoiding unrealistic oscillation without expensive computational cost.

Material and geometric non-linearity was considered in the analysis. The inelastic behavior of concrete was represented by the concrete damaged-plasticity model in ABAQUS, whereas the plasticity of steel was represented by the metal plasticity model in ABAQUS, using the von Mises yield criteria. Mechanical properties of steel (i.e., structural steel in beams and columns, and reinforcing steel in slabs) and lightweight concrete at elevated temperature follow Eurocode 4 [5], and no strain hardening was considered in this study. Thermal properties (i.e., thermal expansion, thermal conductivity, and specific heat) of steel and lightweight concrete are taken from Eurocode 4 [5]. Details on material properties at elevated temperatures are described in Section 5.2.1 and 5.2.2.

The measurements for the structural robustness evaluation include:

- For insulation: deflections of beams and lateral displacements of columns
- For integrity: deflection of slabs and rotations at beam ends
- For stability: internal forces (i.e., axial force and moments in two directions) in columns, and internal forces (i.e., axial force, shear force, and moment) at beam ends

In this study, Life Safety is assumed as the designed performance level for the two buildings. For insulation criterion, the deflection limit of beams was chosen as $L_{span}/40$ [6] and the lateral displacement limit of columns was chosen as 120 mm [6]. For integrity criterion, the deflection limit of the slabs was chosen as $L_{span}/20$ [6]; and the rotation limit at beam ends was $6\theta_y$ (for primary beams) and $9\theta_y$ (for secondary beams), where θ_y is the yielding rotation, according to ASCE/SEI 41-06 [7].

For convenience, the time limit for satisfying all three criteria is denoted as T, while the time limit associated with insulation criterion is denoted as $T_{insulation}$, the time limit associated with integrity criterion is denoted as $T_{integrity}$, and the time limit associated with stability criterion is denoted as $T_{stability}$. Then $T = min\ (T_{insulation}, T_{integrity}, T_{stability})$.

6.3.2. Results for Structure A

In a first-floor fire, when fire spread on four compartments, the building could remain robust for 64 min, and the failure was governed by the insulation criterion (i.e., insulation failure in the interior column at 56 min, leading to subsequent collapse of the heated structure at 64 min). The critical case is case 1, as shown in Fig. 6.6.

When fire spread on six compartments, the building could remain robust for 55 min (i.e., less than one-hour standard for fire resistance), and the failure was governed by stability criterion. The stability failure (i.e., buckling in all heated columns) led to immediate insulation failure (i.e., high deflection of beams and high lateral displacement of columns) and integrity failure (i.e., high deflection of slab). This suggests that one-hour fire protection for beams and columns is adequate for the four-compartment fire but not so for the six-compartment fire. The critical case of six-compartment fire is case 7, 10, and 12, as shown in Fig. 6.6.

Table 6.4 summarizes the time limit and failure mechanisms of Structure A for the first-floor fire.

Table 6.4. *Time limit and failure modes of Structure A for the first-floor fires*

Heated Area	Case	Time Limit (min)				Stability Failure Description
		$T_{insulation}$	$T_{integrity}$	$T_{stability}$	T	
4 comp.	1	64	75	75	**64**	At t = 56 min, buckling of interior column & load redistribution
	2	67	69	69		At t = 60 min, buckling of interior column & load redistribution
	3	67	78	78		At t = 60 min, buckling of interior column & load redistribution
	4	75	88	88		Failures of all heated columns nearly at the same time
	5	66	76	76		At t = 59 min, buckling in interior column & load redistribution

	6	66	76	76		At t = 59 min, buckling in interior column & load redistribution
6 comp.	7	55	55	55	**54**	Failures of all heated columns nearly at the same time
	8	61	61	61		Failures of all heated columns nearly at the same time
	9	65	75	75		At t = 58 min, buckling in interior columns & load redistribution
	10	55	55	55		Failures of all heated columns nearly at the same time
	11	65	65	65		At t = 58 min, buckling in interior columns & load redistribution
	12	55	55	55		Failures of all heated columns nearly at the same time

(Green color indicates the governing failure mode, i.e., the lowest time limit among the three)

In brief,

Heated Area	Time Limit	Governing Failure Mechanism	Critical Case
4 compartments	64'	Insulation failure in beams	1
6 compartments	55'	Insulation failure in beams and columns	7, 10, 12

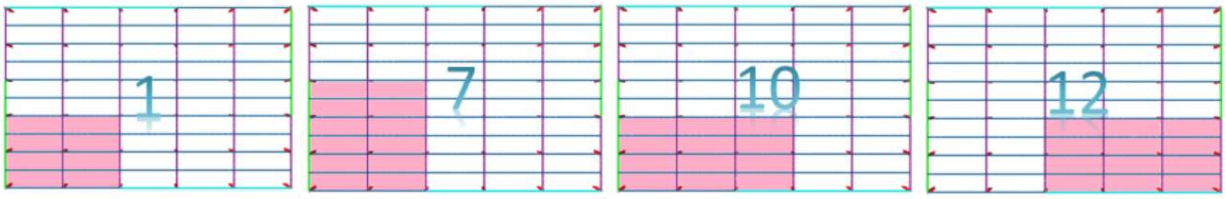

Fig. 6.6. *Four critical fire cases of Structure A*

Regarding the influence of the vertical fire location, when fire occurred on the middle story (i.e., the fifth floor) or top story (i.e., the ninth floor), the columns failed after a longer time of fire exposure (i.e., $T_{stability}$ = 87 min or beyond in the fifth-floor and ninth-floor fire vs. $T_{stability}$ = 55 min in the first-floor fire). Fire on the first floor is therefore the critical scenario for structural design in fire in this structure. The time limit of the building in upper-story fire (the fifth and ninth floor) was governed by the insulation failure due to a limiting deflection of L/40 in beams, i.e., $T = T_{insulation}$ = 80 min. Table 6.5 summarizes different structural response to different vertical location of fire.

Table 6.5. *Influence of the vertical location of fire on the structural robustness*

Floor	# comp.	Time Limit (min)				Governing Failure Mechanism
		$T_{insulation}$	$T_{integrity}$	$T_{stability}$	T	
1	4	64	69	69	64	Insulation failure in interior column
	6	55	55	55	55	Stability failure in columns
5	4	82	87	105	64	Insulation failure in beams
	6	80	85	87	64	Insulation failure in beams
9	4	82	87	125	64	Insulation failure in beams
	6	80	85	124	64	Insulation failure in beams

(Green color indicates the governing failure mode)

In most of fire cases, the structural failure was governed by insulation failure while in the critical cases (i.e., the first-floor six-compartment fire), the structural failure was governed by stability failure. In fact, in the first-floor six-compartment fire, the heated columns experienced higher temperatures compared to those in the first-floor four-compartment fire, and higher gravity loads compared to those in the fifth-floor or ninth-floor fires due to the existence of more floors above the heated floor. This caused the earlier stability failure in the columns on the first-floor six-compartment fire case (i.e., at time T = 55 min). Whereas in upper-floor fires, the columns could remain stable for a substantially longer time (around 85 min) and the failure was triggered by insulation failure in multiple beams due to large deflections.

In addition to DCR > 1, the stability failure can also be indicated in the time history of internal forces (especially axial forces) and lateral displacements in columns. More specifically, the buckling instability in a column is marked by a significant decrease in axial force in the column, coupled with an increase in axial force in the adjacent columns, which indicates load redistribution, as shown in Fig. 6.7. At the same time, the buckling column also experiences a significant change in lateral displacement, as shown in Fig. 6.8. The pattern of stability failure observed in Structure A was the buckling in an interior column in the heated area, which initiated load redistribution to

the adjacent columns, eventually resulting in failure of all heated columns. In Case 1 of the first-floor fire, for example, column B5 started to buckle at $t = 56\ min$, which caused load redistribution to the surrounding columns (i.e., columns A5, C5, B4, and B6), until eventually all columns failed at $t = 76\ min$. In other cases (i.e., Cases 4, 7, 8, 10, 12), all heated columns failed almost simultaneously, resulting in a sudden loss of stability. Fig. 6.11 illustrates the failure corresponding to Case 10 of the first-floor fire, which had a sudden stability failure at $t = 55\ min$ simultaneously with insulation and integrity failures. In Structure A, sudden stability failures tended to occur in larger-scale fires (i.e., six compartments) while gradual stability failures tended to occur in smaller-scale fires (i.e., four compartments).

The integrity failure is assumed to occur when the vertical displacement of the slab exceeds the limit of $L_{span}/20$ or the rotation at the beam ends exceeds the limit of $6\theta_y$ for primary beams and $9\theta_y$ for secondary beams. In the structure analyzed here, the integrity failure was usually determined by the vertical displacement of the slabs. Fig. 6.9 illustrates the integrity failure in Structure A for Case 1 of the first-floor fire.

The insulation failure is assumed to occur when the deflections of beams exceed L/40 or lateral displacements of columns exceed 120 mm. Fig. 6.10 illustrates the insulation failure in Structure A for Case 1 of the first-floor fire. In Case 1, at t = 56 min, the interior column B5 started to buckle, resulting to redistribution to the adjacent columns (i.e., columns B4, B6, A5, C5) and the lateral displacements of column B5 exceeding the limit of 120 mm. Thus, at t = 56 min, the fire insulation for column B5 was assumed to fail and the temperature in B5 quickly increased beyond the critical temperature, as shown in Fig. 6.10. This "new" temperature of B5 was updated to the "new" structural analysis to predict the subsequent response of the building structure. As can be seen in Fig. 6.10, about 8 min later (i.e., at t = 64 min), all heated columns buckled, along with large deflections of slabs exceeding a limit of L/20, resulting to structural failure. In other words, in Case 1, the insulation failure at t = 5 min in the interior column B5 led to the time limit of Structure A $T_{limit} = 64\ min$.

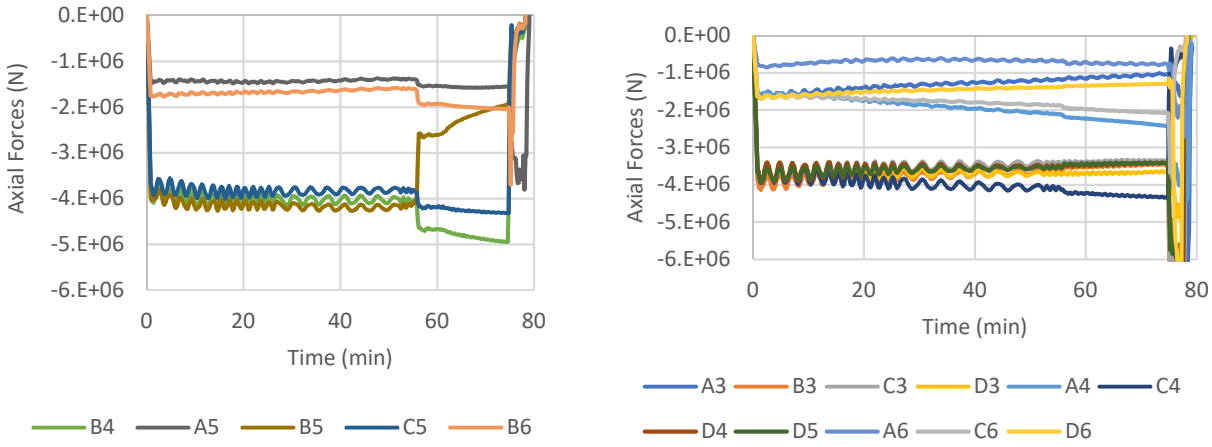

(a) *(b)*

Fig. 6.7. *Axial forces in heated columns (a) and adjacent columns (b) on the first floor in Structure A for the first-floor fire (Case 1). Stability failure occurred at 76 min, initiated by buckling of the interior column (B5) at 56 min*

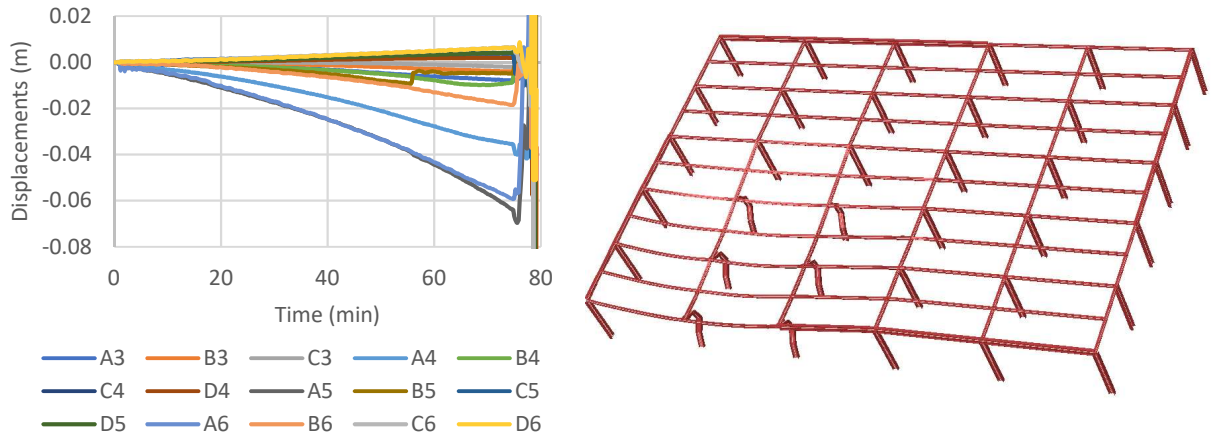

(a) *(b)*

Fig. 6.8. *Lateral displacements of columns (a) and deformed shape of the first floor (b) in Structure A for the first-floor fire (Case 1). Stability failure occurred at 76 min*

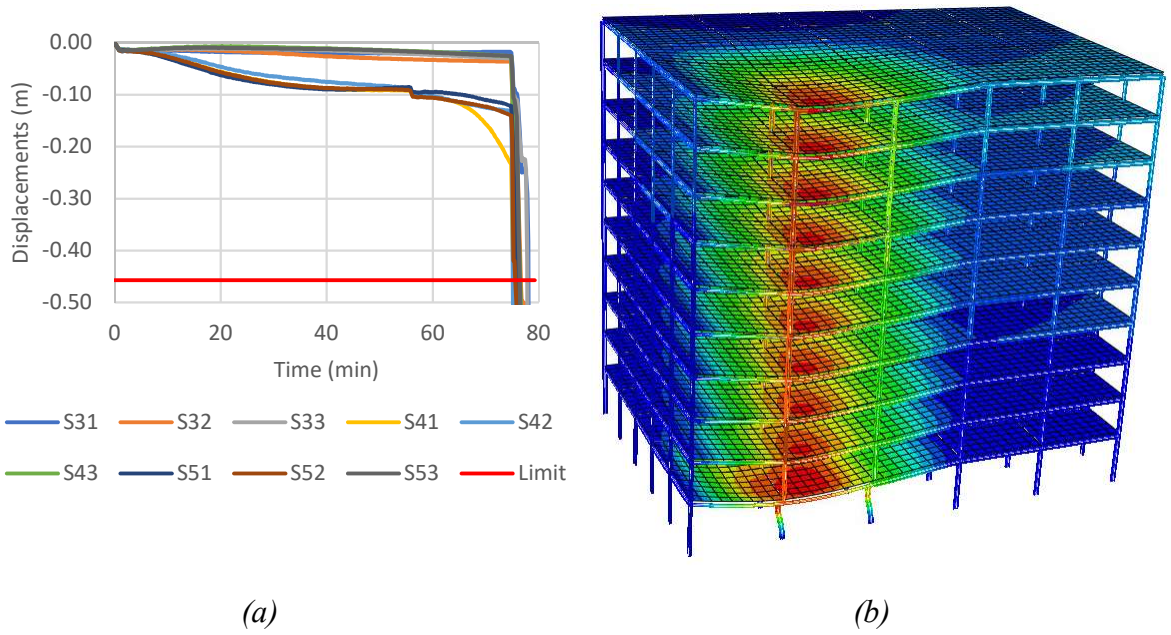

(a) *(b)*

Fig. 6.9. *Deflections of the first-floor slabs (a) and deformed shape of building (b) in Structure A for the first-floor fire (Case 1). Integrity failure occurred at 76 min*

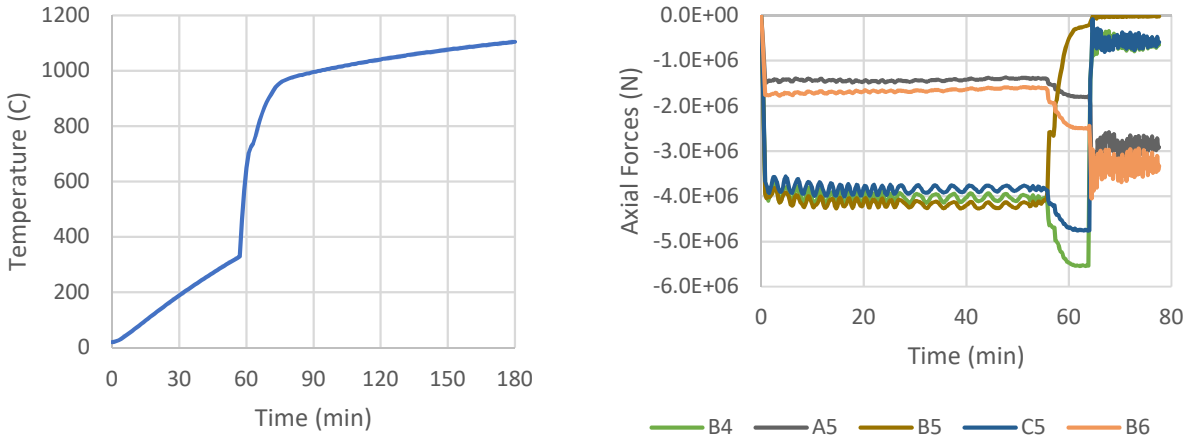

Fig. 6.10. *Quick temperature rise in column B5 (a) and axial forces in heated columns (b) in Structure A for the first-floor fire (Case 1) with failure in fire protection in col B5 at 56 min. Structure A failed at* T_{limit} *= 64 min*

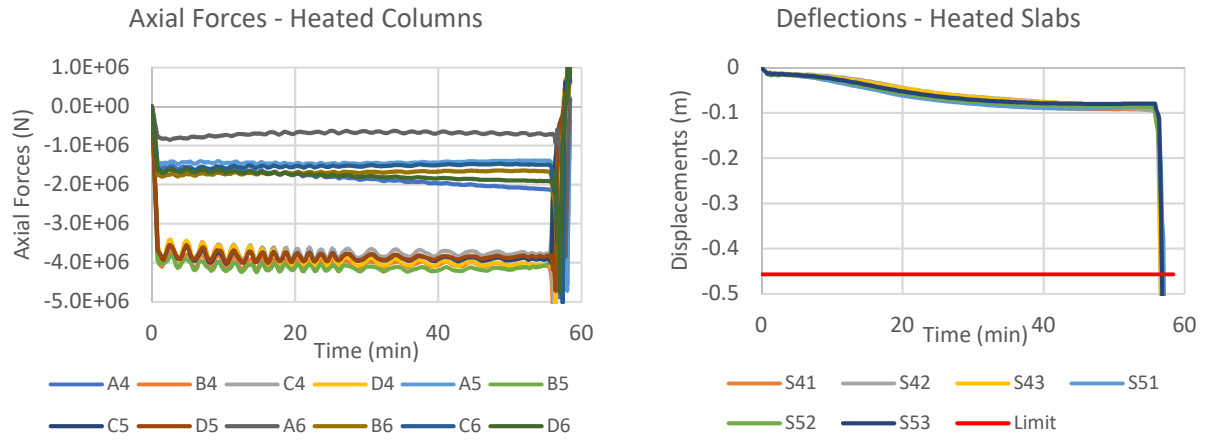

(a) *(b)*

Fig. 6.11. *Axial forces in the heated columns (a) and deflections of the heated slabs (b) in Structure A for the first-floor fire (Case 10). Stability and integrity failures occurred at 56 min*

6.3.3. Results of Structure B

In a first-floor fire, Structure B remained robust for 70 min for fire occurring in six compartments, 75 min for fire occurring in four compartments, 75 min for fire occurring in three compartments, 76 min for fire occurring in two compartments, and 80 min for fire occurring in a single compartment. In all cases, the failure was governed by the insulation criterion, assuming the limiting deflection for beams is L/40 and the limiting lateral displacement for columns is 120 mm. Table 6.6 summarizes the time limit and failure mechanisms of Structure B in the first-floor fire.

Because the first-floor fire is the critical case for structural design in fire for Structure A, other cases of fire on upper floors were not considered in Structure B to save the computational cost of conducting those analyses.

Table 6.6. *Time limit and failure modes of Structure B in the first-floor fires*

Heated Area	Case	Time Limit (min)			Time Limit	Stability Failure Description
		Insulation	Integrity	Stability		
1 com.	1	82	99	159	80	Failures of all heated columns simultaneously
	2	80	95	157		Failures of all heated columns simultaneously
	3	80	95	157		Failures of all heated columns simultaneously

	4	82	99	160		Failures of all heated columns simultaneously
2 com.	5	76	85	105	76	Failures of all heated columns simultaneously
	6	77	87	108		Failures of all heated columns simultaneously
	7	76	84	119		Failures of all heated columns simultaneously
4 com.	8	75	84	91	75	At t = 81 min, buckling in interior columns & load redistribution
6 com.	9	70	79	87	70	At t = 79 min, buckling in interior columns & load redistribution
3 com.	10	75	75	117	75	Failures of all heated columns simultaneously
	11	75	82	104		Failures of all heated columns simultaneously
	12	75	85	117		Failures of all heated columns simultaneously

(Green color indicates the governing failure mode)

Similar to Structure A, the stability failure can be determined by DCR > 1 or observation of significant changes in the time history of internal forces (especially axial forces) and lateral displacements in columns. More specifically, the buckling instability in a column is marked by a significant decrease in axial force of the column, along with a substantial increase in the value of its lateral displacement, as shown in Fig. 6.12, which corresponds to Case 8. Different from Structure A with gradual stability failure, the primary pattern of stability failure observed in Structure B was the simultaneous buckling and failure of all heated columns, as shown in Fig. 6.12.

The possible reason for the sudden stability failure in Structure B is that at the time of load redistribution, the internal forces in the adjacent columns had already reached their capacity. It is also worth noting that in the gradual stability failure of Structure A, column buckling appeared relatively early (i.e., around 60 min or earlier), as shown in Table 6.4. At that time, temperature in the adjacent columns was still low enough that their temperature-dependent capacity could accommodate the additional loads caused by load redistribution. After approximately 10-20 min, the load exceeded the capacity and the adjacent columns failed, leading to stability failure of the building. In contrast, in Structure B, column buckling appeared relatively late (i.e., around 90 min and up to 160 min, depending on the fire exposure), as shown in Table 6.6. At that time, the

temperature in the adjacent columns was so high that the capacity could not accommodate any additional loads, resulting in nearly immediate failure after the buckling of one column.

The integrity failure occurred in Structure B primarily when vertical displacement of the slabs exceeds the limit of $L_{span}/20$, as shown in Fig. 6.13 for Case 8.

It can be seen that the stability failure occurred in Structure B at a later time than that in Structure A (i.e., 87 min vs. 55 min). The time limit of Structure B (i.e., 70 min), which was governed by the insulation failure, was also longer than the time limit of Structure A (i.e., 55 min), which was governed by the stability failure (also occurring simultaneously with integrity and insulation failures). This indicates Structure B has a higher robustness against fire-induced progressive collapse than Structure A. Several factors may contribute to this difference, such as the selection of member sizes, the gravity loads, the dimensions of the compartments and building.

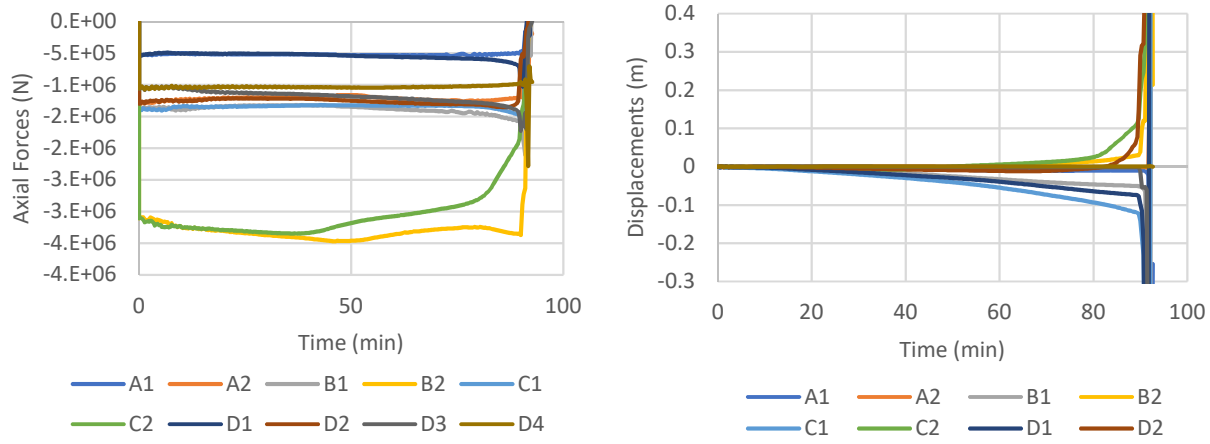

(a) *(b)*

Fig. 6.12. *Axial forces (a) and lateral displacements (b) in heated columns on the first floor in Structure B for the first-floor fire (Case 8). Stability failure occurred at t=92 min*

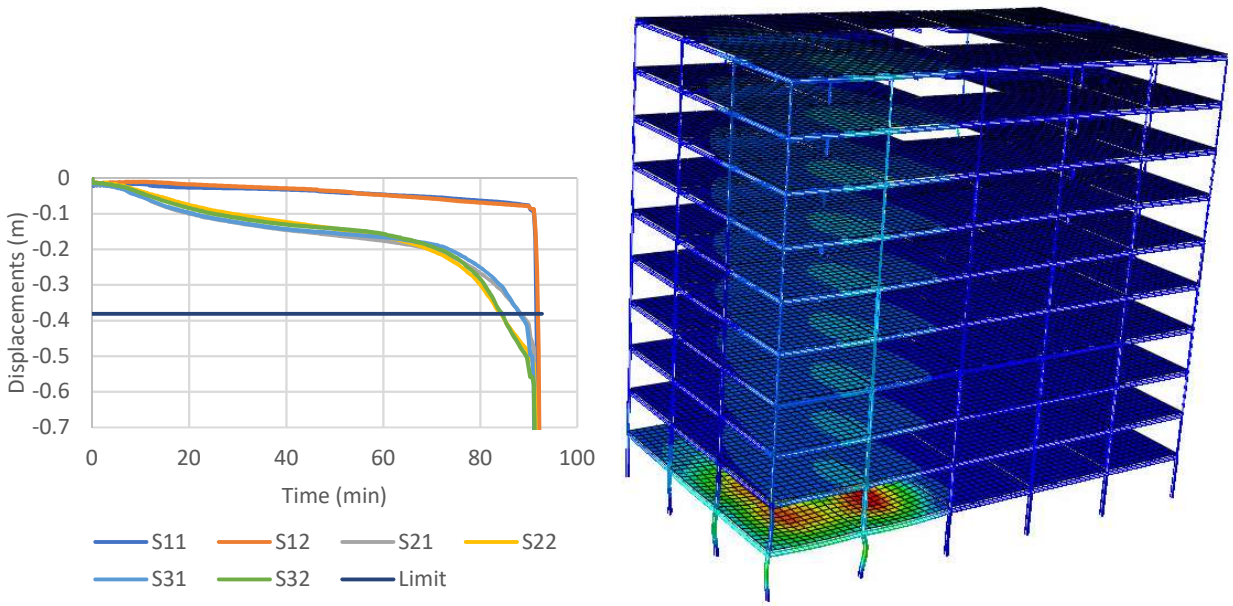

(a) *(b)*

Fig. 6.13. *Vertical displacements of heated slabs (a) and deformed shape of building (b) in Structure B for the first-floor fire (Case 8). Integrity failure occurred at t=84 min*

6.4. Discussions

Findings from this case study can be summarized into three primary categories below.

6.4.1. General failure pattern and quantitative structural evaluation

Fire on the first floor was found to be the critical case for structural design in fire. The larger the area is under fire, the more dangerous it is for the structure. The most extreme case is when fire occurs in six compartments in the corner of the building (i.e., Case 7, 10, 12 for Structure A, and Case 9 for Structure B).

In Structure A, the pattern of stability failure tends to be a gradual failure (i.e., the failure of the entire structure occurs several minutes after the initiation of column buckling and load redistribution) for the four-compartment fires, and a sudden failure (i.e., the failure of the entire structure occurs immediately after the initiation of column buckling) for the six-compartment fires. In Structure B, the pattern of stability failure is sudden, and stability failure tends to occur after insulation failure and integrity failure.

The time limit of Structure A and Structure B were 55 min and 70 min respectively, which corresponded to the most extreme case with fire in six compartments. In Structure A, the time limit is lower than the insulation rating and shows the fire resistance rating is not a true indicator of how a structure perform as a system in fire.

In both buildings, the time limit was primarily governed by the insulation failure. The exception is that in the critical cases (i.e., Case 7, 10, and 12) of Structure A, stability failure governed the time limit.

6.4.2. Comparison between the 2D and 3D analysis

The 2D model (described in Chapter 5) analyzes the exterior moment frame (i.e., axis A) of Structure A with the assumption that fire spreads through entire moment bay of the frame (i.e., from column A3 to column A6). Therefore, the comparison between the 2D and 3D model only considers the 2D model with Case 7 of Structure A under the 3D analysis. This comparison is summarized in Table 6.7.

Table 6.7. *Comparison between 2D and 3D analysis*

	2D Model	3D Model
Analysis approach	- Non-linear static analysis (e.g., ABAQUS Implicit) - Fixed temperature-increased load scenario (assumption: column buckles and is removed when temperatures in structural members reaches a steady state after a period of fire exposure)	- Non-linear dynamic analysis (e.g., ABAQUS Explicit) - Fixed load-increased temperature (i.e., column buckles & loads are redistributed when fire-induced temperatures in structural members still develop)
Failure mechanism	Stability failure for the first-floor fire Integrity failure for the fifth-floor and ninth-floor fires	Stability failure (simultaneously with integrity failure and insulation failure) for the first-floor fire Insulation failure for the fifth-floor and ninth-floor fires

Time limit	120 min	55 min
Critical case	Fire on the ninth floor	Fire on the first floor

The 3D model with nonlinear dynamic analysis is more realistic for considering transient effect of fire. In the dynamic analysis, the column removal happens automatically as a consequence of the growing fire, compared to the static analysis in which the column removal is done manually. Thus, the dynamic analysis can reduce a number of unrealistic scenarios in which the loss of a specific column is unlikely to occur in fire. Because of the difference in analysis approach between the 2D and 3D models, it is not appropriate to simply compare the quantitative results between the 2D and 3D analyses. However, the 2D analysis still provides important qualitative findings on the overall structural performance in fire, especially the role of insulation failure (or limiting deflection of beams) in the time limit of the structure.

In addition to different analysis approach, another reason for such a big difference regarding the time limit between the 2D and 3D models is that the 2D model considers only the perimeter moment frame, which has higher stiffness and lower average temperatures than the rest of the building (i.e., interior gravity frames) even when being subjected to the same fire. Also, due to the nature of 2D model, all out-of-plane lateral displacements of structural members were restrained and the non-uniform temperature between the exposed and unexposed sides of perimeter members was neglected in the 2D model. Consequently, the fire-induced deformations predicted by the 2D analysis are less than actuality, giving a prediction that the structure has a higher time limit when a 2D model is used. This level of inconsistency between 2D and 3D structural models has been identified by other authors in the analysis of structures at room temperature.

The 3D model includes the contribution of the composite floor system, which improves load redistribution from a buckled column to the adjacent columns in all directions, as compared to the 2D model, which has only beams bridging the buckled column with the adjacent columns in one direction. Therefore, the consideration of the composite floor system makes the 3D analysis more realistic, which is similar to the findings in Alashker et al. [8].

The effect of the composite floor system on structural response to fire-induced progressive collapse is also shown in the 3D analysis where integrity time limit (or deformation-controlled failure) did

not decrease in the upper-floor fires. More specifically, in the 2D analysis, because only beams (on the heated floors and above) helped redistribute loads in an upper-floor fire, fewer beams contributed to bridging a lost column compared to those in lower-floor fires. This resulted in larger deformations in the beams and a shorter integrity time limit. In contrast, in the 3D analysis, because both slabs and beams in two directions helped redistribute loads, in an upper-floor fire, a large portion of the floor system contributed to bridging a lost column, resulting in smaller deformations in the beams and a longer integrity time limit.

6.4.3. Comparison between the two structural types

Because fire cases analyzed in Structure A involved either four or six compartments involved in fire, the comparison between Structure A (i.e., perimeter moment frame with interior gravity frame, designed for seismic design category C) and Structure B (i.e., rigid core center with gravity frame, designed for seismic design category B) only considers four- and six-compartment fire cases (i.e., Cases 8 and 9) of Structure B. The comparison is summarized in Table 6.8.

Table 6.8. *Comparison between two types of structure*

	Structure A (perimeter moment frames)	Structure B (rigid core with gravity frames)
Stability Failure	- Primarily gradual failure: the failure of the entire structure occurs around 10 min or more after the initiation of column buckling and load redistribution In extreme cases with six-compartment fire, failure is sudden. - Stability time limit (assuming the structure did not fail earlier according to the insulation criterion) is: 69 min for four-compartment fire 55 min for six-compartment fire	- Primarily sudden failure: the failure of the entire structure occurs immediately after the initiation of column buckling, although it occurs at later time - Stability time limit (assuming the structure did not fail earlier according to the insulation criterion) is: 91 min for four-compartment fire 87 min for six-compartment fire

Governing Failure	- In 4-compartment fire, insulation failure - In 6-compartment fire, stability failure	Insulation failure in beams in all cases
Time limit	55 min for six-compartment fire; 64 min for four-compartment fire	70 min for six-compartment fire; 75 min for four-compartment fire
Critical case	Fire at the corner over six compartments	Fire at the corner over six compartments

In most fire cases, both structures share the same governing failure, that is insulation failure. In both buildings, the larger area is heated, the shorter time the structure can remain robust; six-compartment fire is the critical case for design.

The longer time limit of Structure B (compared to Structure A) may indicate that Structure B is more robust against fire-induced progressive collapse than Structure A. The reason can be a more effective choice of the member sizes, the effect of the structure type, and the effect of the floor layout.

6.5. Design improvement

Design improvement process is conducted for Structure A to explore the effectiveness of different strategies in preventing progressive collapse within a desired time of fire exposure. Based on the governing failure and critical fire scenario, there are two major approaches for design improvements:

(1) Fire prevention and suppression: aims to prevent fire from spreading through 6 compartments. This can be achieved by improving compartmentation, opening protection, and fire stopping.

(2) Structural enhancement: aims to enhance structural resistance to 6-compartment fire. This can be achieved by increasing fire protection level for the structural members (as described in Section 6.5.1), and increasing capacity of the structural members (as described in Section 6.5.2).

In this study, the focus is on the structural enhancement.

As mentioned earlier in Section 6.3.2, Structure A can withstand a standard fire for 55 min if fire occurs in six compartments on the first floor and 64 min if fire occurs in four compartments on the first floor or six compartments on the fifth or ninth floor). All the beams and columns are fire protected with one-hour fire resistance rate.

The desired performance level for the building is assumed to be Life Safety for at least one hour. It is clearly seen that the current design is sufficient for the first-floor four-compartment fires, the fifth-floor fires, and the ninth-floor fires. Thus, the improvement is only for the extreme cases with fire occurring in six compartments on the first floor, as shown in Fig. 6.14. All these fire cases follow the same failure pattern, that is stability failure at 55 min, which causes integrity and stability failures at the same time.

Fig. 6.14. *Three extreme fire cases with fire spreading in 6 compartments*

In the following sections, various structural enhancement strategies are explored in order to meet the Life Safety performance objective. It is noted that original fire protection is sufficient for fire on the middle and upper floor, as described in Section 6.3.2. Thus, there is no change in members on the fourth floor and above; the adjustment is only applied to members on the first, second, and third floor.

6.5.1. Increasing fire protection

Increasing fire protection aims to reduce the temperature rise in the steel members during the duration of fire exposure, resulting in higher capacity and lower deformation in the structure under fire.

The method of increasing fire protection is to increase the thickness of the spray-applied fire resistive material (SFRM). The SFRM thickness follows the guideline provided by the manufacturer and was checked via thermal analysis (i.e., using a heat transfer model to verify that the temperature in the member is under a limit for a specified period of fire exposure). Table 6.9. describes the appropriate thickness of CAFCO 300 for beams [9].

Table 6.9. *Appropriate SFRM thickness (in.) for beams [9]*

Rating Hour	Restrained	Unrestrained
1 hr.	3/8 in.	3/8 in.
1.5 hr.	7/16 in.	11/16 in.
2 hr.	3/4 in.	1 in.
3 hr.	1-1/4 in.	1-5/8 in.

The thickness of SFRM applied to columns follows the formulae below [2]:

$$h = \frac{R}{75(W/D) + 32} \text{ (for column } W/D \text{ range of 0.33 to 2.51)} \quad (6\text{-}1)$$

$$h = \frac{R}{75(W/D) + 15} \text{ (for column } W/D \text{ range of 2.51 to 6.68)} \quad (6\text{-}2)$$

where:

h = thickness of SFRM (in.), h = 1/4 to 4-1/2 in. (rounded up to the nearest 1/16 in.)

R = fire resistance rating period (min), R = 60 to 240

W = weight of the steel column (lb./ft.)

D = heated perimeter of the steel column (in.)

Table 6.10. summarizes different attempts of improving fire protection for columns and/or beams. It also includes one attempt of leaving secondary beams unprotected in order to investigate its influence on the global performance and potential of saving material cost.

Table 6.10. *Attempts of enhancing fire protection for structural members*

Attempt	Fire Proofing Rate			Time Limit (min)			
	Columns	Primary Beams	Secondary Beams	$T_{insulation}$	$T_{integrity}$	$T_{stability}$	T
Original	1 hr.	1 hr.	1 hr.	55	55	55	**55**
#1	2 hr.	1 hr.	1 hr.	> 67	85	87	**> 67**
#2	1.5 hr.	1 hr.	1 hr.	> 64	71	72	**> 64**
#3	1 hr.	2 hr.	1 hr.	58	60	60	**58**
#4	1 hr.	1 hr.	0	53	54	54	**53**

(Green color indicates the governing failure mode)

It can be seen that increasing fire protection for columns has a significant effect on the three failure modes of the global structure (i.e., insulation, stability, and integrity). This is because buckling in the columns is the primary reason for the stability, integrity, and insulation failures. Thus, delaying the time when columns buckle by increasing fire protection for columns can substantially extend the time limit.

Increasing fire protection for beams has a small effect on the three failure modes of the global structure (i.e., insulation, stability, and integrity). This is because stability and integrity failures are primarily determined by buckling in the columns. Insulation failure is determined by both buckling in columns and large deflections in beams. Thus, strengthening the beams by adding fire protection without strengthening columns does not have a significant impact.

The combination of 1.5-hour fire protection for all columns and 1-hour fire protection for all beams is sufficient for the building to remain robust at the Life Safety performance level for one-hour standard fire exposure.

Leaving secondary beams unprotected has an insignificant effect on the global structural robustness (i.e., very small decrease in time limit of all different failure modes). This provides a potential of saving fire insulation materials. However, to satisfy the objective of one-hour fire resistance for the building, more trials of fire protection for members should be conducted to find the most cost-effective option.

6.5.2. Increasing load-bearing capacity

There are three ways of increasing load-bearing capacity: increasing the capacity of slabs, of beams, and of columns. They are described below.

Increasing the capacity of slabs:

As shown earlier in Table 6.3, four different methods to increase the capacity of the slabs include increasing the thickness of slab, the strength of concrete, the strength of steel mesh, and the size of steel mesh. The strength of steel mesh used in this building is Grade 60 (σ_y = 60 ksi = 420 MPa), which is the highest steel grade available for reinforcement, so the strength of the mesh is kept unchanged. Thus, Table 6.11 shows the design combinations that involve increasing the compressive strength of the concrete and increasing the size of the mesh.

Table 6.11. *Attempts of enhancing capacity of slab*

Attempt	Column			Time Limit (min)			
	Concrete strength	Slab thickness	Steel mesh	$T_{insulation}$	$T_{integrity}$	$T_{stability}$	T
Original	3 ksi	3-1/4” on top of 3” deck	A185	55	55	55	**55**
#5	6 ksi	3-1/4” on top of 3” deck	A185	55	55	55	**55**
#6	3 ksi	3-1/4” on top of 3” deck	A370	55	55	55	**55**

It can be seen that increasing the concrete strength and the reinforcement provided insignificant improvement in structural robustness (i.e., the time limit is unchanged). In other words, strengthening the capacity of slabs is not an effective method of improving structural robustness in fire.

Increasing the capacity of beams:

Larger beam sections are used to increase the capacity of beams, as shown in Table 6.12. Because no failure (i.e., no large displacement or large strain) was observed in the edge beams with moment beam-to-column connections during the structural analysis of three-hour standard fire exposure, the sizes of these beams were kept unchanged. Therefore, the size increase is for the interior beams

and edge beams with shear beam-to-column connections. The beams are color coded in Fig. 6.15 and the sizes are given in Table 6.12.

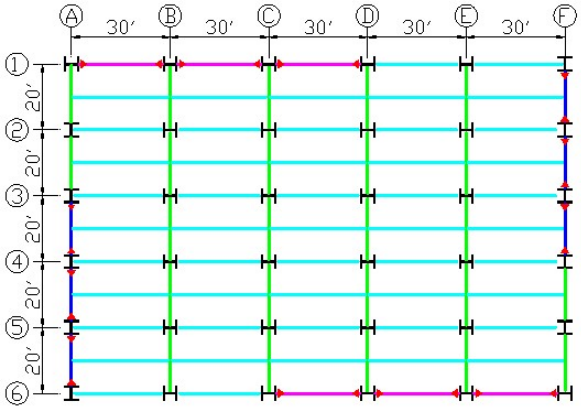

Fig. 6.15. *Floor layout of the building (members of the same color are of the same sections)*

Table 6.12. *Attempts of increasing capacity of beams*

Attempt	East-West Beam		North-South Beam		Time Limit (min)			
	Moment (Purple)	Shear (Cyan)	Moment (Blue)	Shear (Green)	$T_{insulation}$	$T_{integrity}$	$T_{stability}$	T
Original	W24x76	W14x22	W21x73	W16x26	55	55	55	**55**
#7	W24x76	W16x26	W21x73	W18x35	56	56	56	**55**
#8	W24x76	W18x35	W21x73	W21x44	62	62	62	**62**

(Green color indicates the governing failure mode)

It can be seen that increasing the sizes of beams provides an insignificant improvement in the global structural robustness in fire. It is similar to the impact of increasing fire protection for beams. The reason is also the same, i.e., stability failure and integrity failure is primarily determined by buckling in columns; and insulation failure is determined by both buckling in columns and large deformation in beams. In other words, enhancing the capacity of beams is not as effective to the global structural performance as enhancing the capacity of columns.

Increasing the capacity of columns:

Larger column sections are used to increase the capacity of columns, as shown in Table 6.13.

Table 6.13. *Attempts of increasing capacity of columns*

Attempt	Column				Time Limit (min)			
	Section	Area ($in.^2$)	Modulus W_x ($in.^3$)	Modulus W_y ($in.^3$)	$T_{insulation}$	$T_{integrity}$	$T_{stability}$	T
Original	W18x119	35.1	231	44.9	55	55	55	**54**
#9	W21x147	43.2	329	60.1	> 65	85	85	**> 65**
#10	W21x122	35.9	273	49.2	> 62	64	64	**> 62**

(Green color indicates the governing failure mode)

Increasing the size of columns provides a significant improvement in the stability and integrity but a modest effect on the time limit determined by insulation, similar to the impact of increasing fire protection for columns. However, adding a few minutes to the time limit can be crucial to ensuring that the design satisfies the objective of one-hour robustness. It was found that increasing the column size on the first, second, and third floors to W21x122 and keeping the rest of the structure unchanged is an effective way to ensure the Life Safety performance of one-hour under standard fire exposure.

6.6. Conclusions and limitations

6.6.1. Conclusions

Applying the 3D analysis method that was described in Chapter 5, two types of structure were studied to evaluate their structural robustness against fire-induced progressive collapse. One structure consists of perimeter moment frames and interior gravity frames (called Structure A), and the other consists of a central core and gravity frames (called Structure B). These structures are both 10-story composite buildings with steel columns, steel beams and reinforced concrete slabs. 2-node beam-column elements (i.e., B31 type) were used for modeling the beams and columns, 4-node shell elements (i.e., S4R type) were used for modeling the slabs, and simple joints (i.e., kinematic coupling constraints) were used for modeling the connections. To simulate fire-induced progressive collapse hazard, the fixed-load increased-temperature scenario was adopted and implemented in ABAQUS.

A parametric study was conducted to analyze the influence of different factors on the structural robustness in fire as well as the effectiveness of different strategies for design improvement. The case study part (described in Section 6.3 and 6.4) focuses on evaluating the structural robustness and the effect of fire-related factors (i.e., fire location, fire scale, and fire type) while the design improvement part (described in Section 6.5) focuses on the effect of structure-related factors (i.e., fire protection, capacity of the slabs, capacity of the beams, and capacity of the columns).

Three criteria were used to evaluate structural robustness in fire for these buildings, namely integrity, insulation, and stability. The term "time limit" was used to quantify structural robustness. Because there are three criteria, the time limit of the structure is the minimum of three limits corresponding to three criteria, i.e., $T = min\ (T_{insulation},\ T_{integrity},\ T_{stability})$.

Several major conclusions from the case study and design improvement are as follows:

- Composite floor systems help redistribute loads from the buckled columns to the adjacent columns, improving the structural resistance to fire-induced progressive collapse. As a result, the effect of the composite floor should be included in structural analysis and thus the 3D model is expected to be more accurate than the 2D model. This is in agreement with studies of structural systems at room temperature.

- Because nonlinear dynamic analysis with fixed-load increased-temperature scenario was used in the 3D model, the loss of a column happens naturally during the progression of fire, whereas in the static analysis used in the 2D model, the loss of a column was manually imposed on the structure. Therefore, the 3D model can provide a more realistic prediction than the 2D model.

- The 2D model overestimated the structural robustness compared to the 3D model. It is because the 2D model only analyzed the perimeter moment frame of the building, which has higher stiffness but lower fire temperature than the remaining structure. The 2D model restrains out-of-plane deformation, which also contributes to higher predicted robustness. Therefore, for a more accurate and realistic structural evaluation, the 3D model with nonlinear dynamic analysis and consideration of composite floor system is recommended. The 3D model can also accommodate more fire scenarios and complicated structural arrangements.

- In most of fire cases, insulation failure determined the time limit of structure. In some extreme cases (e.g., fire occurring in six compartments at the corner of Structure A), stability failure determined the time limit, and happened simultaneously with stability and integrity failures.

- Prescriptive design may be insufficient to ensure structural robustness in fire. For example, Structure A with one-hour fire insulated beams & columns can withstand a single-floor standard fire for only 55 min.

- Structure B (i.e., rigid core structure and gravity frames) is more robust against fire-induced progressive collapse than Structure A (i.e., exterior moment frames and interior gracity frames). The reason can be a better choice of member sizes, a difference in loading value, or the effect of layout.

- The improvement of structural resistance against fire-induced progressive collapse can be achieved in two ways, adding fire protection to steel members, and increasing capacity of structural members. Adding fire protection for columns and increasing the sizes of columns were found to be the most effective ways to enhance structural robustness. Adding fire protection to beams and increasing the sizes of beams provided small and insufficient improvements. Increasing the capacity of slabs did not affect the global structural robustness in fire.

- To enhance the design for Structure A, the two most cost-effective methods are: (1) increasing the size of columns on the lower three floors to W21x122 and keeping all the rest unchanged, and (2) using 1.5-hour fire proofing for columns on the lowest three floors and 1-hour fire proofing for all beams and the remaining columns. To select the best design improvement, a financial analysis should be conducted to estimate the costs (i.e., material cost, construction cost, maintenance, environmental impacts, etc.) and benefits of each method; a good design is the one satisfying the design objectives at a low cost. It is also noted that the two selected methods are only suitable with the assumed objective, which in this case was a Life Safety performance level for one-hour standard fire exposure. Depending the building requirements (e.g., building importance, occupancy, number of floors, fire evacuation strategy), the objective may be different and thus the selected design may be different.

6.6.2. Limitations and discussion

Due to computational challenges, beam-to-column connections were modeled as simple joints in these 3D analyses instead of non-linear springs (as presented in Chapter 3). This method may not be very accurate for fire conditions because of thermal expansion and material degradation at elevated temperatures. For higher accuracy, further research is needed to include more accurate connection models.

As mentioned earlier in Section 6.2, this study only considered ISO 834 standard fire curve. The purpose is to generalize the conclusions on structural robustness in fire, which can then serve as guidance for design practice. Additional study on other fire exposures should be conducted in the future to expand the findings to more realistic fire scenarios, and to explore the influence of other fire-related factors such as fire duration, the effect of the cooling phase, and creep failure of steel.

Due to time constraints, only several samples of design improvements were analyzed. More cases may need to be considered, and a complete design should include a financial analysis in order to find the most cost-effective design, which satisfies the objective at the lowest cost.

The assumed objective in this study is the Life Safety performance at one-hour standard fire exposure. In reality, many factors can affect the objective such as the importance of the building, the number of occupants, and the fire evacuation strategy. In the scope of this study, other factors and different objective scenarios were not considered.

The design improvement focused on adjusting the structure-related factors (i.e., fire protection and the capacity of structural members). However, as mentioned in Section 6.5, there is at least another way to mitigate progressive collapse in fire, i.e., using fire prevention and suppression strategies. Their goal of fire safety engineering is to prevent the propagation of fire horizontally and vertically. More specifically, in Structure A, it is conceivable that the partitions could be designed to prevent fire from occurring in six compartments simultaneously. To achieve fire prevention, the designer needs to satisfy all three components of fire prevention, i.e., compartmentation, opening protection, and fire stopping, which are detailed in Aker [10]. For better assurance, it is also important to have redundancy in fire protection. Passive fire protection, along with active fire protection (e.g., detection system and fire-sprinkler system) and occupant education, is a safer approach to protecting buildings and people.

Reference

[1] Sadek F., Main J., Lew H., Robert S., Chiarito V., El-Tawil S. (2010). "An Experimental and Computational Study of Steel Moment Connections under a Column Removal Scenario." NIST Technical Note 1669, *National Institute of Standards and Technology*, Gaithersburg, MD.

[2] FEMA 353. (2000). "Recommended Specifications and Quality Assurance Guidelines for Steel-Moment Frame Construction for Seismic Applications." Federal Emergency Management Agency (FEMA).

[3] Agarwal, A., Varma, A. (2014). "Fire Induced Progressive Collapse of Steel Building Structures: The Role of Interior Gravity Columns." *Engineering Structures*, *58,* 129-140.

[4] Eurocode 1. (2002). "Actions on Structures, Part 1-2: General Actions - Actions on Structures Exposed to Fire." *Commission of European Communities*, Brussels, Belgium.

[5] Eurocode 4. (2005). "Design of Composite Steel and Concrete Structures, Part 1-2: General Rules - Structural Fire Design." *Commission of European Communities*, Brussels, Belgium.

[6] Lawson, R., Newman, G. (1990). "Fire Resistant Design of Steel Structures - A Handbook to BS 5950: Part 8". *The Steel Construction Institute*, SCI publication 080.

[7] ASCE/SEI 41-06. (2007). "Seismic Rehabilitation of Existing Buildings." *American Society of Civil Engineers (ASCE)*, Reston, VA.

[8] Alashker, Y., Li H., El-Tawil S. (2011). "Approximations in Progressive Collapse Modelling." *Structural Engineering*, v 137 (9), 914-924.

[9] "BXUV.N735 Fire Resistance Ratings - ANSI/UL 263."

[10] Aker, J. (2008). "The Basics of Passive Fire Protection." Buildings.com <www.buildings.com/article-details/articleid/5851/title/the-basics-of-passive-fire-protection-> (07/01/2017)

CHAPTER 7. CONCLUSION AND FUTURE WORK

Chapter 7 summarizes the research conclusions on structural robustness against fire-induced progressive collapse. It also describes the limitations of this dissertation and discusses possible areas for future research.

7.1. Conclusion

This dissertation addresses the need of analyzing the structural performance against fire-induced progressive collapse as well as improving existing designs to resist this extreme hazard. It also presents a comprehensive method of quantifying structural robustness in fire, closing the gap in current research and design codes. The focus is on framed building structures with steel columns and beams with composite reinforced concrete slabs. The research was conducted via computational analyses which were validated against experimental tests.

The study presented in this dissertation used sequentially coupled thermal - structural analyses in ABAQUS (i.e., a thermal analysis was conducted to obtain temperatures in structural members during fire, which were then inputted into the structural analysis to predict the structural response in fire-induced progressive collapse) with consideration for geometric and material nonlinearity. The progressive collapse scenario was simulated by removing a column from the structural system, which is otherwise known as the Alternate Path Method within the Direct Approaches in the GSA [1] and UFC [2] guidelines. In addition to fire, the loading included gravity loads and lateral loads. The most appropriate and realistic analysis method was found to be the nonlinear dynamic analysis (e.g., explicit dynamic analysis in ABAQUS) but the dynamic analysis required a high computational cost. A more cost-effective method was to perform the nonlinear static analysis (e.g., implicit analysis in ABAQUS) with a dynamic amplification factor to consider the dynamic effect of the column removal.

Due to the development of axial forces in floor beams, it was not appropriate to model beam-to-column connections as simple joints (i.e., perfectly rigid or pinned) in the structural system. A simplified model for the welded unreinforced flange - bolted web (WUF-B) connection was proposed to provide an accurate prediction of structural performance in fire at a reasonable computation cost. The connection model was a system of nonlinear springs (i.e., connector elements in ABAQUS), each of which represents a failure mechanism of the connection. The model for WUF-B connection was validated against high-resolution FE models and experimental tests at room temperature and elevated temperatures.

The proposed method of evaluating structural robustness in fire combines the principles of fire protection criteria and acceptance criteria with research findings on fire insulation materials. There are three performance level - Immediate Occupancy (IO), Life Safety (LS), and Collapse Prevention (CP); each performance level requires different limits and calculation coefficients. The structure is considered robust if it satisfies three criteria: (1) *integrity* (i.e., to prevent fire spread through openings, which involves limiting the rotations at beam ends and deflections of slabs), (2) *insulation* (i.e., to prevent unacceptable temperature rise at the unexposed surface of structures, which involves limiting strains to avoid damage in SFRM), and (3) *stability* (i.e., to prevent the loss of load-bearing capacity of structures, which involves preventing forces in beams and columns from exceeding the capacity). The time limit was defined as the maximum duration of ISO 834 standard fire exposure that the structure could withstand before the performance criteria were no longer met. The time limit was useful for quantitatively comparing the robustness of different structures threaten by fire-induced progressive collapse.

Simplified 2D models and 3D models were applied in the study to evaluate the building performance in the fire-induced progressive collapse events. The 2D model used beam-column elements to represent steel beams and columns, and the connection model to represent beam-to-column connections. With the assumption that during fire, the member temperatures reach a steady-state when a column begins to buckle, the 2D model adopted the fixed-temperature increased-load scenario and used the nonlinear static analysis in ABAQUS, in which a column was manually removed at the beginning of the loading step. It was found to be appropriate to integrate the connection model into the 2D analysis of a frame but too expensive to do so in the 3D analysis of an entire building. Thus, the 3D model used simple joints (i.e., perfectly pinned or rigid) to

represent the connections, but the composite floor system was more accurately modelled using beam and shell elements. The 3D model adopted the fixed-load increased-temperature scenario and used the nonlinear dynamic analysis in ABAQUS, in which a column removal occurs naturally with reduced capacity and load redistribution in the structure during fire.

A ten-story composite building with perimeter moment resisting frames and interior gravity frames, unprotected concrete slab, and one-hour fire protected steel columns and beams was used as a case study. The 2D model analyzed the perimeter moment frame while the 3D model analyzed the entire structural system. A parametric study was conducted to investigate the influence of different factors such as the vertical location of fire, the location of column loss, and the scale of fire (i.e., the number of compartments exposed to fire, and the number of floors exposed to fire). The 2D model predicted that the frame remained robust for at least 120 min in a single-floor standard fire and 90 min in a three-floor standard fire; fire on the ninth-floor was found to be the critical case; and insulation failure determined the time limit in the upper-floor fire while stability failure determined the time limit in the lower-floor fire. In comparison, the 3D model predicted that the building would remain robust for 55 min in a single-floor standard fire, and fire on the first-floor was found to be the critical case; insulation failure determined the time limit in all cases. The reason for such a big difference in results between the 2D and 3D models is the membrane action of the composite floor system, which redistributes loads from the buckled columns to the adjacent columns. The higher stiffness and lower temperature of exterior moment frame also caused the 2D model to overestimate the structural robustness. Therefore, it is recommended to use 3D models for accurate evaluations of entire buildings exposed to fire-induced progressive collapse scenarios.

It was found from the 3D analyses that there is no difference in robustness against fire-induced progressive collapse between two types of structure (i.e., framed structure vs. core structure) although it took longer time for the core structure to lose its load-bearing capacity. The reason can be a better choice of the member sizes, a difference in the gravity loads, or the effect of design layout. Further research should be carried out for a more accurate conclusion.

Despite being rarely considered in studies on structural robustness in fire, for the structures considered here, insulation failure under high strains determined the time limit in almost all cases.

It was assumed that the insulation would be damaged at a strain of 0.01. Fire protection materials (e.g., intumescent, gypsum board, etc.) may have different deformation limits.

There are two ways to enhance the design for improved robustness, namely fire prevention (to limit the spread of fire in multiple compartments), and structural enhancement (to improve the structural resistance). Fire prevention can be achieved by improving compartmentation, opening protection, and fire stopping. These are prescriptive approaches that can also prevent fire and smoke migration, and protect evacuation routes. Structural enhancement can be achieved by adding fire protection to steel members (i.e., beams and columns), and increasing capacity of structural members (i.e., slabs, beams, and columns). Adding fire protection to columns and increasing the sizes of columns were found to be the most effective ways to enhance structural resistance. In contrast, adding fire protection to beams and increasing the sizes of beams provided small and insufficient improvement in performance; increasing the capacity of the slab did not provide much improvement either.

7.2. Limitation and future work

In the proposed method of quantifying structural robustness in fire, the strain limit of 0.01 was used to define failures of the insulation. This value is applicable for SFRM as the fire insulation material. For better accuracy, it is recommended that the mechanical properties of insulation be determined from experimental tests, including their dependence on temperature and strain. Other factors which may affect the insulation performance (e.g., the story drift) and the integrity performance (e.g., partition walls and claddings) were not considered in this study. This is a possible area for future research.

The 3D analysis did not include the connection model (i.e., the system of spring elements to represent the connections' performance at elevated temperatures) due to the extreme computational cost. Future research should investigate the effects of considering temperature-dependent stiffness of connections on the global robustness of an entire building under fire through 3D analyses with connection models. In addition to standard fire curve, natural fire exposure should be applied to further study the robustness of structures in real fire scenarios.

Apart from standard fire, the study did not consider other types of fire such as compartment fire and localized fire. The effect of cooling phase, traveling fire, and creep failure of steel were not considered either.

As mentioned earlier, it is the safest to combine active fire protection (i.e., fire detection and fire suppression systems) and passive fire protection (i.e., fire insulation for steel members, compartmentation, opening protection, etc.). The focus of this dissertation was on the structure-related factors, i.e., using adequate fire insulation and strengthening the capacity of structural members, of which the effectiveness can be easily quantified. For a better practicality, future research should explore the fire protection measures such as compartmentation, opening protection, and fire stopping. A financial analysis and probabilistic analysis may also be included to weight the effectiveness of those approaches and provide suggestions for design improvement.

Reference

[1] U.S. General Service Administration. (2003). "Progressive Collapse Analysis and Design Guidelines for New Federal Office Buildings and Major Modernization Projects." Washington, D.C.

[2] Unified Facilities Criteria. (2009). "Design of Buildings to Resist Progressive Collapse. Department of Defense." Washington, D.C.